Seismic body-wave imaging with and without earthquakes

Hsin-Hua Huang[1,2,3]

Fan-Chi Lin[3]

Victor Tsai[2]

Brandom Schmandt[4]

Jamie Farrell[3]

Robert Smith[3]

Keith Koper[3]

1 Academia Sinica, Taiwan

2 California Institute of Technology, U.S.A.

3 University of Utah, U.S.A.

4 University of New Mexico, U.S.A.

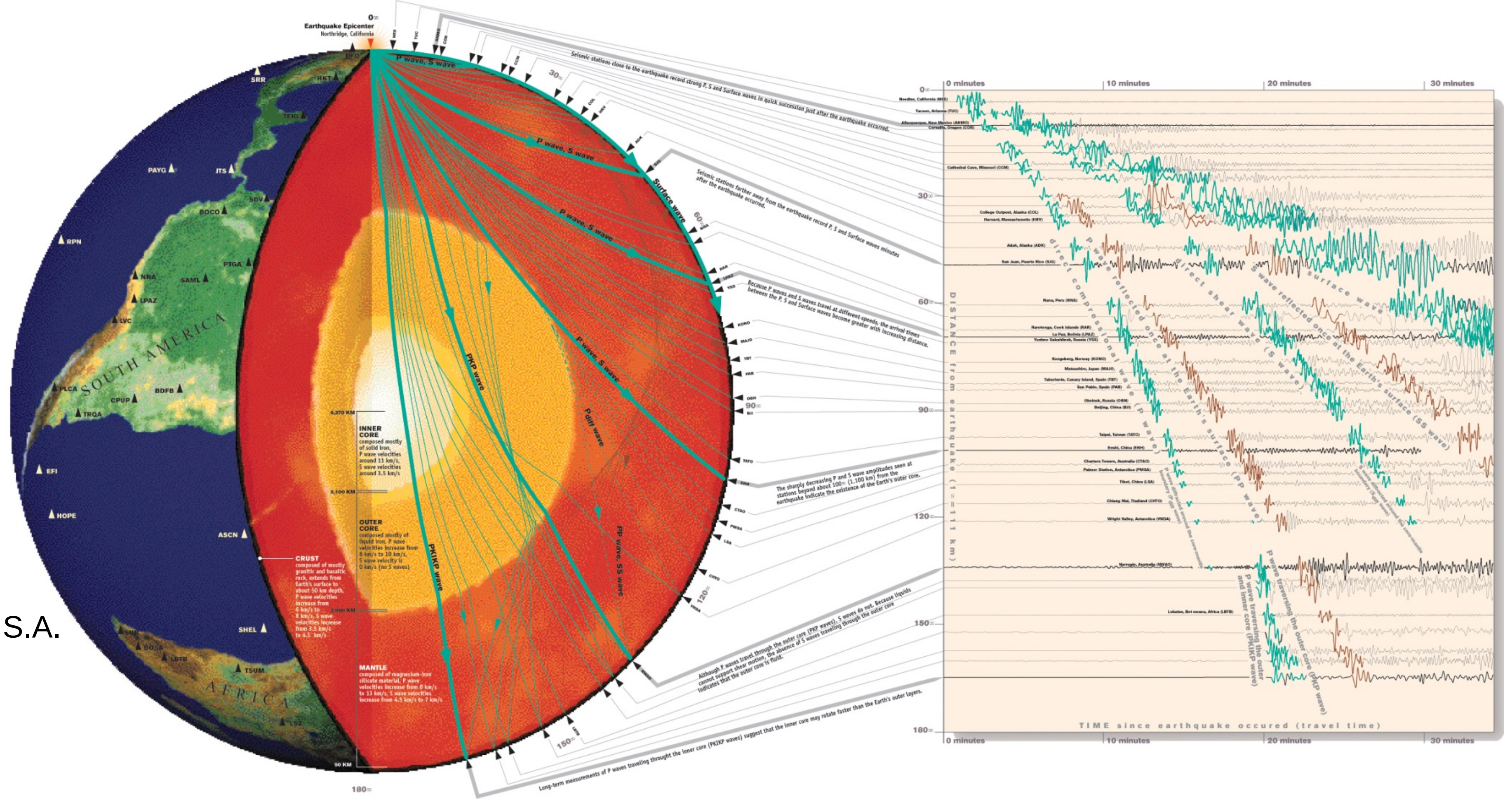

Multi-scale Earth structure

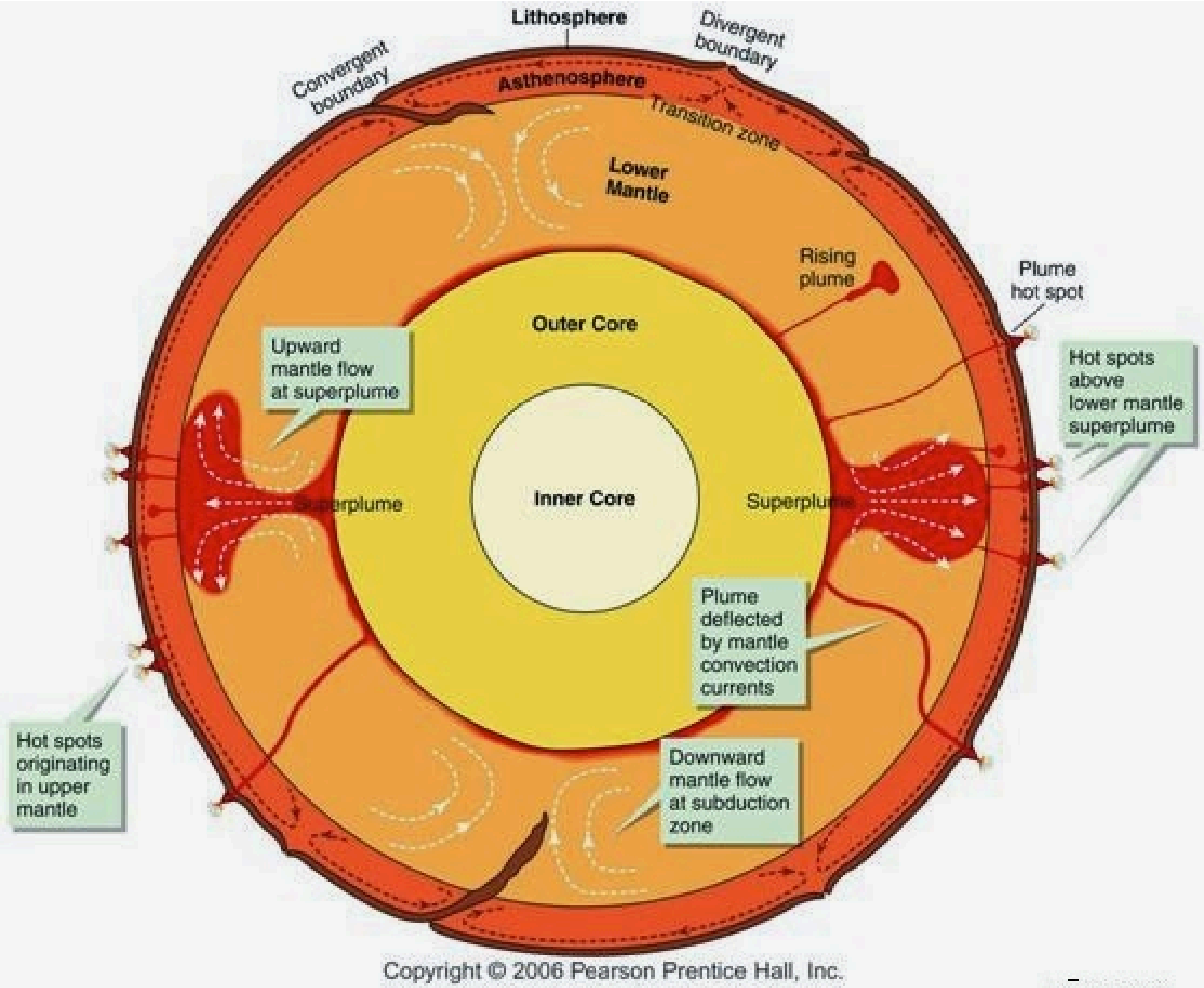

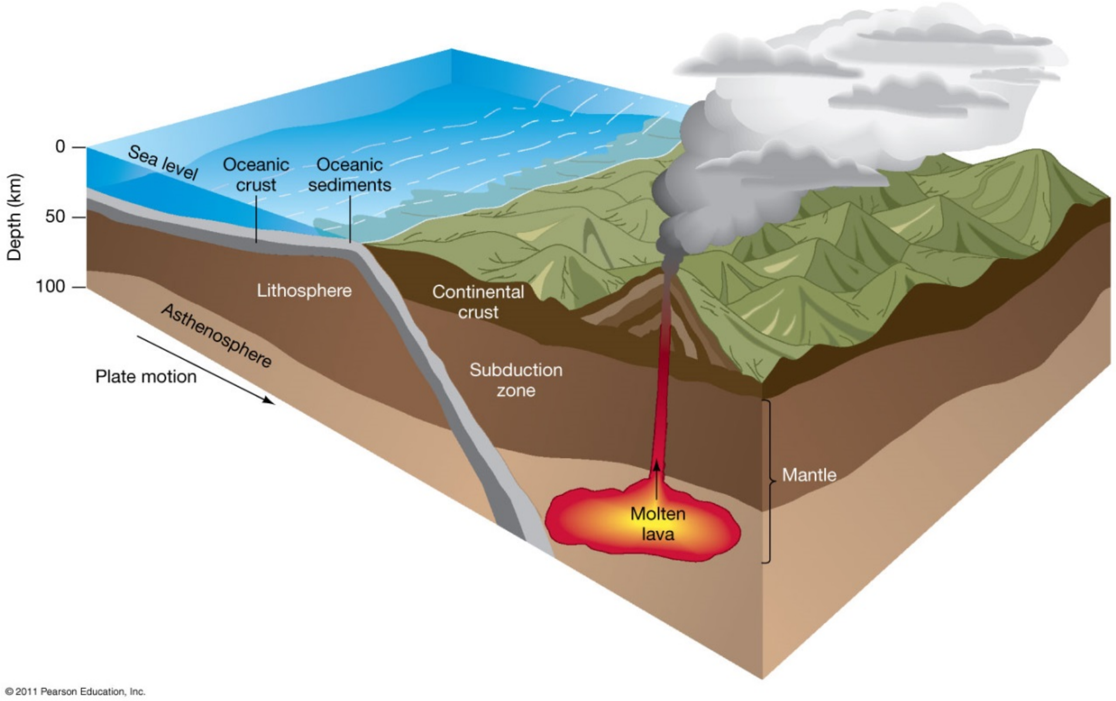

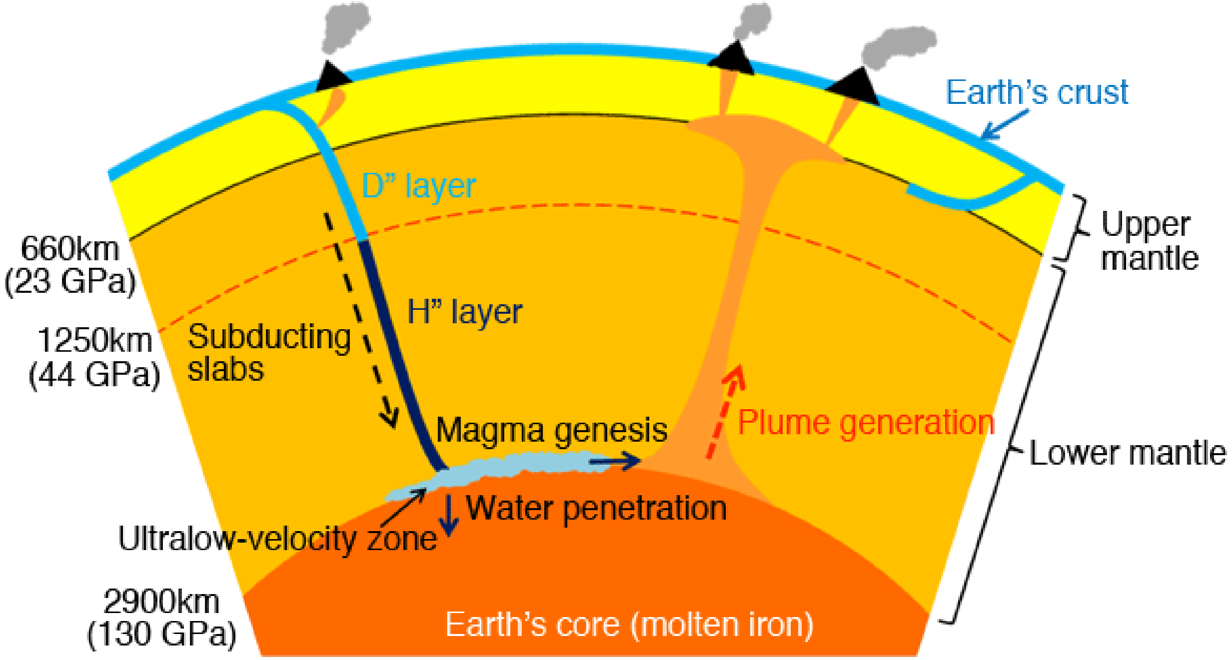

Complex structure of Earth's inner core

Differential rotation (Song & Richards,1996; Tkalcic, et al., 2013)

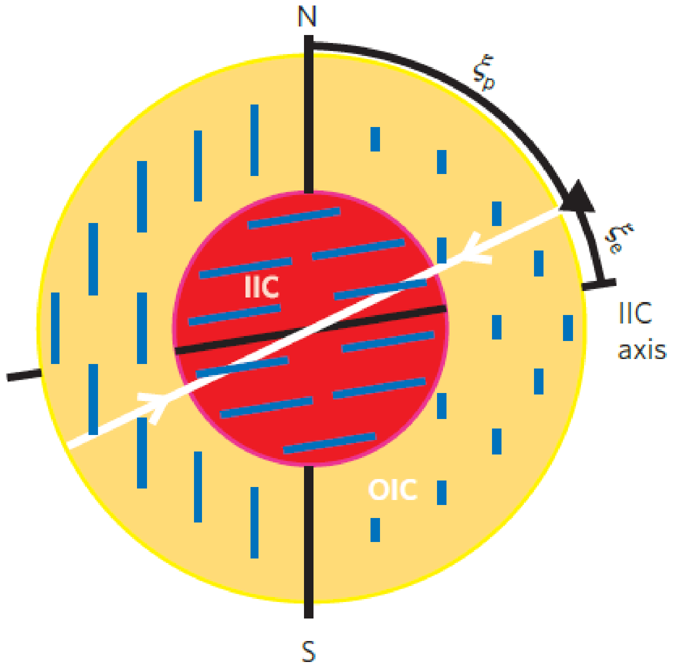

Innermost inner core (Ishii & Dziewonski, 2002; Wang et al., 2015)

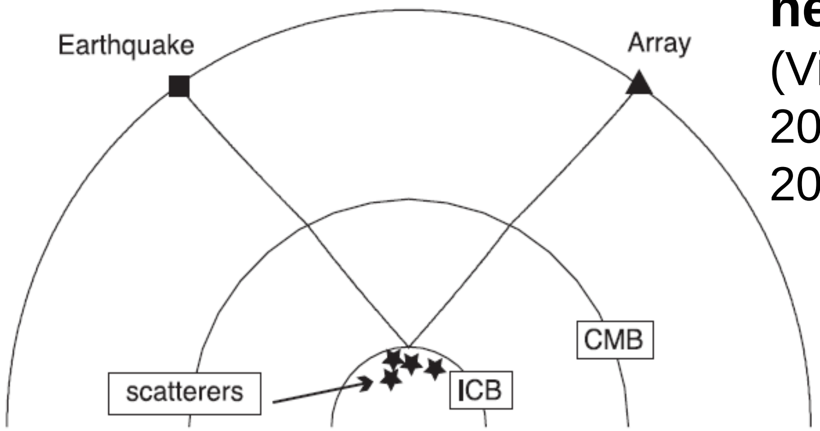

Fine-scale heterogeneity (Vidale & Earle, 2000; Koper et al., 2004)

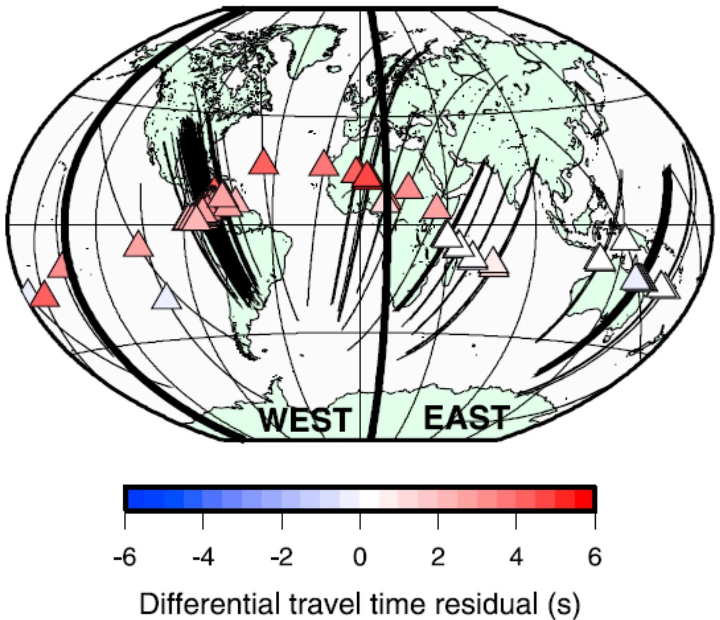

hemispherical structure (Tanaka and Hamaguchi, 1997; Irving & Deuss, 2011)

Yellowstone w/ eqk.

- 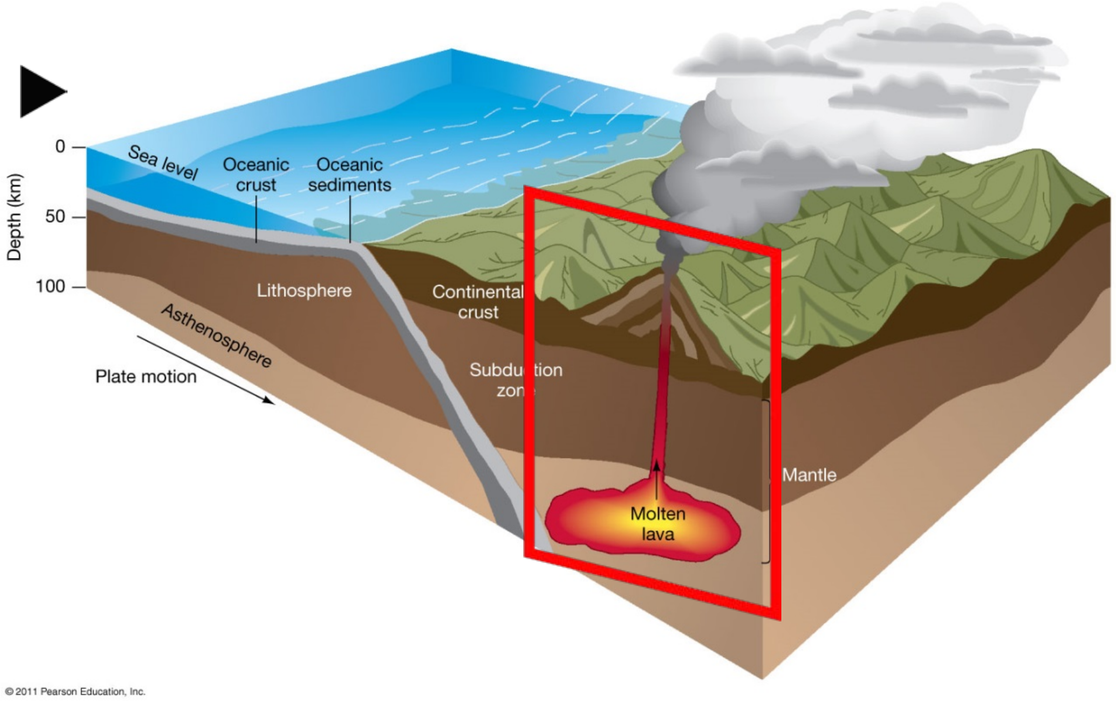

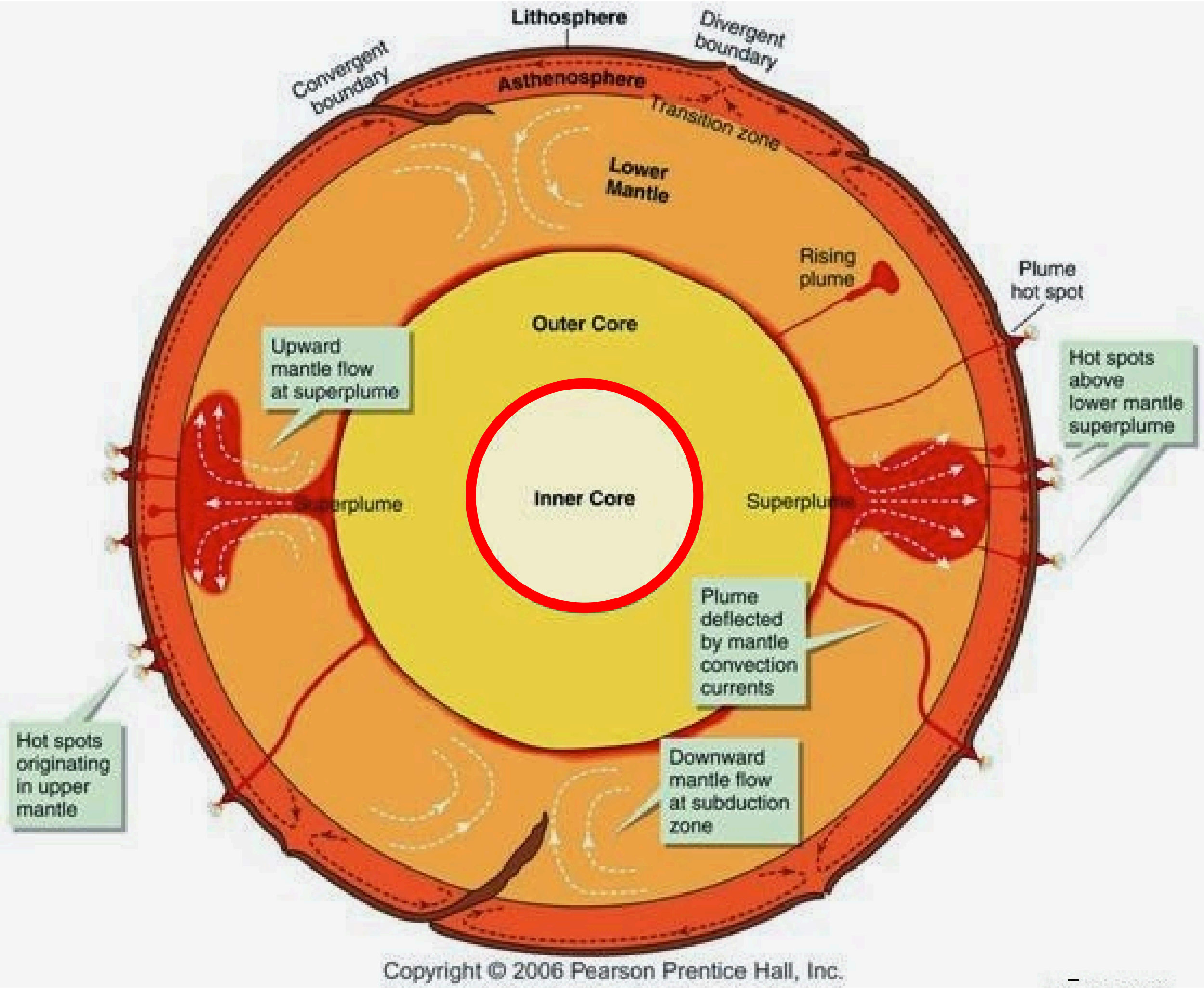

- Inner core w/o eqk.

Why we care about Yellowstone?

− Huge and active (supervolcano)

− Plume-originated (intraplate)

− most vigorous hydrothermal system

− Basalt-rhyolite bimodal system

Yellowstone hotspot & Snake River Plain

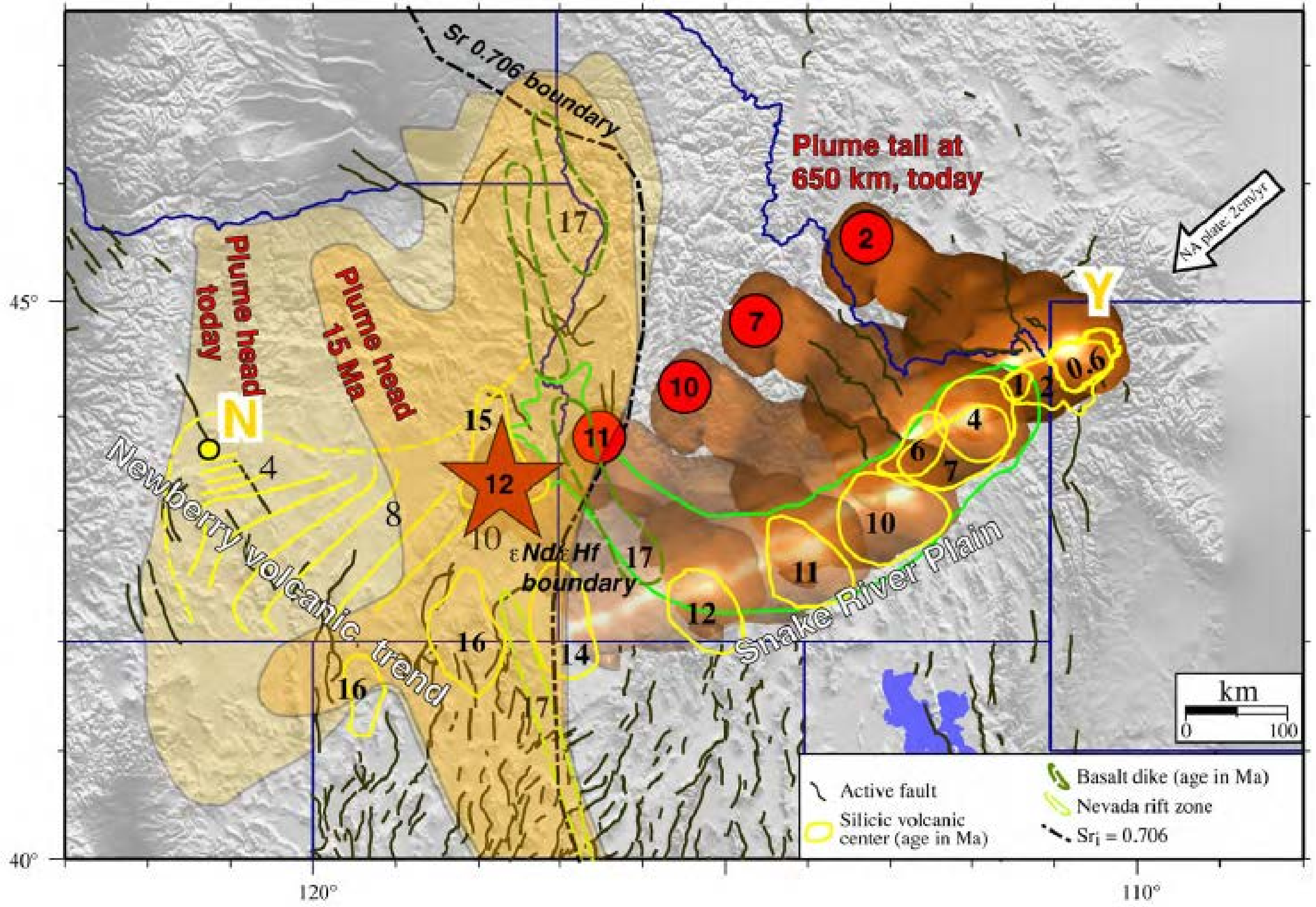

(Smith et al., 2009)

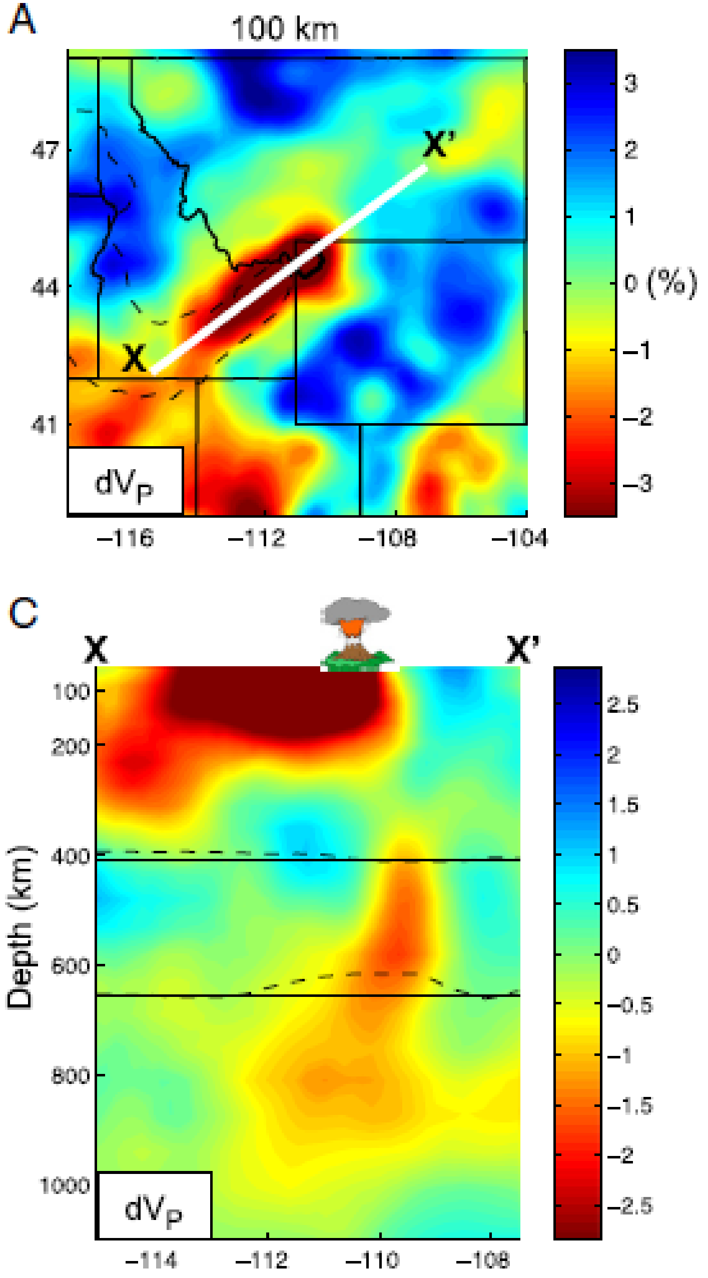

(Schmandt et al., 2012)

Crustal magmatic system from local seismic tomography

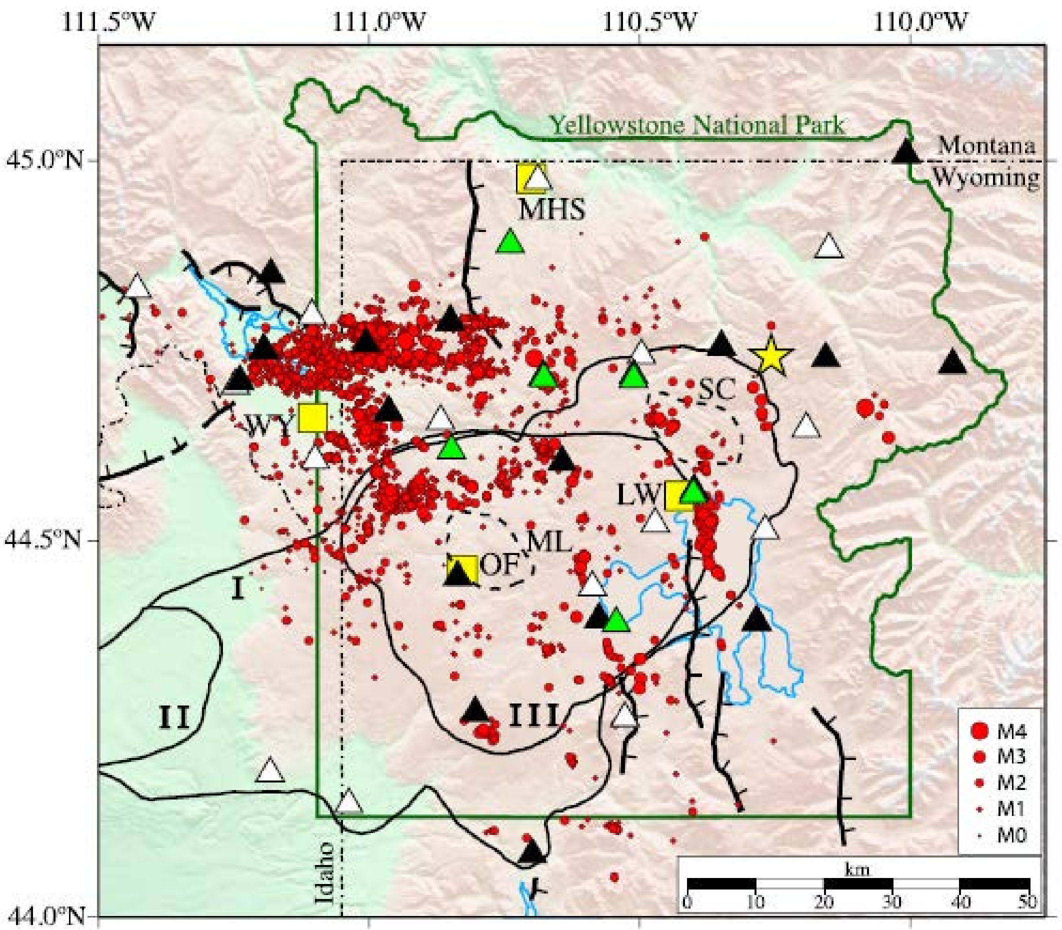

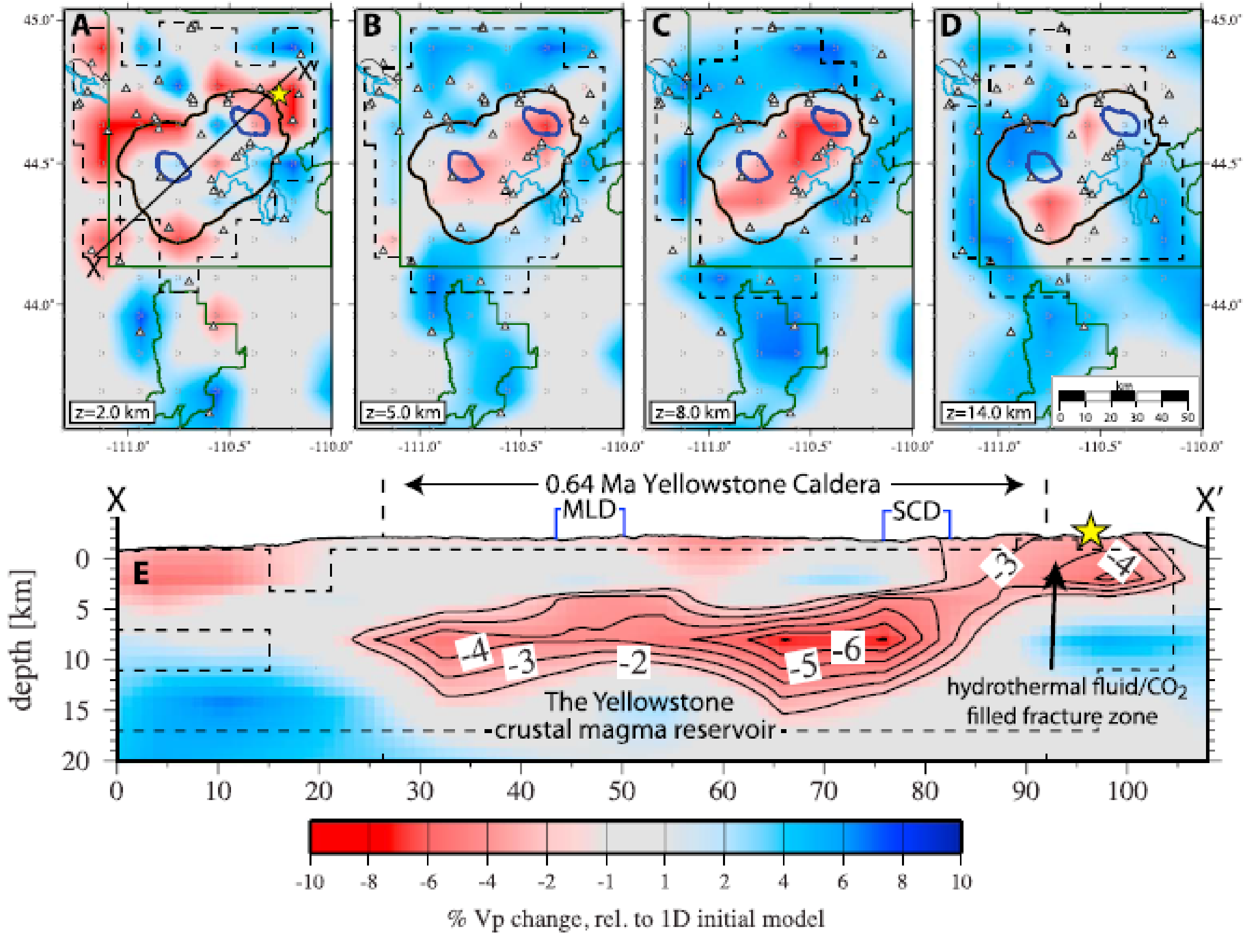

(Farrell et al., 2014)

Yellowstone schematic model from seismic observations

- A elongated shallow magma reservoir

- A NW-tilted deep-seated mantle plume

(Farrell et al., 2014)

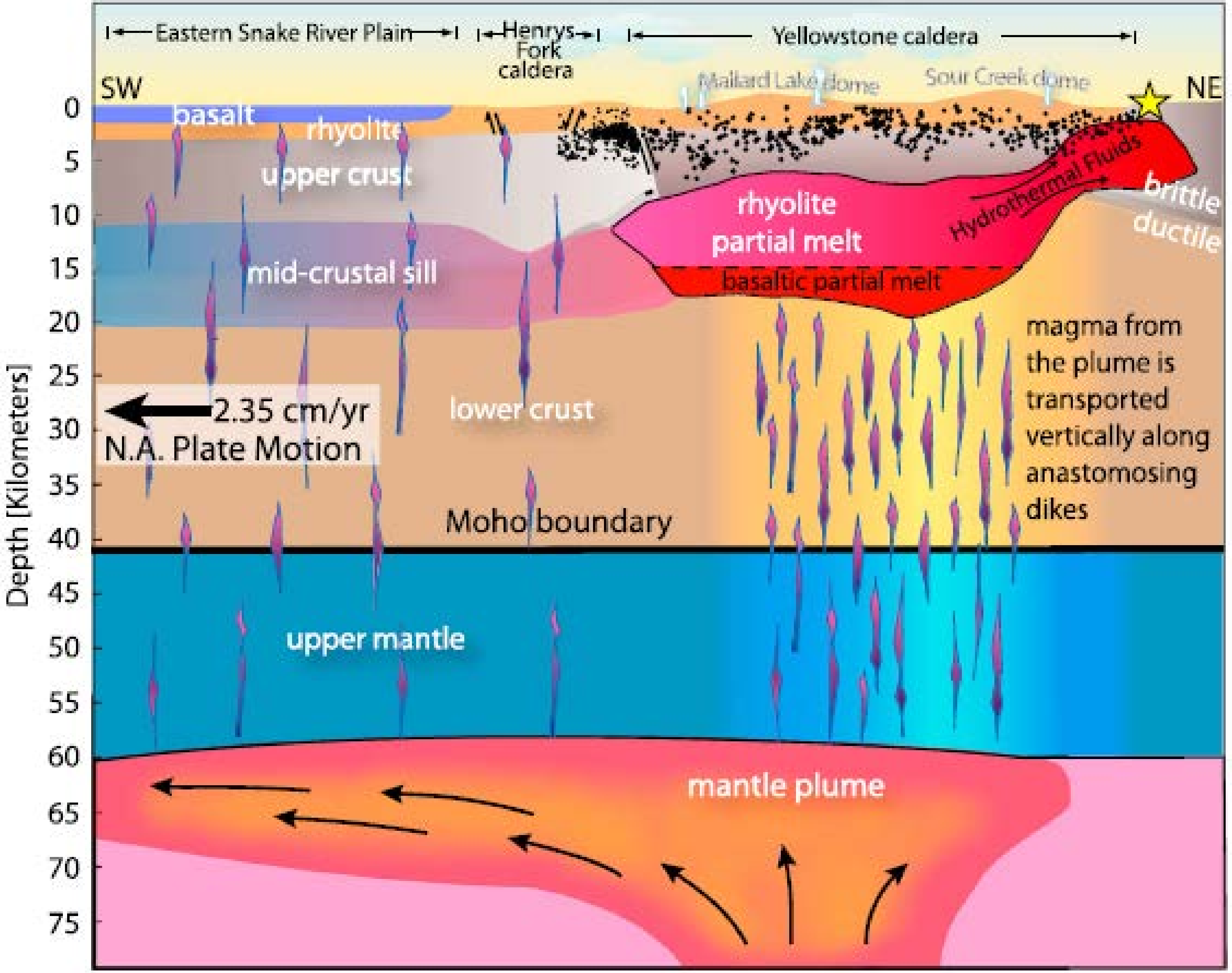

Yellowstone schematic model from geochemical observations

Extremely high..

- Heat flow (thermal gradient ~700-1000 °C/km)
- CO_2 (~5% of global volcanogenic CO_2 flux)
- Lasting for a long time (~15,000 years)

But..

- The upper-crustal rhyolitic reservoir can not account for these solely

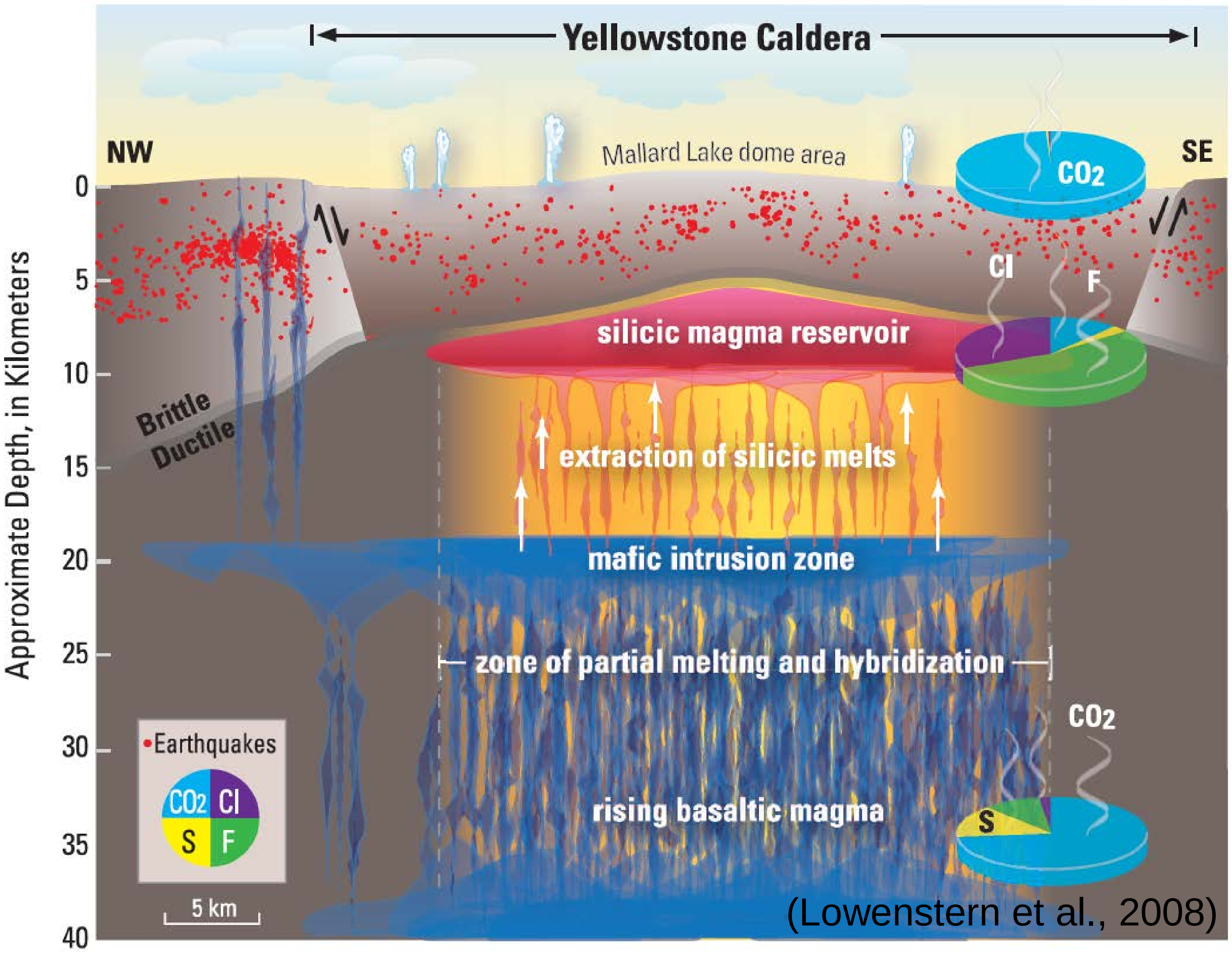

(Lowenstern et al., 2008)

Imaging the entire crustal magmatic system

- Shallow seismogenesis
- Limited array aperture

Askja Volcano, Iceland

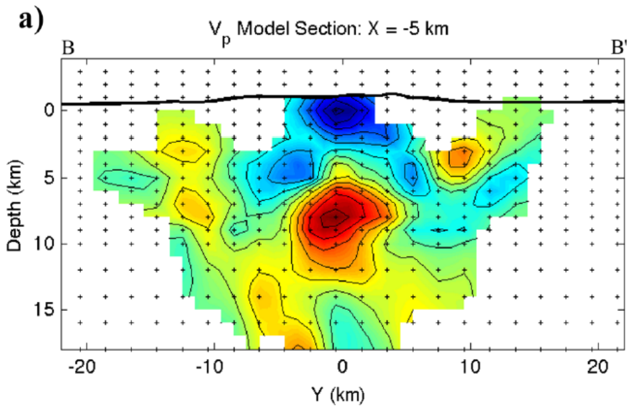

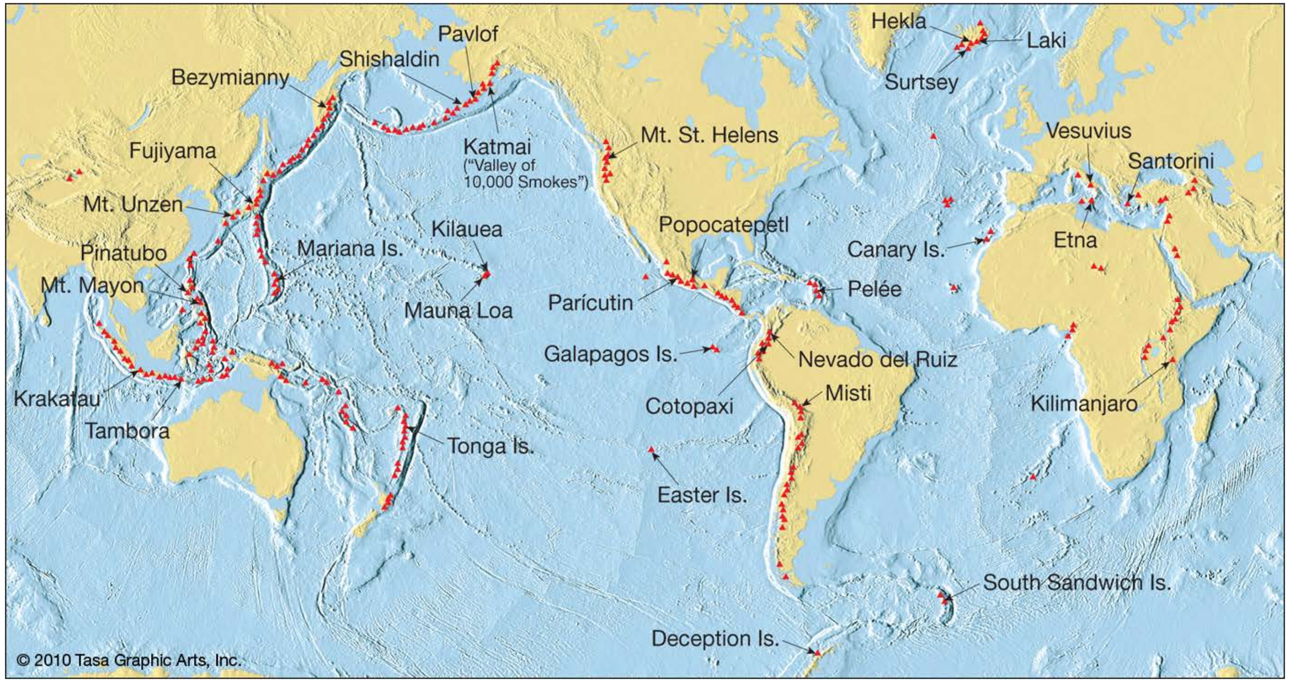

Kilauea Volcano, Hawaii, USA

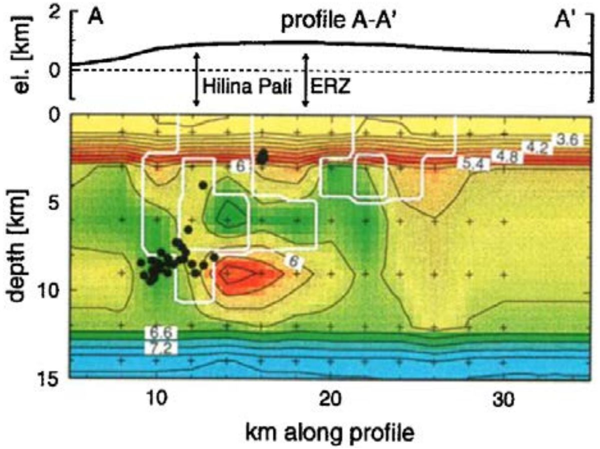

Mount St. Helens, Washington, USA

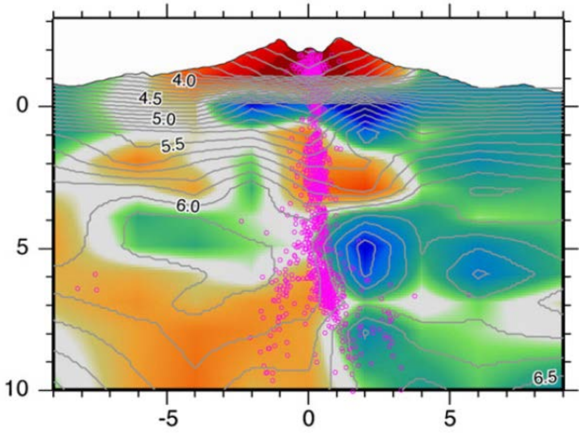

Axial Volcano, Juan de Fuca mid-ocean ridge

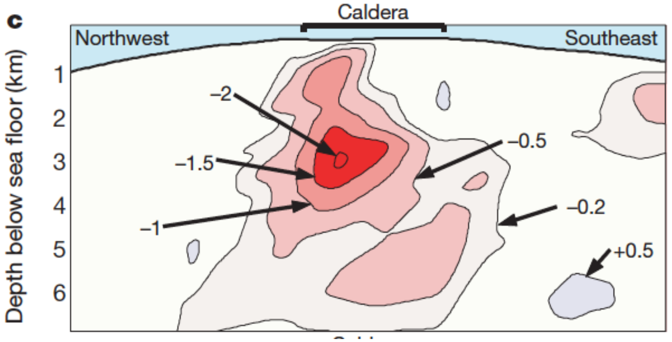

Joint inversion of local earthquake and teleseismic data

$$r_i^j = \int_i^j (s \cdot dl)\left(\frac{\Delta s}{s}\right)$$

Local event absolute arrival times

$$R_i^j = \left(\int_m^j s \cdot dl - \frac{1}{n_s}\sum_{j=1}^{n_s}\int_m^j s \cdot dl\right)\left(\frac{\Delta s}{s}\right)$$

Teleseismic event demeaned relative travel times

To really take the advantage of this..

– local dense array

– wide-aperture array

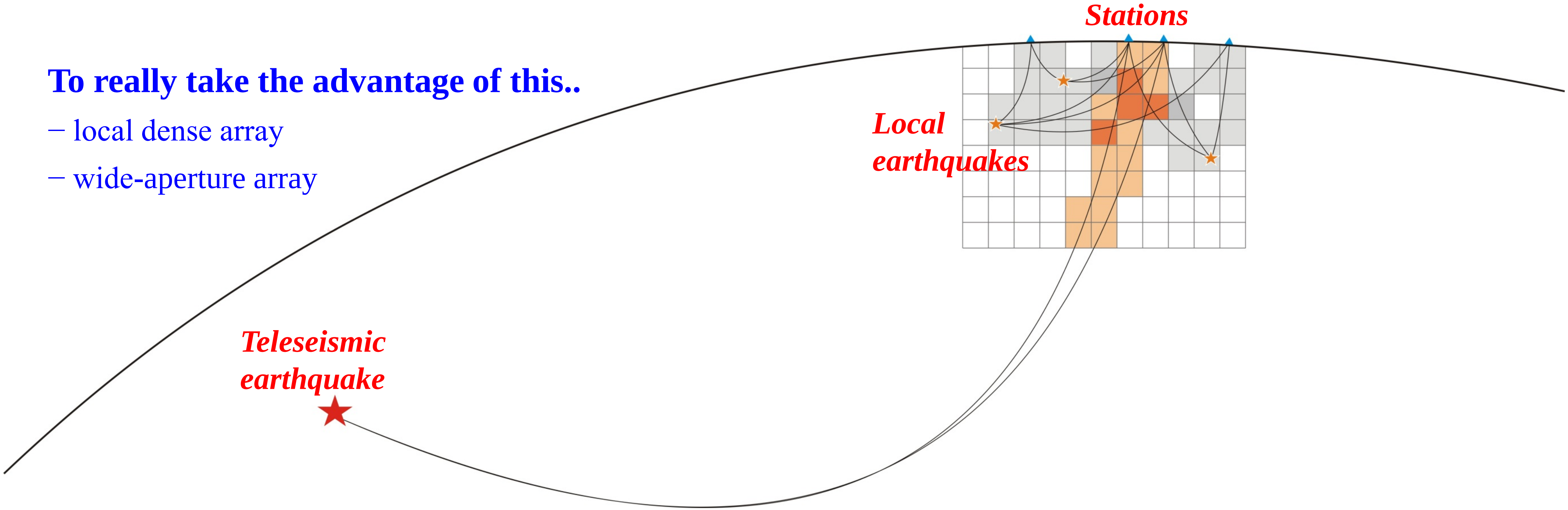

(Roecker et al., 1993; Zhao et al., 1994; Huang et al., 2014)

Data and stations

- Local seismic networks (Farrell et al., 2014)
- Earthscope Transportable Array (Brandon and Lin, 2014)
- 1-D model (ak135+local model)
- Two-step joint inversion (Huang et al., 2014)

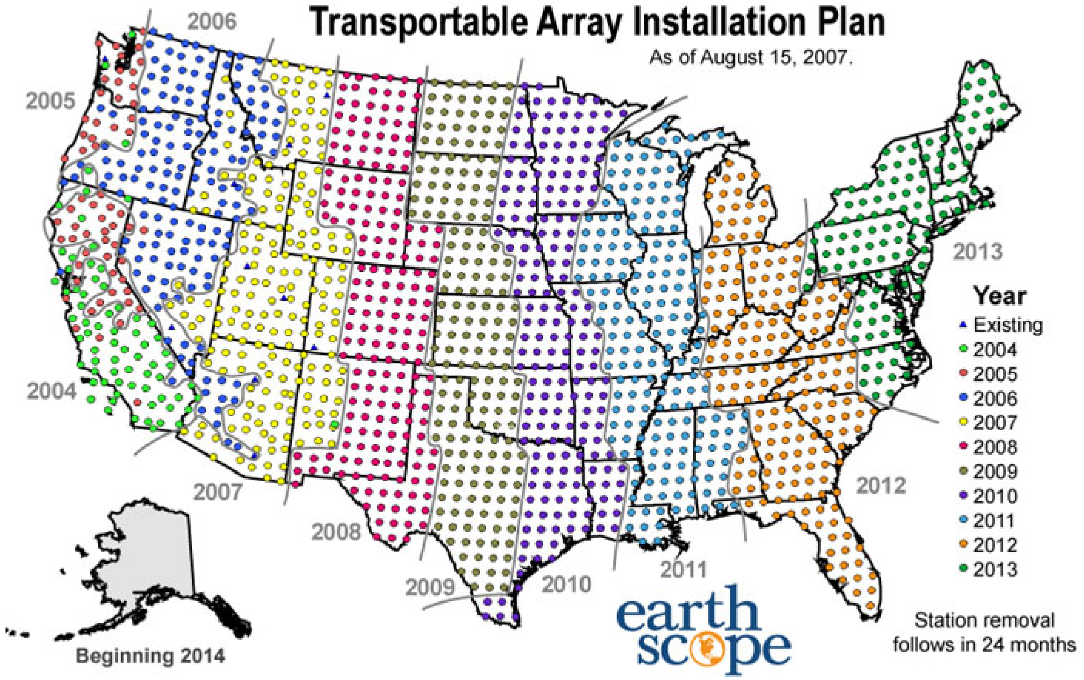

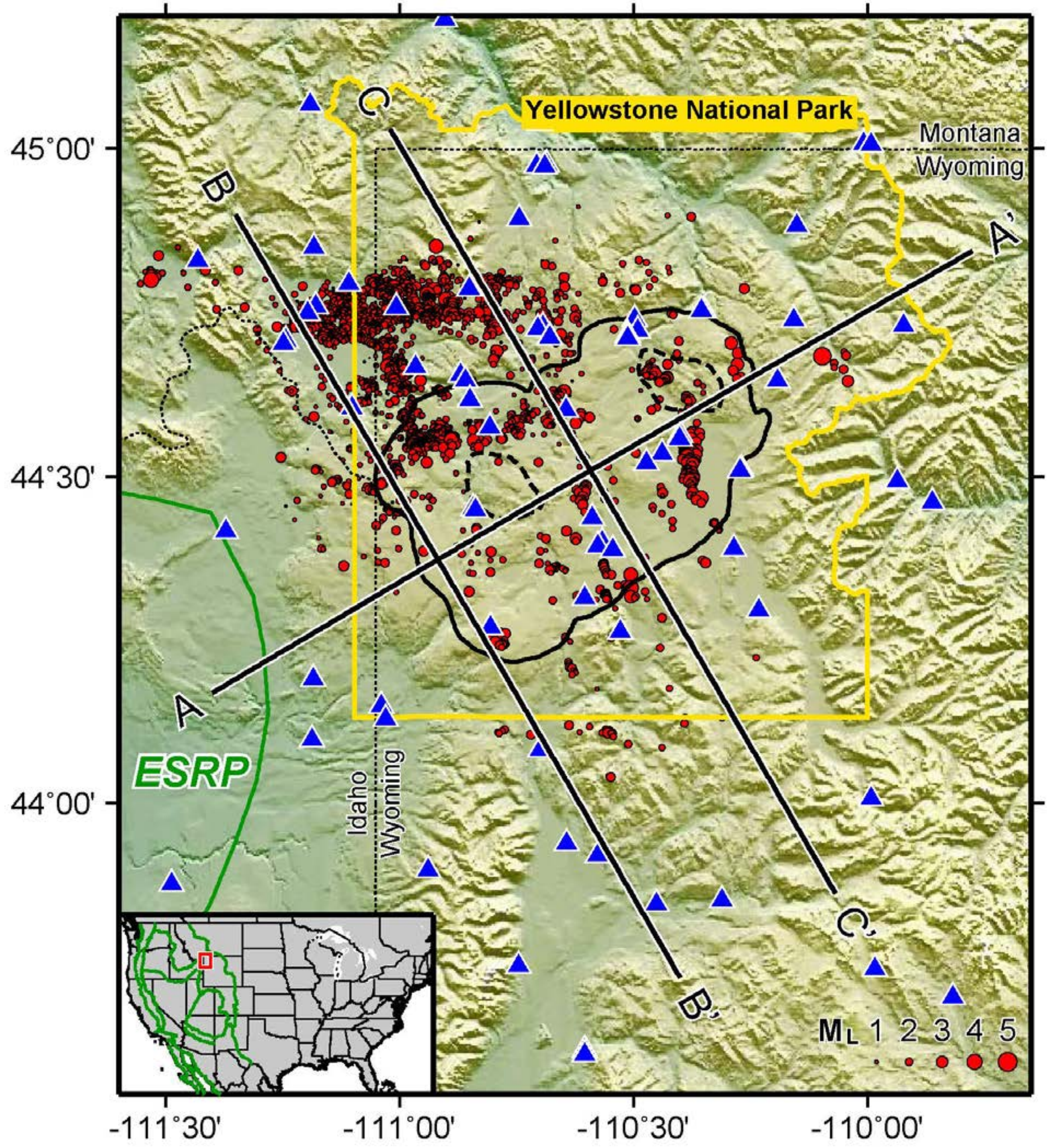

Depth slices of resulting model

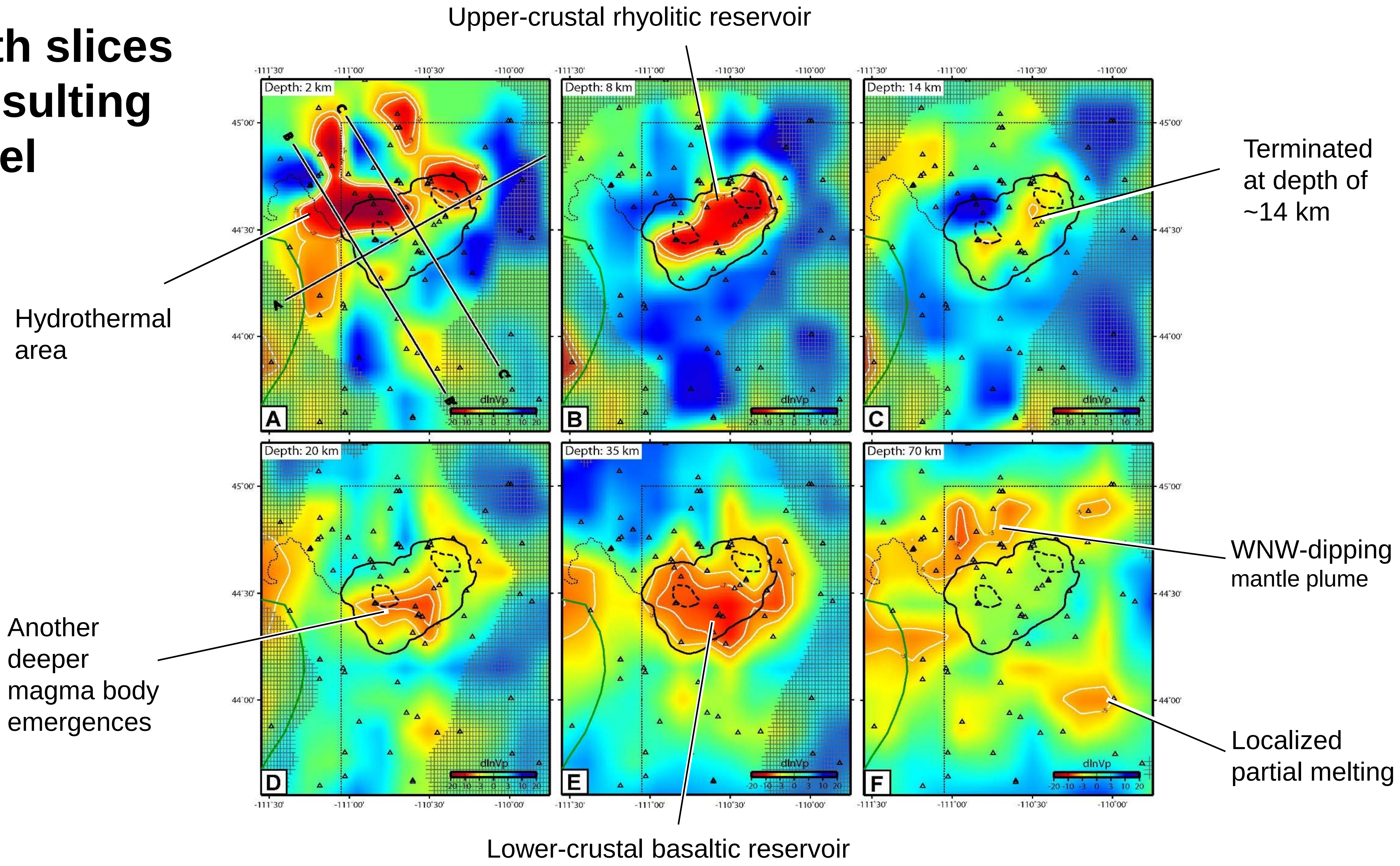

Recovery of checkerboard tests

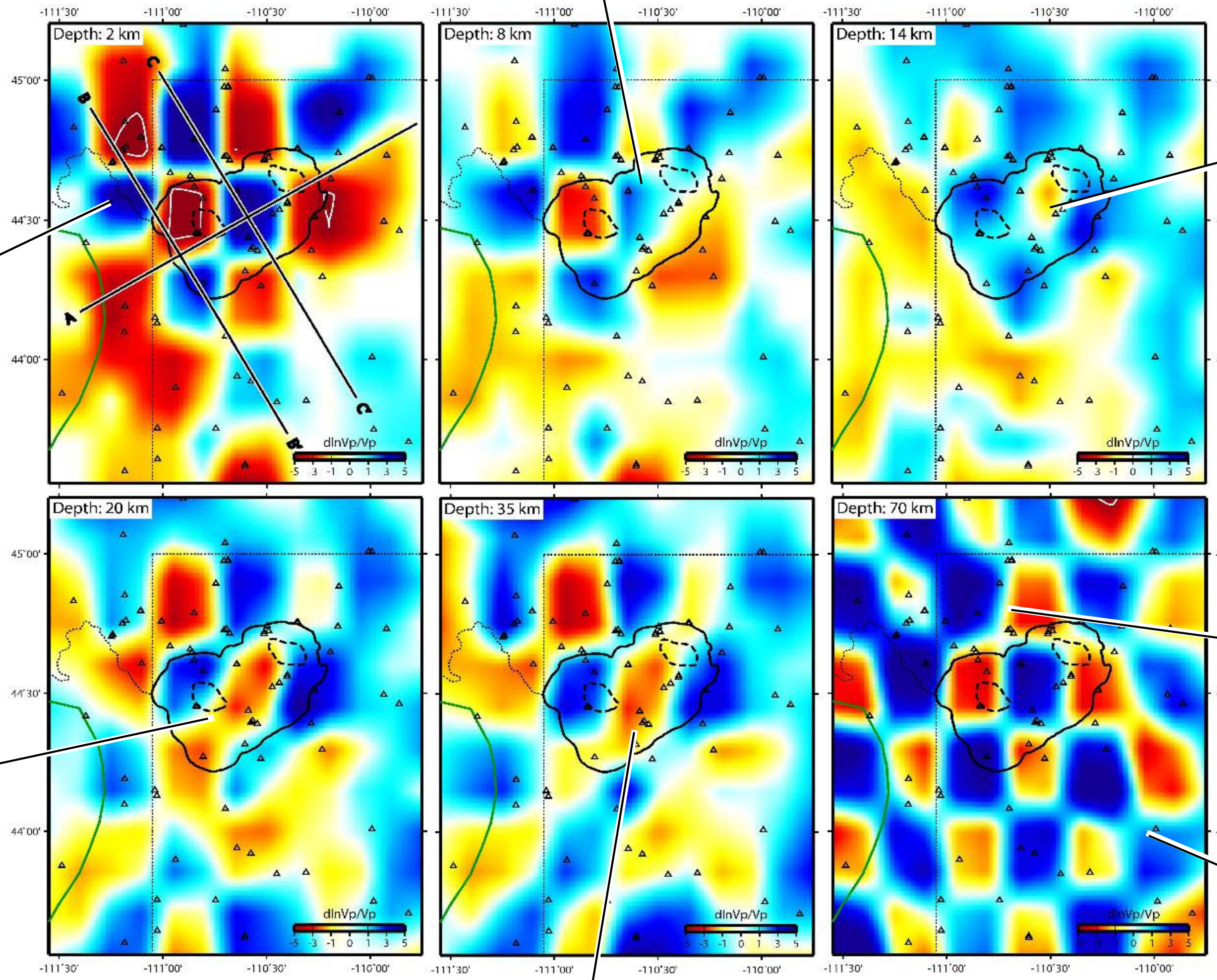

Cross-sections of resulting model

− If the upper- and lower-crustal reservoir separated?

− If the lower-crustal and mantle head separated?

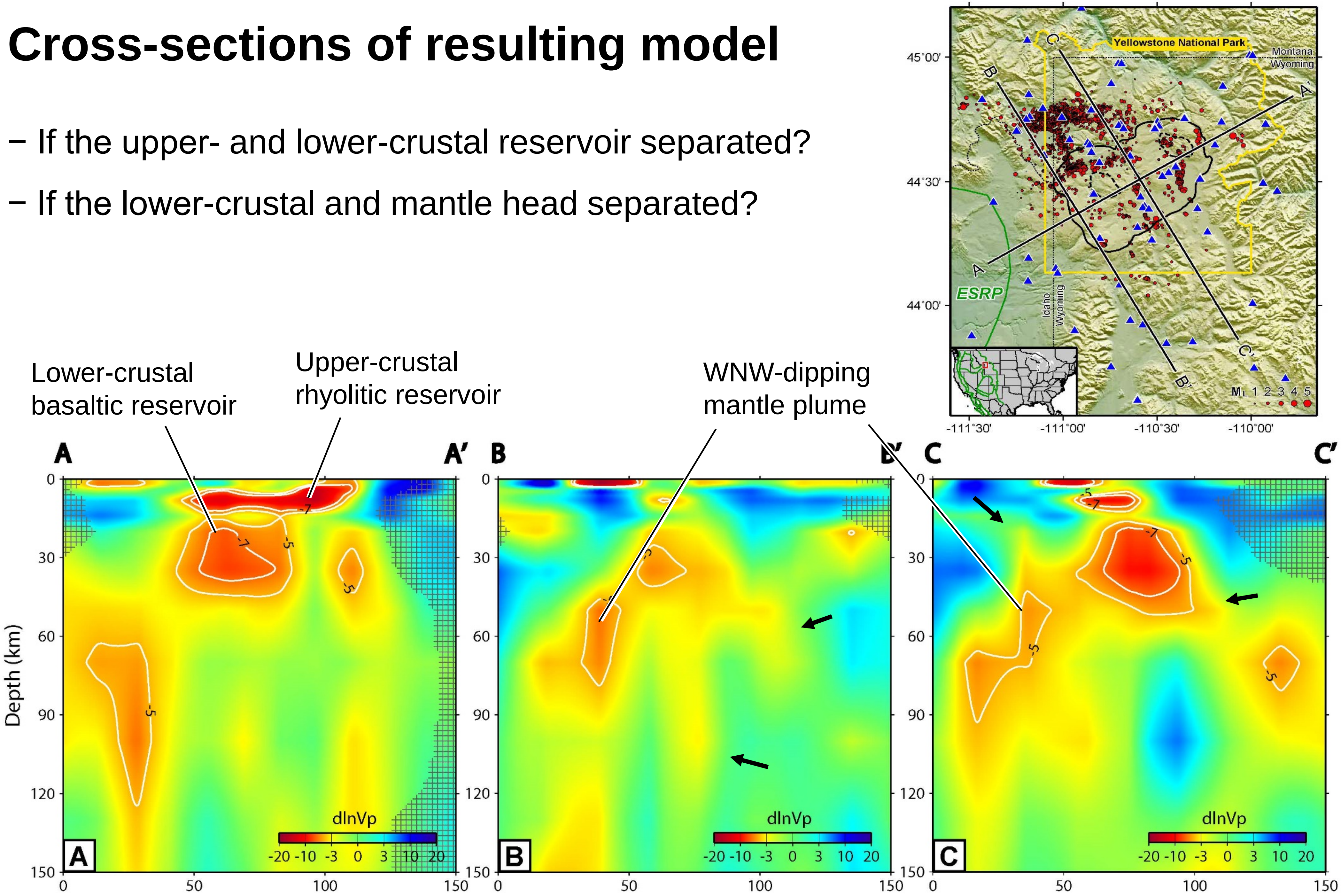

Characteristic model tests

- With lower-crustal low velocity anomaly
- Only joint inversion is capable of resolving a image from the upper crustal to the mantle
- The lower-crustal low velocity anomaly is connected with the plume due to the smearing effect of similar ray incident angles

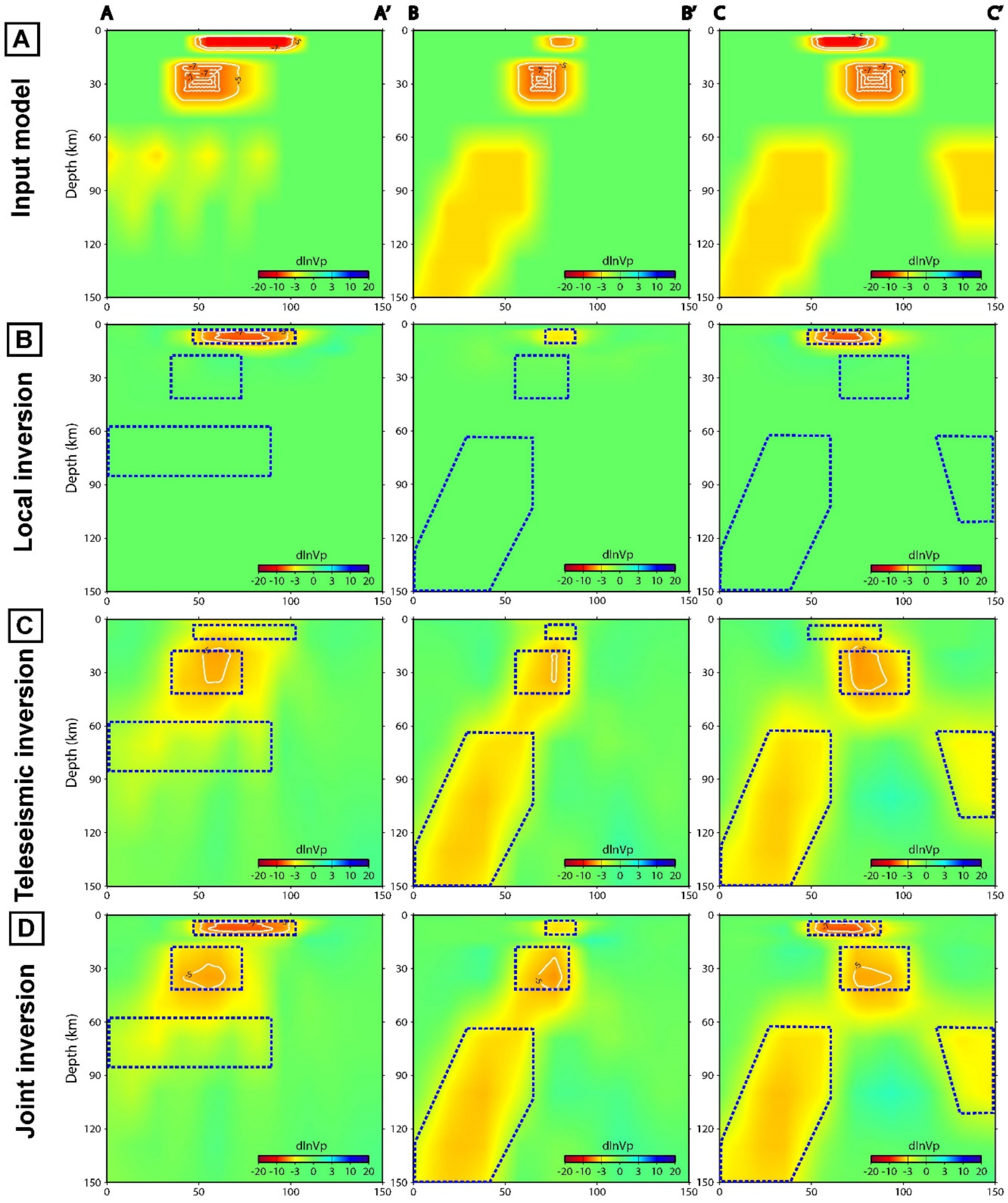

Characteristic model tests

- With noise level of 0.13 s according to the final RMS of travel time residuals of real inversion

- The bottom of the lower crustal anomaly is clearly biased

- Black arrows indicate the smearing artifacts

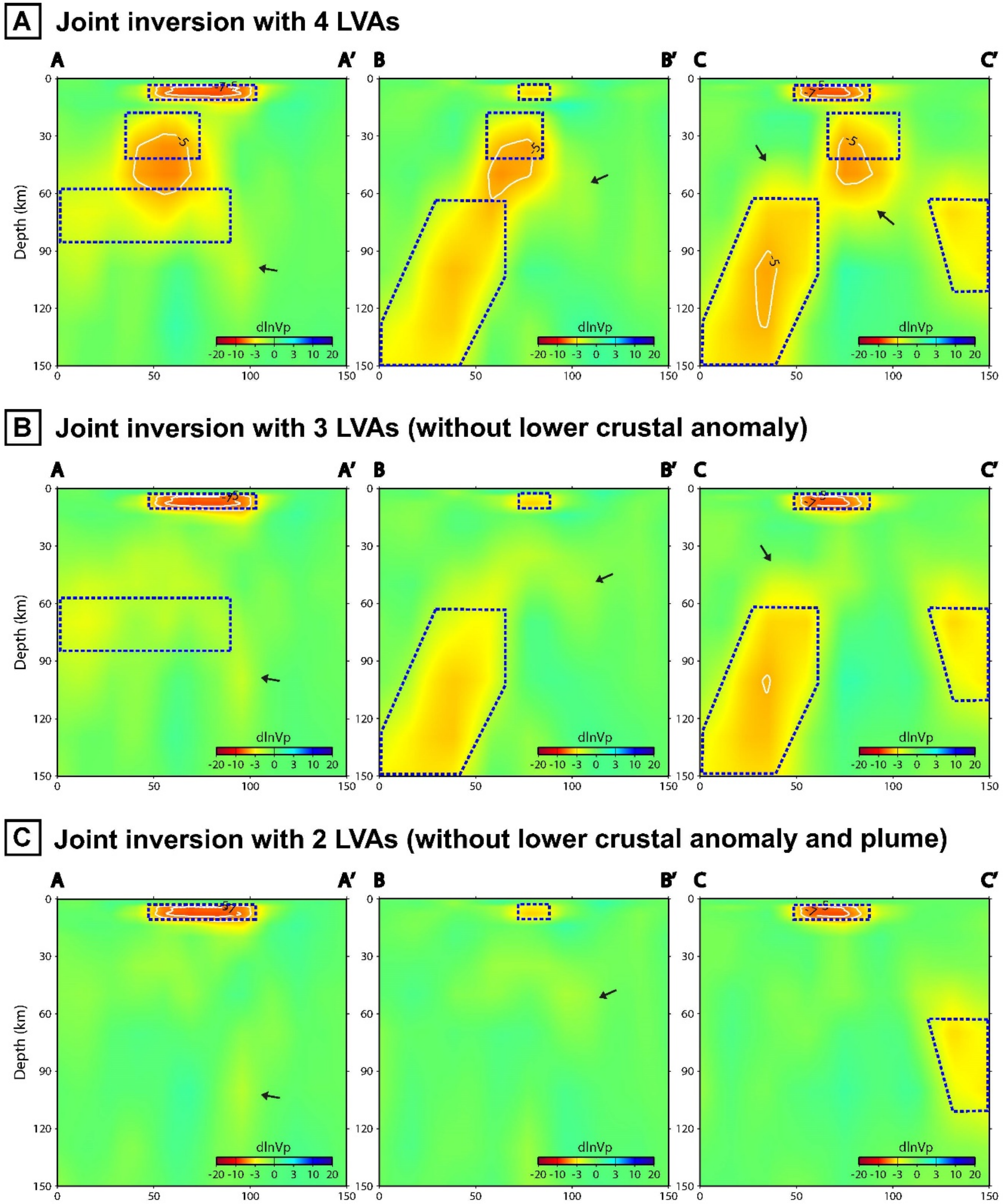

Perspective view of magma bodies

− Isosurfaces of 5% and 3.5% Vp reduction for crustal magma reservoirs and mantle plume

Updated Yellowstone schematic model

Magma body volume (-5% Vp):

– Upper-crustal: ~10,600 km^3

– Lower-crustal: ~46,500 km^3

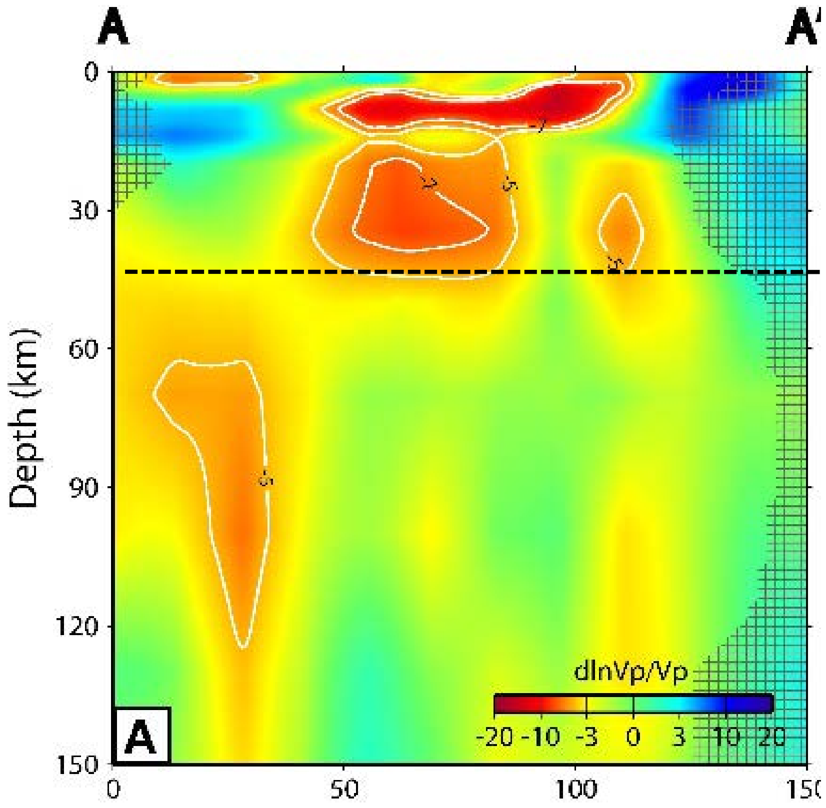

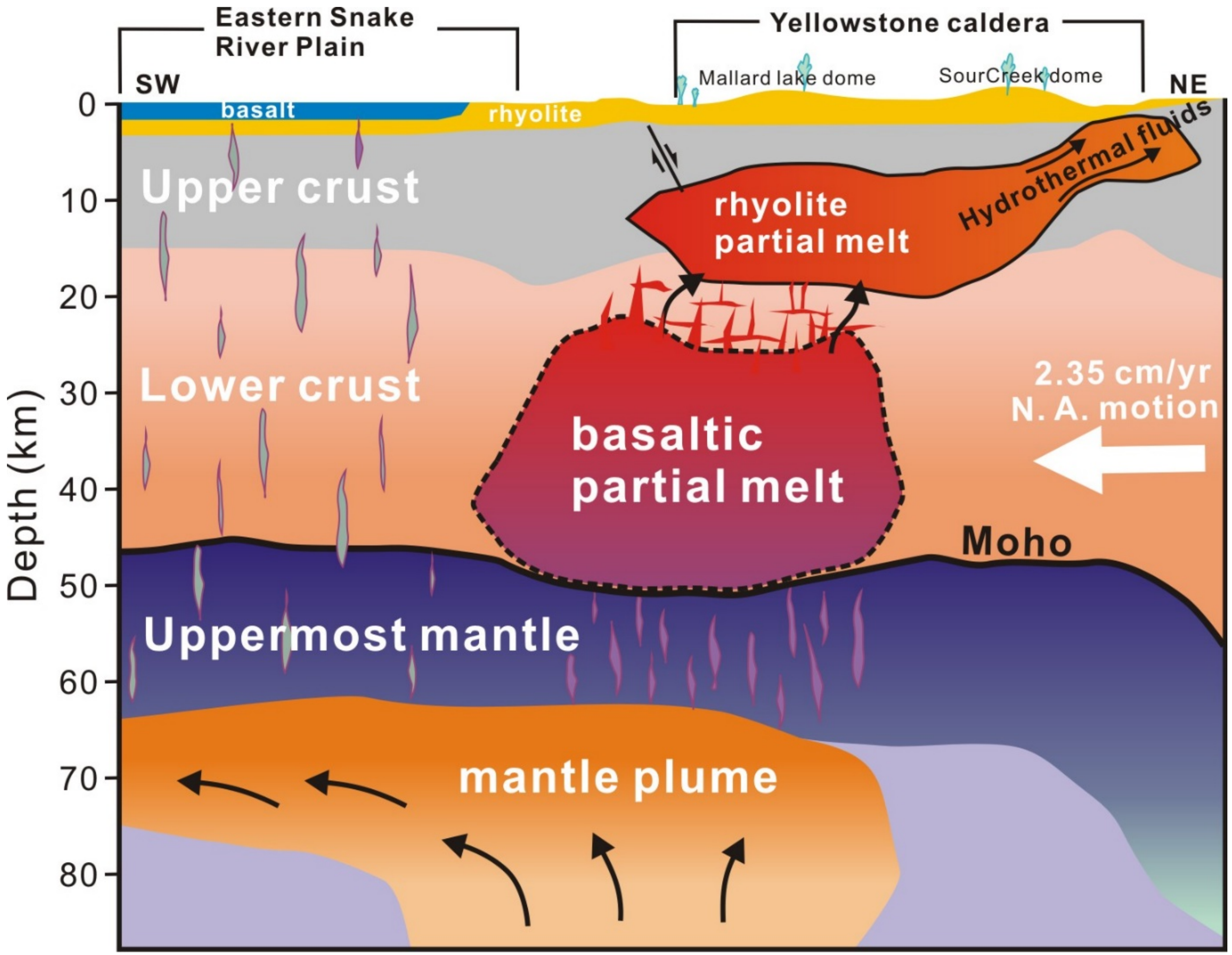

Seismological constraints on CO_2 emission

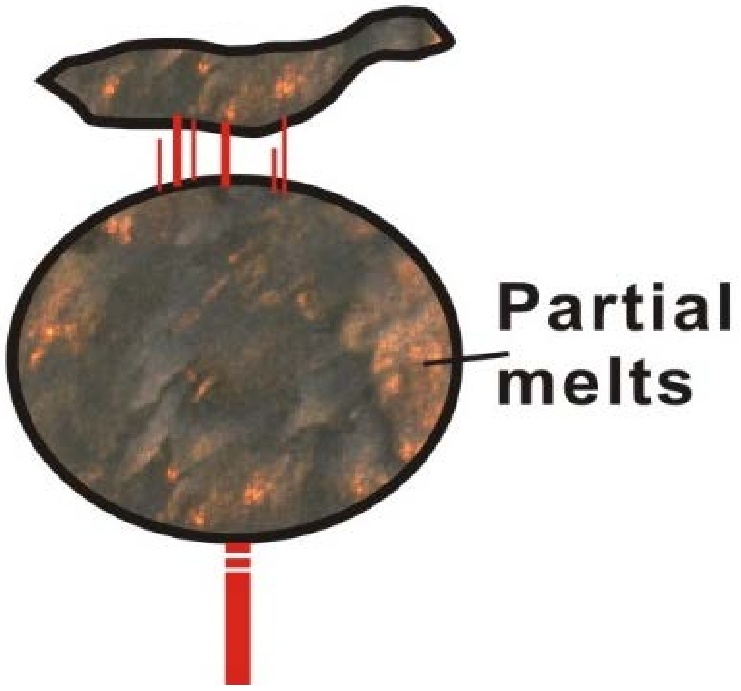

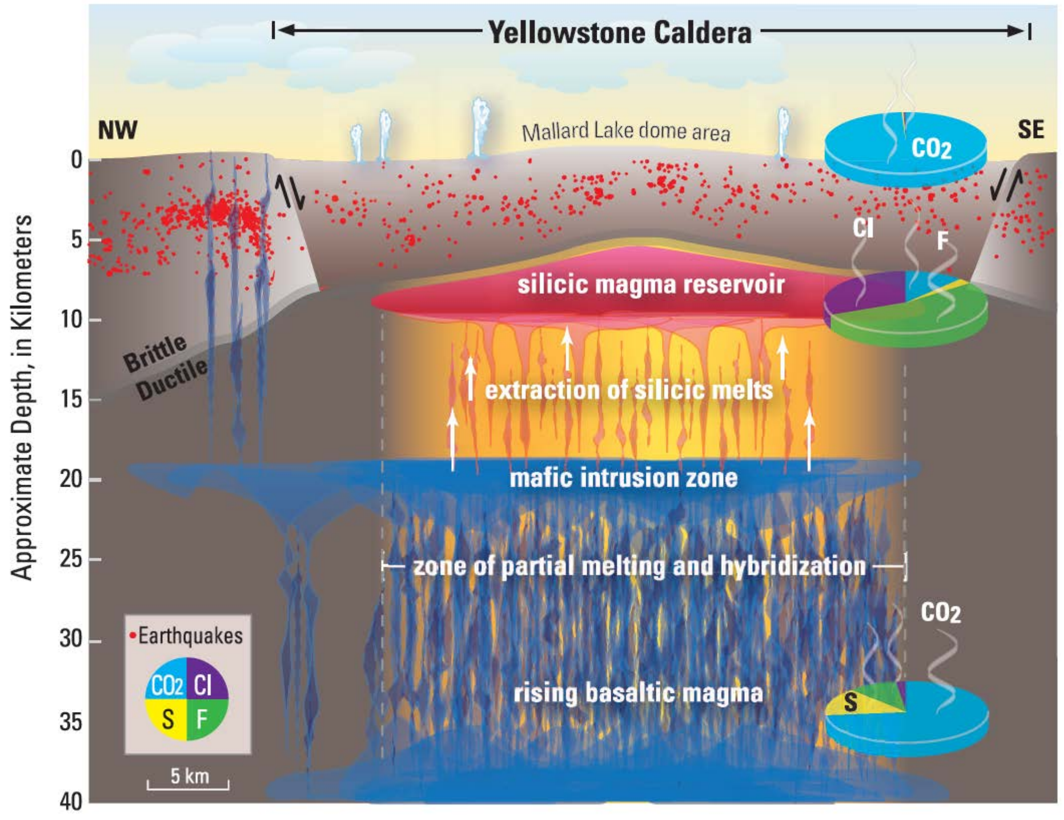

From the study of Werner and Brantley (2003):

→ Annual emission rate of CO_2 from subsurface magma is **8.21×10^{10} kg/yr**

Magma type	Density (kg/km^3)	CO_2 abundance in the melts (ppm)
Basalt	2.9×10^{12} *(28)*	10,000 *(7)*
Rhyolite	2.2×10^{12} *(14)*	400 *(7)*

$$M_{CO_2} = M_{melt} \times r = D_{melt} \times V_{melt} \times r$$

To calculate the melt fraction (and volume)

- Absolute Vp vs. rhyolitic melt fraction

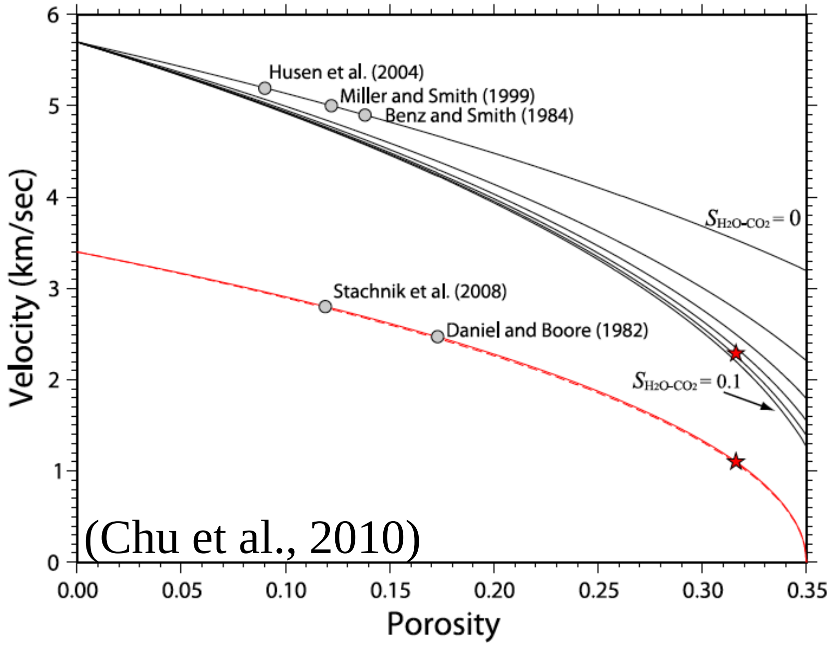

- Vp perturbation vs. basaltic melt fraction

$-\partial \ln V_P/dF$	Melt inclusion description
1.23	Unrelaxed state, dihedral angle typical (*45*)
2.9	Unrelaxed state, organized cuspate shape (*44*)
3.6	Relaxed state, organized cuspate shape (*44*)

[44] Hammond and Humphreys, 2000; [45] Kreutzmann et al., 2004

Upper-crustal reservoir:

− Rhyolite-granite system

− Average Vp of 5.21 km/s

→ ~9% melt fraction

→ 950 km^3 rhyolitic melts

Lower-crustal reservoir:

− Basalt-olvine system

− Average dVp of 6.56%

→ 2-5% melt fraction

→ 930 km^3 basaltic melts

Seismological constraints on CO_2 emission

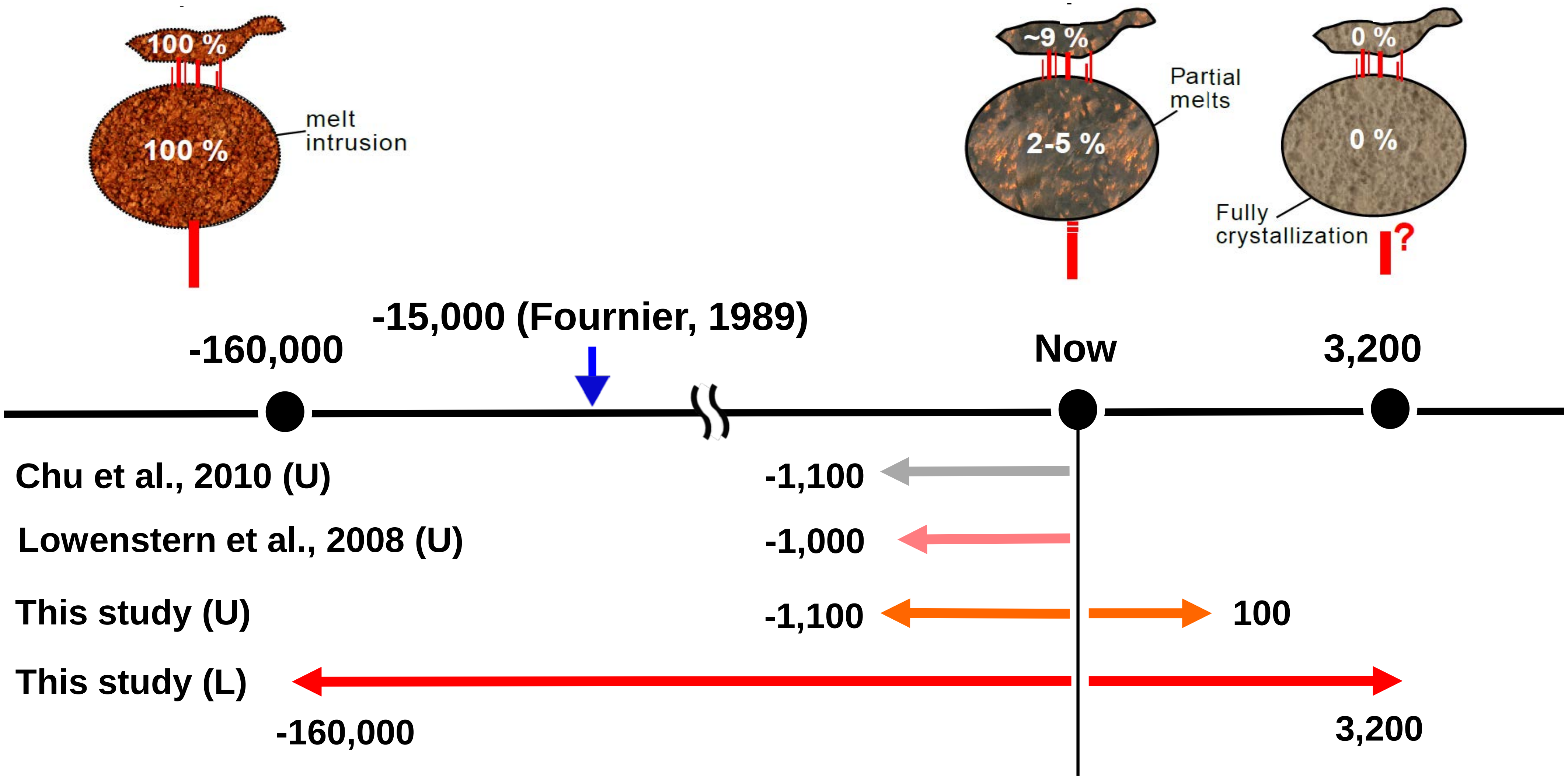

*The high intensity of Yellowstone hydrothermal system has been suggested to last since at least ~15,000 years ago or earlier (Fournier, 1989)

Conclusions

The addition of lower-crustal magma reservoir can help explain the abnomrally large CO2 outflux at Yellowstone

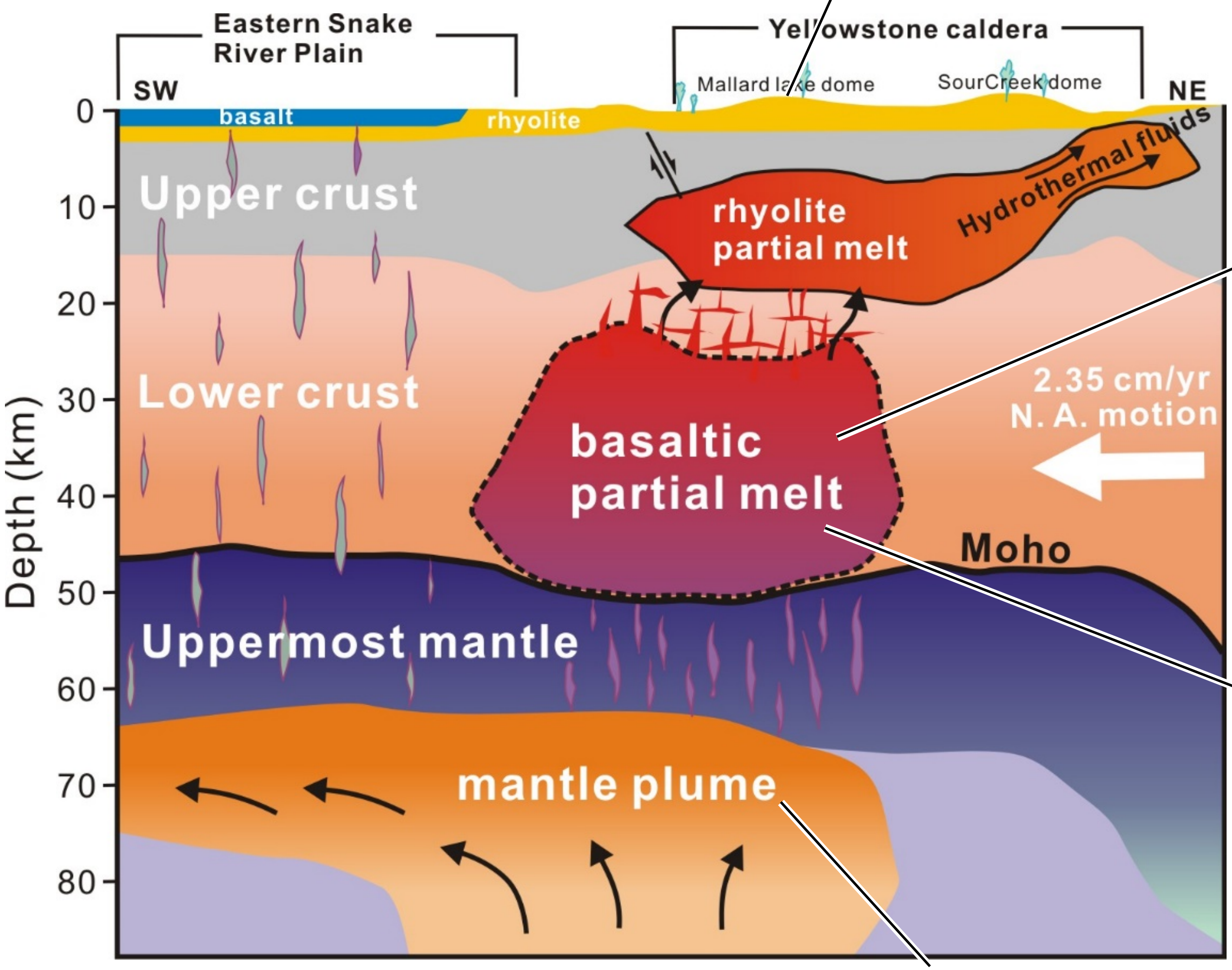

The first image showing entire crustal magmatic system beneath Yellowstone

This model may be representative of other bimodal basaltic-rhyolitic volcanoes around the world

The discovered lower-crustal magma reservoir provides a magmatic link between upper-crustal reservoir and mantle plume

Toward the center of the Earth

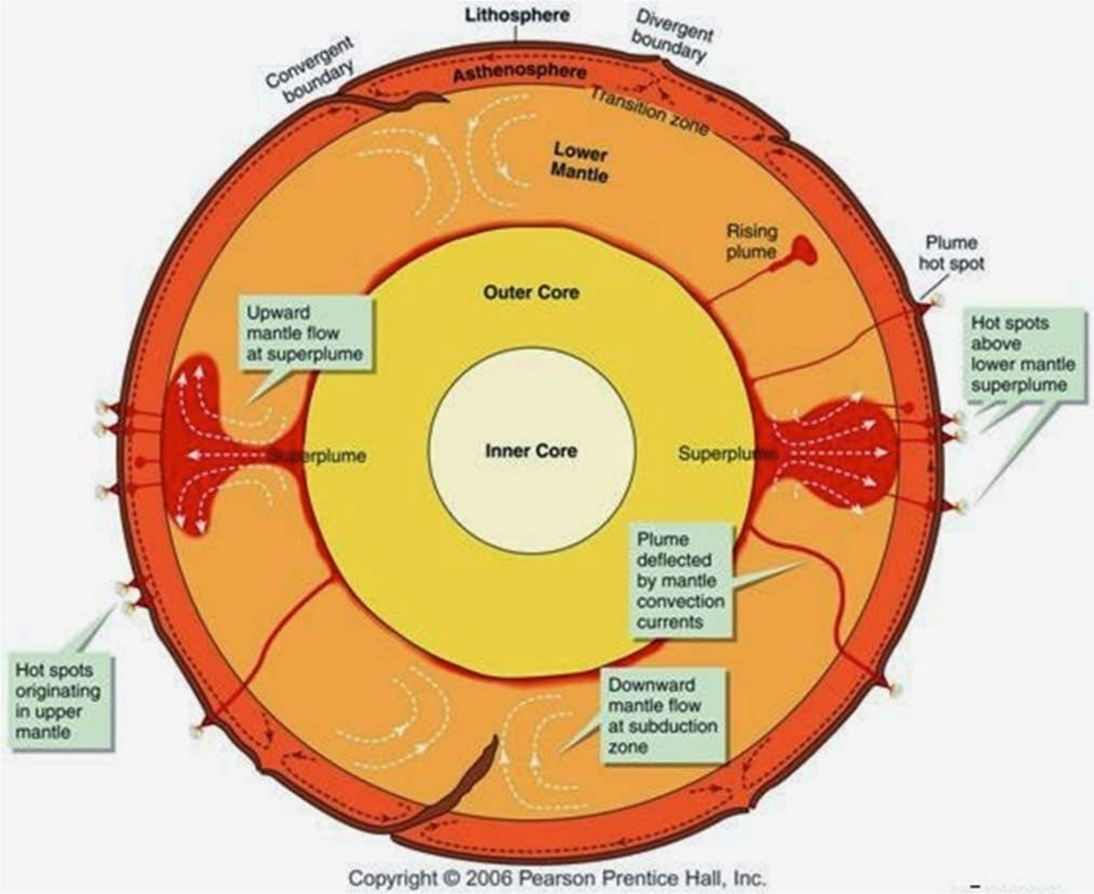

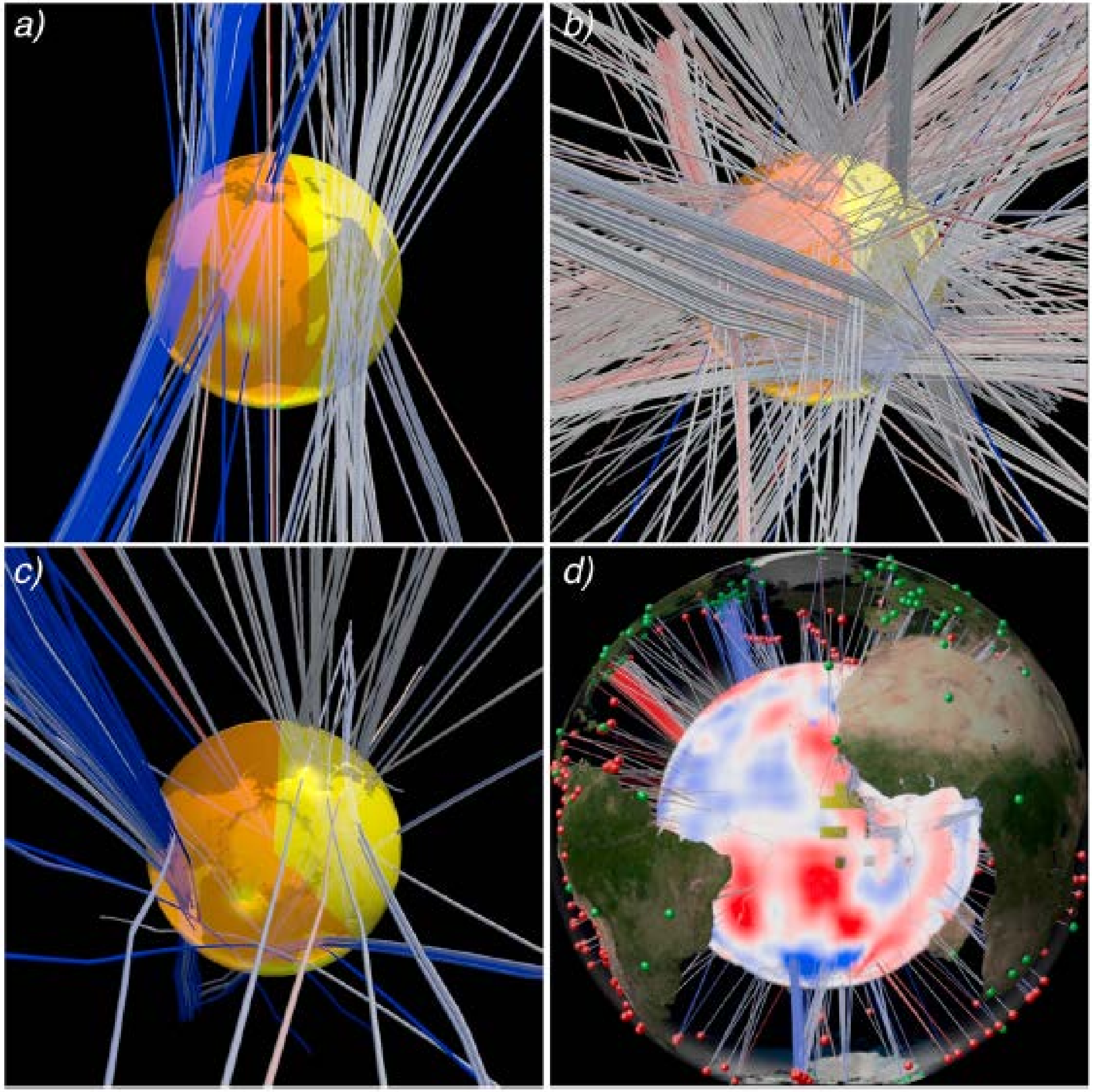

(Tkalcic, 2015)

Seismic interferometry

– Retrieving the Green's function between arbitrary two stations from cross-correlating the ambient noise data

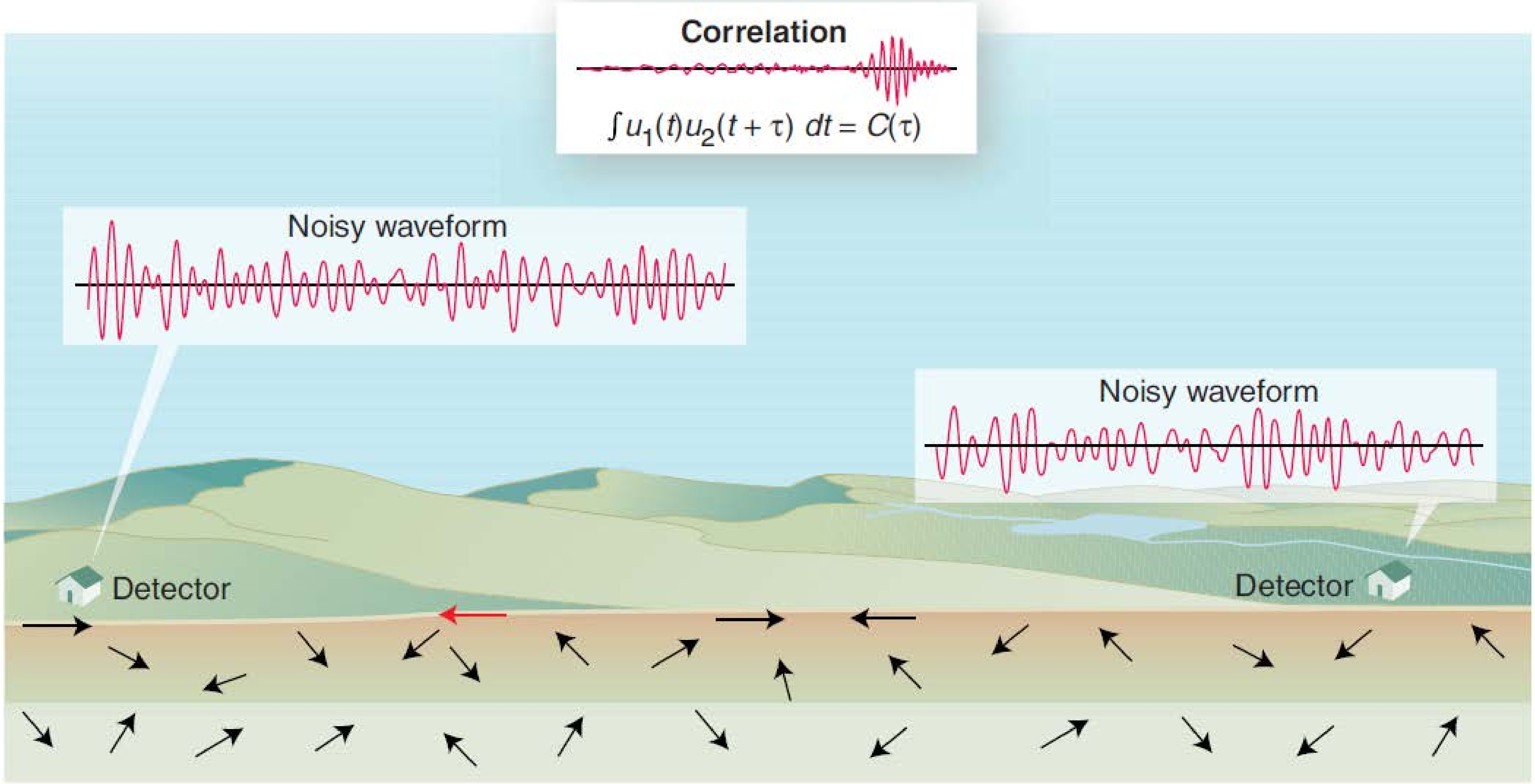

(Weaver, 2004)

Seismic interferometry

– How this actually works..

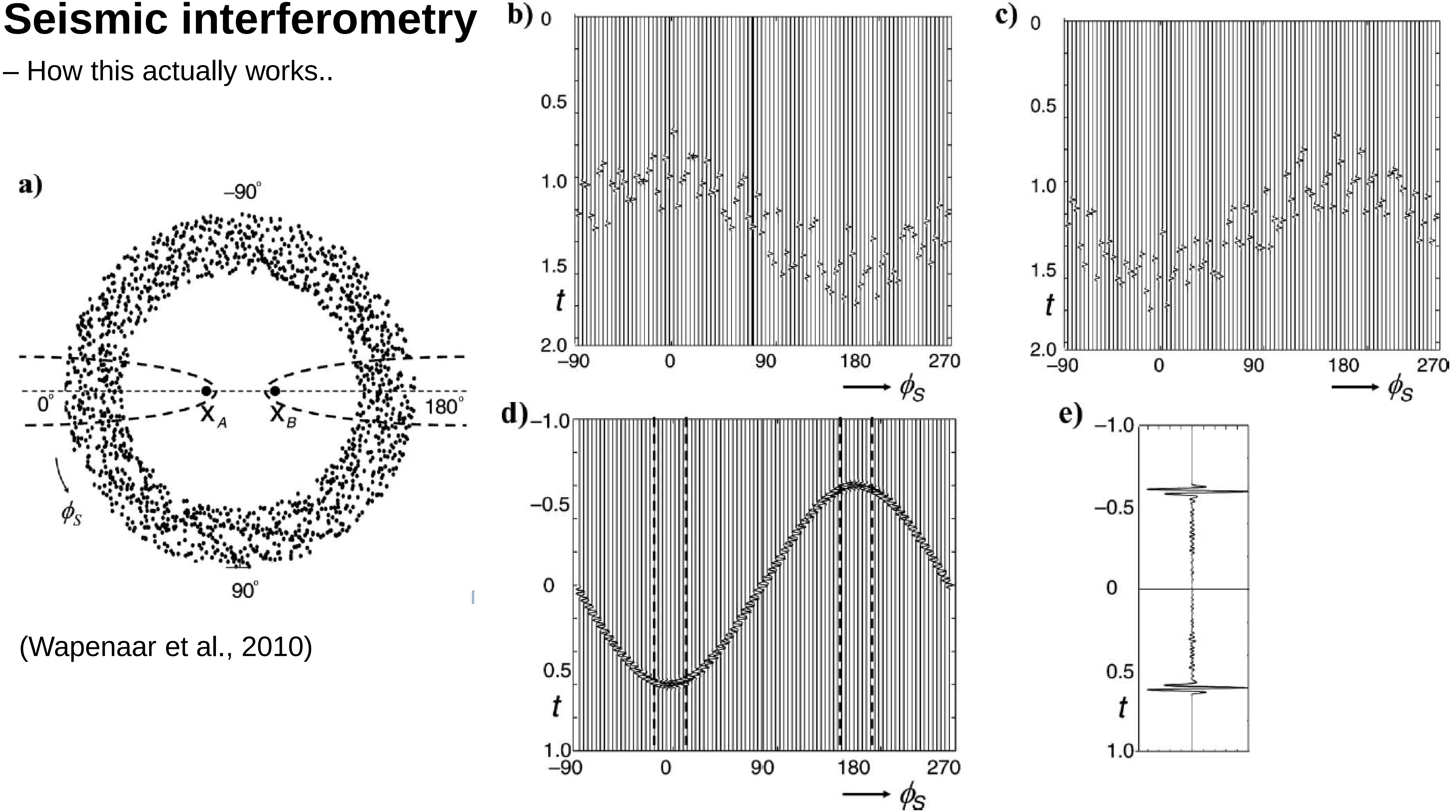

(Wapenaar et al., 2010)

Seismic interferometry

– **Surface wave**

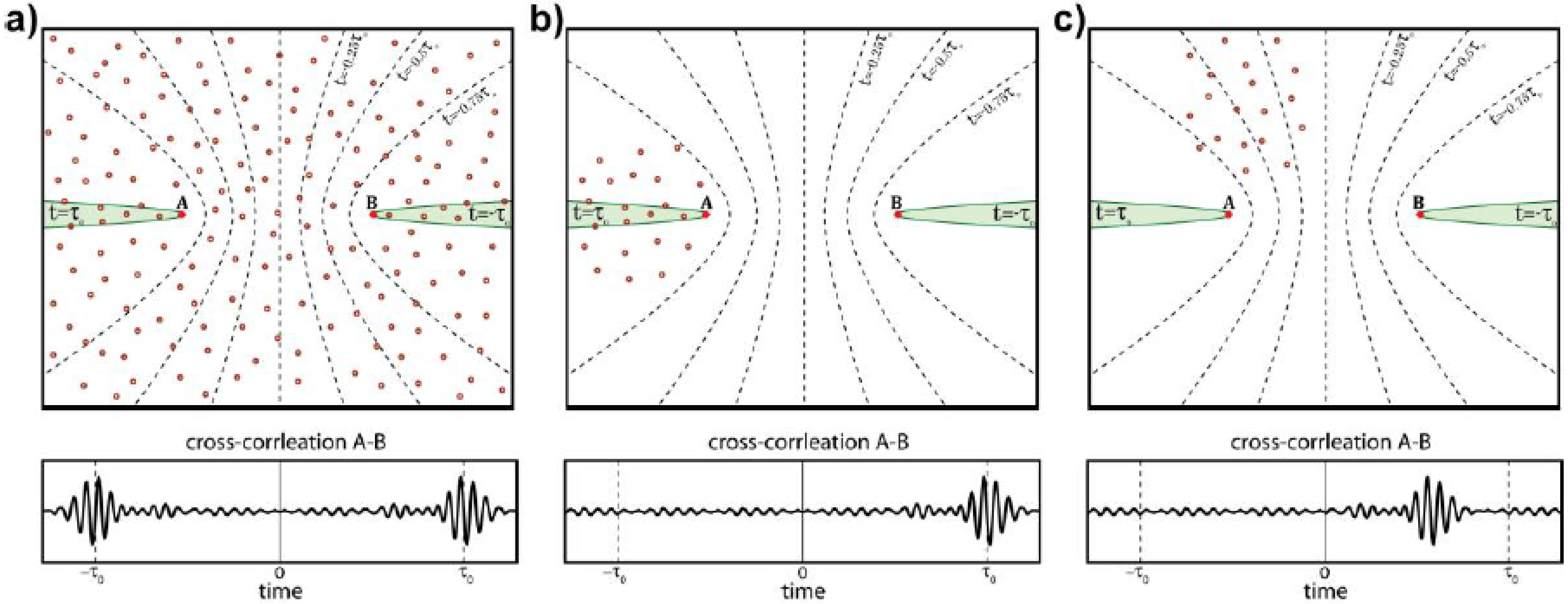

– **Body wave**

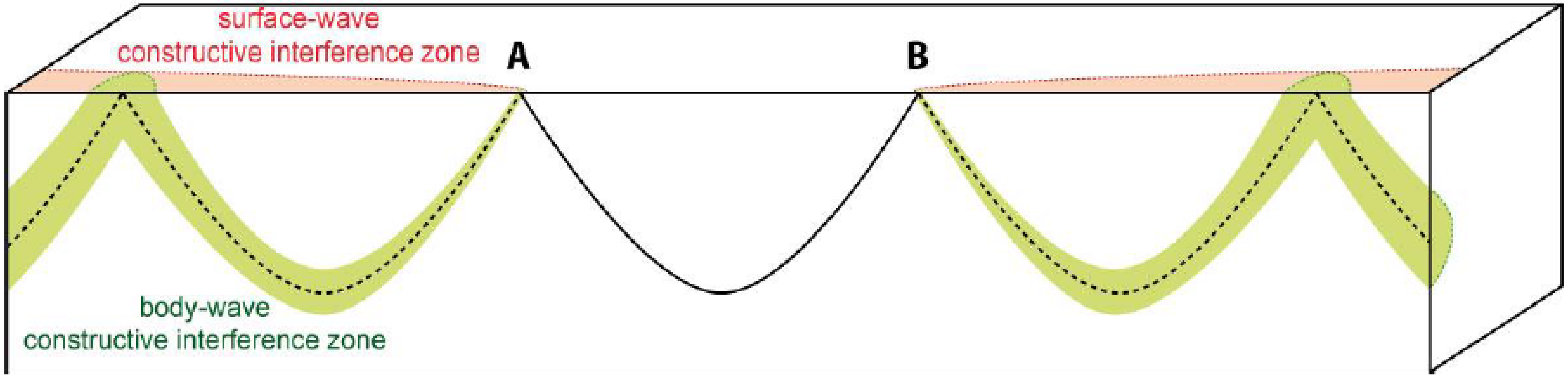

(Shapiro et al., 2015)

Recent development of seismic interferometry

– Not only surface wave, but also body wave

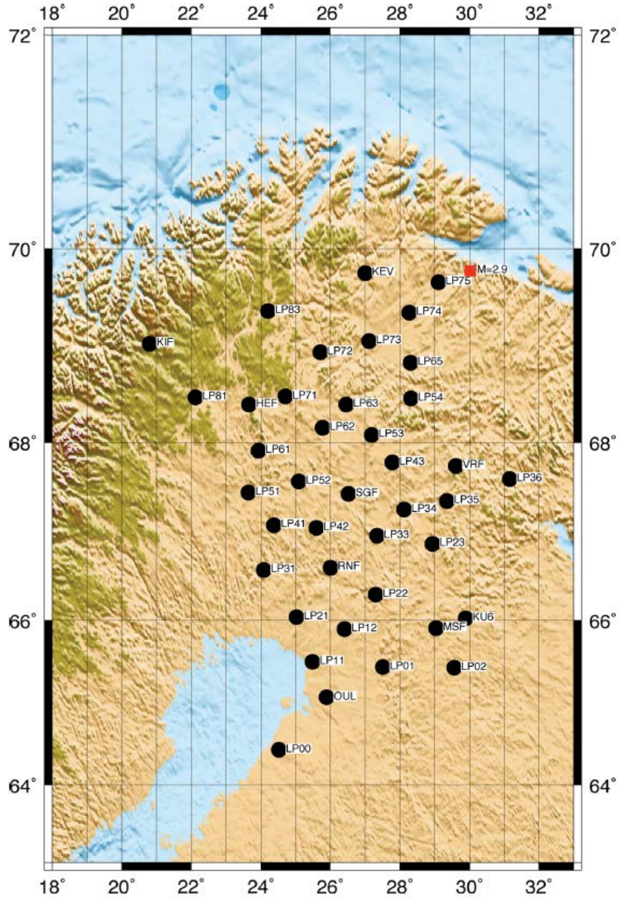

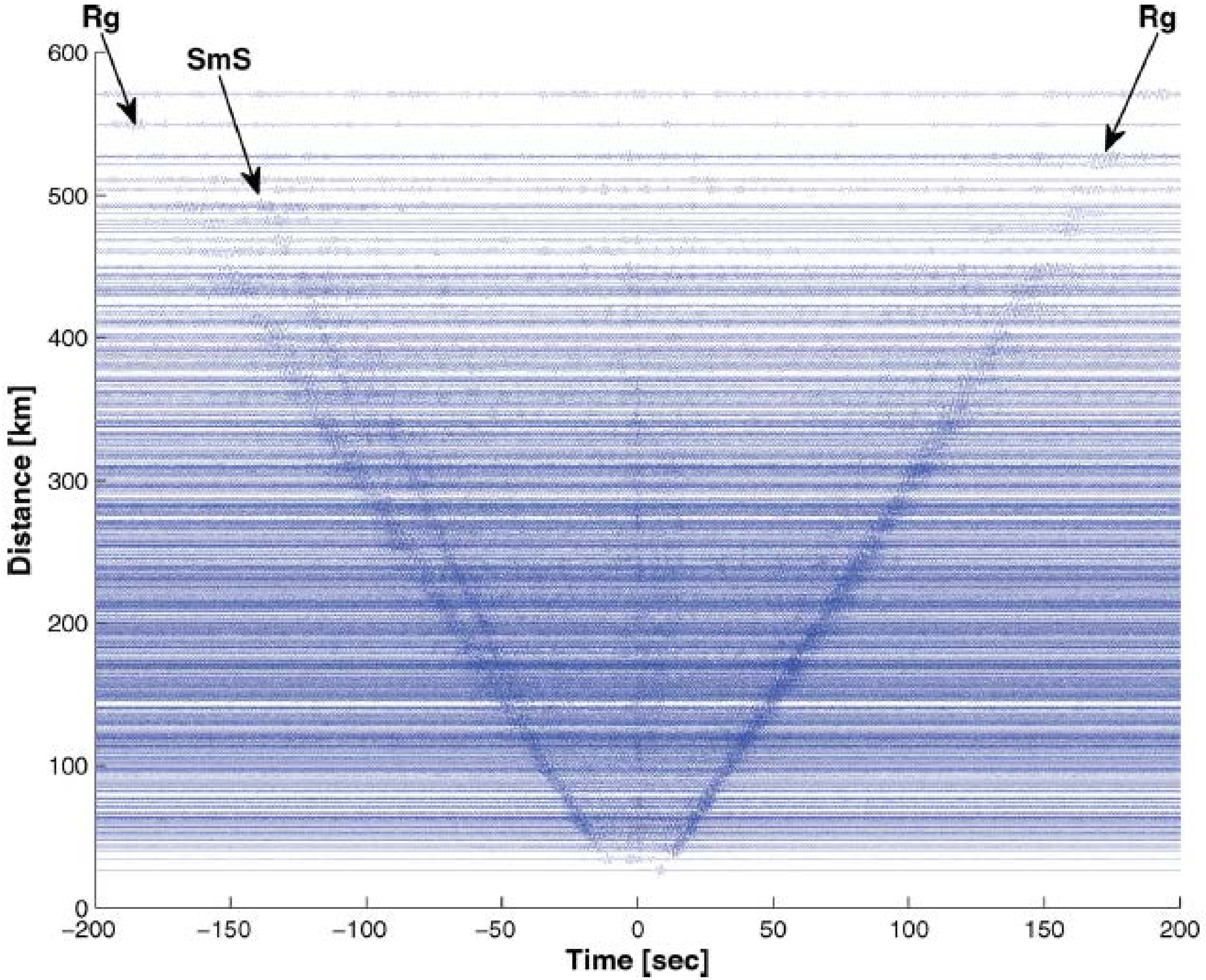

(Poli et al., 2012)

Recent development of seismic interferometry

– Not only surface wave, but also body wave

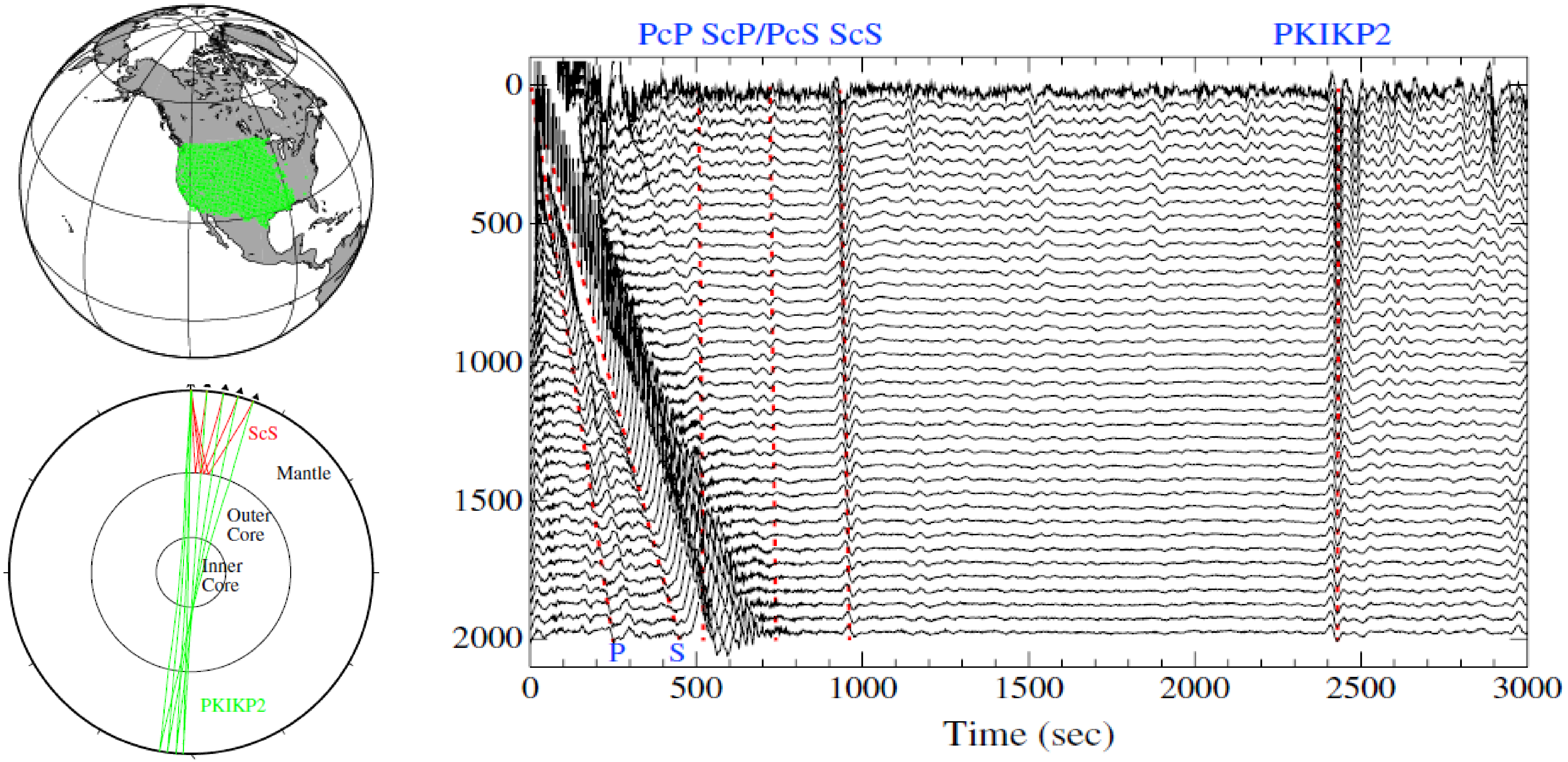

(Lin et al., 2013)

Recent development of seismic interferimetry

– good correlation with the occurrence of large earthquakes, implying that the energy may come from earthquake coda (reverberations)

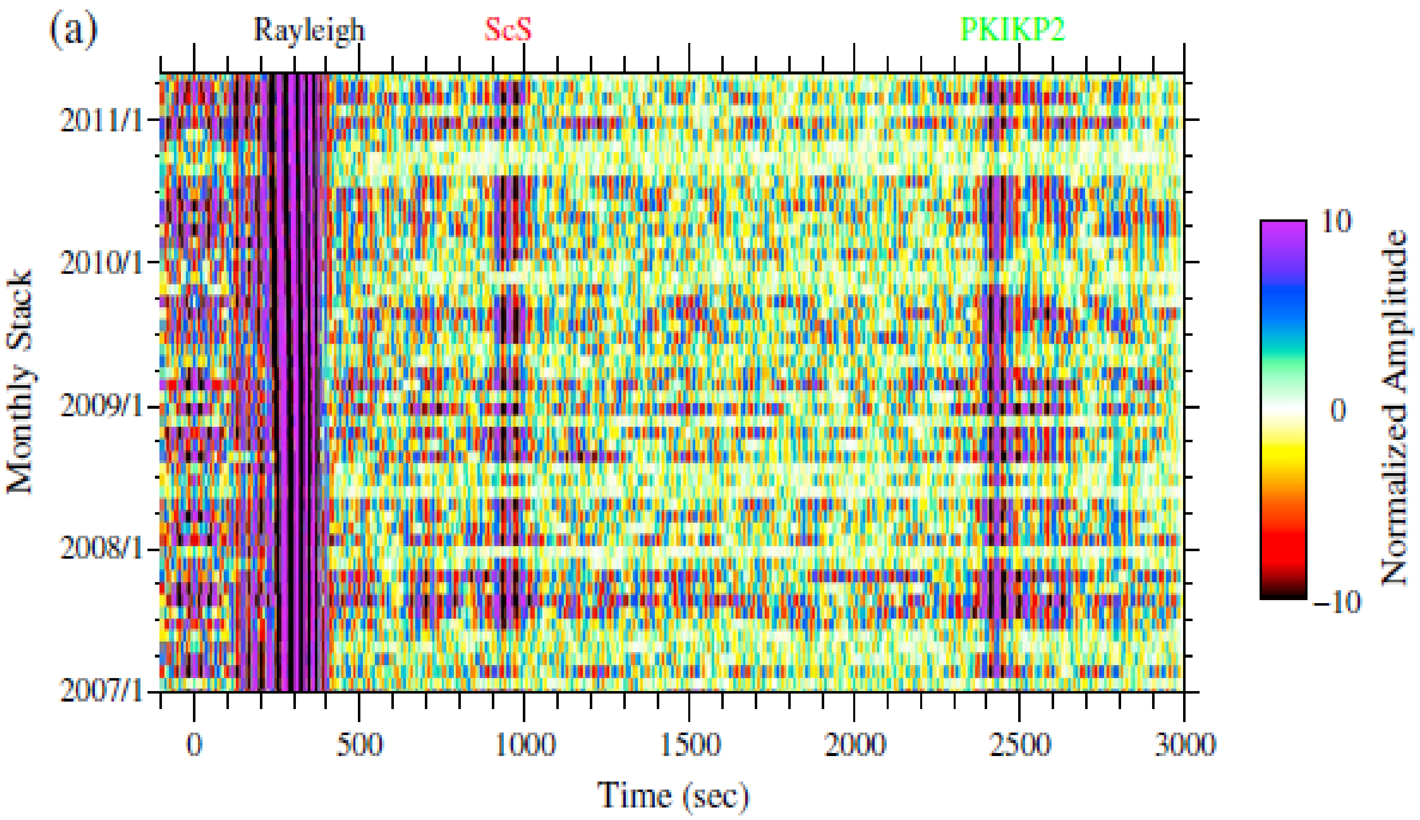

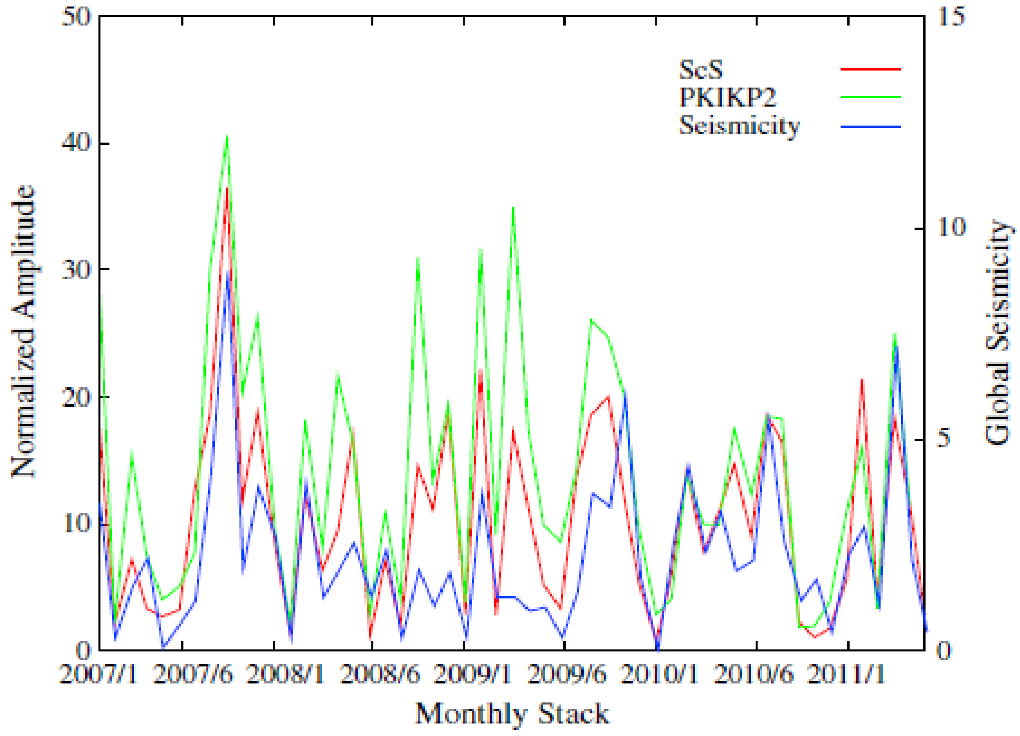

(Lin et al., 2013)

Tohoku global wavefiled simulation

Earthquake coda interferometry

– Temporal normalization (15-50 s) & Spectral wightening (5-800 s)

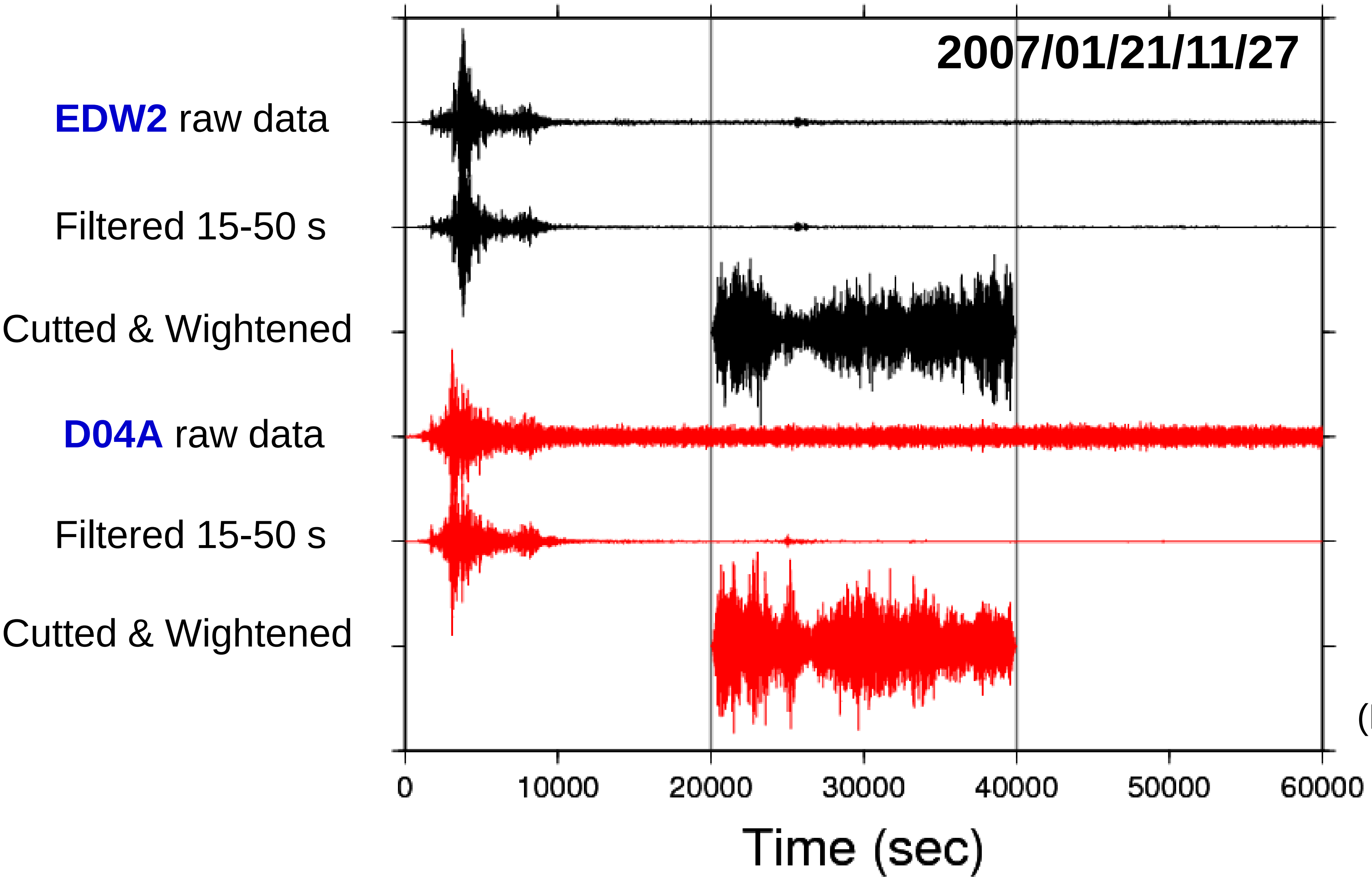

(Huang et al., 2015)

Neighborhood stacking with a radius R

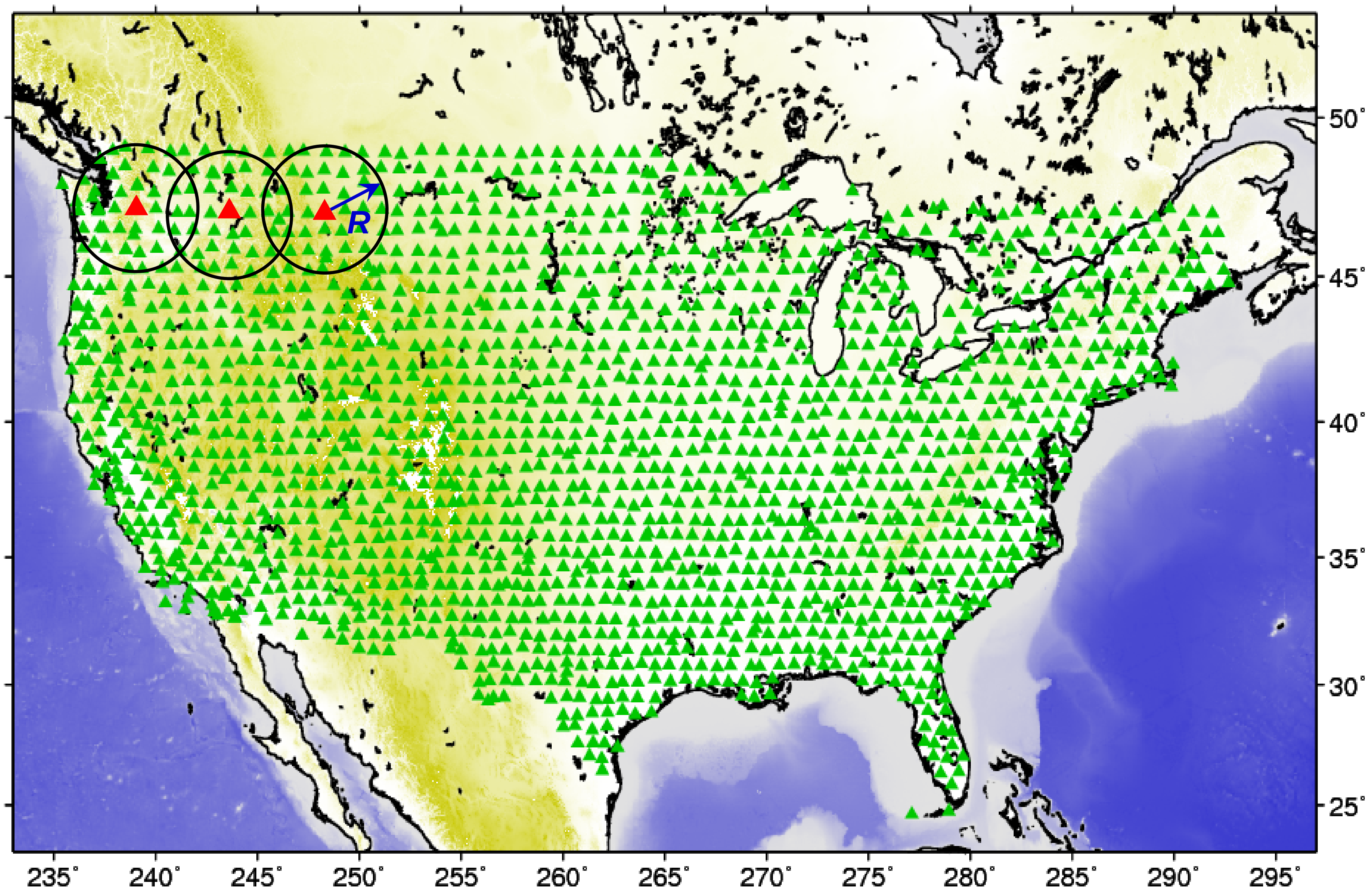

Examples of using radius of 0, 300 km, and measurements

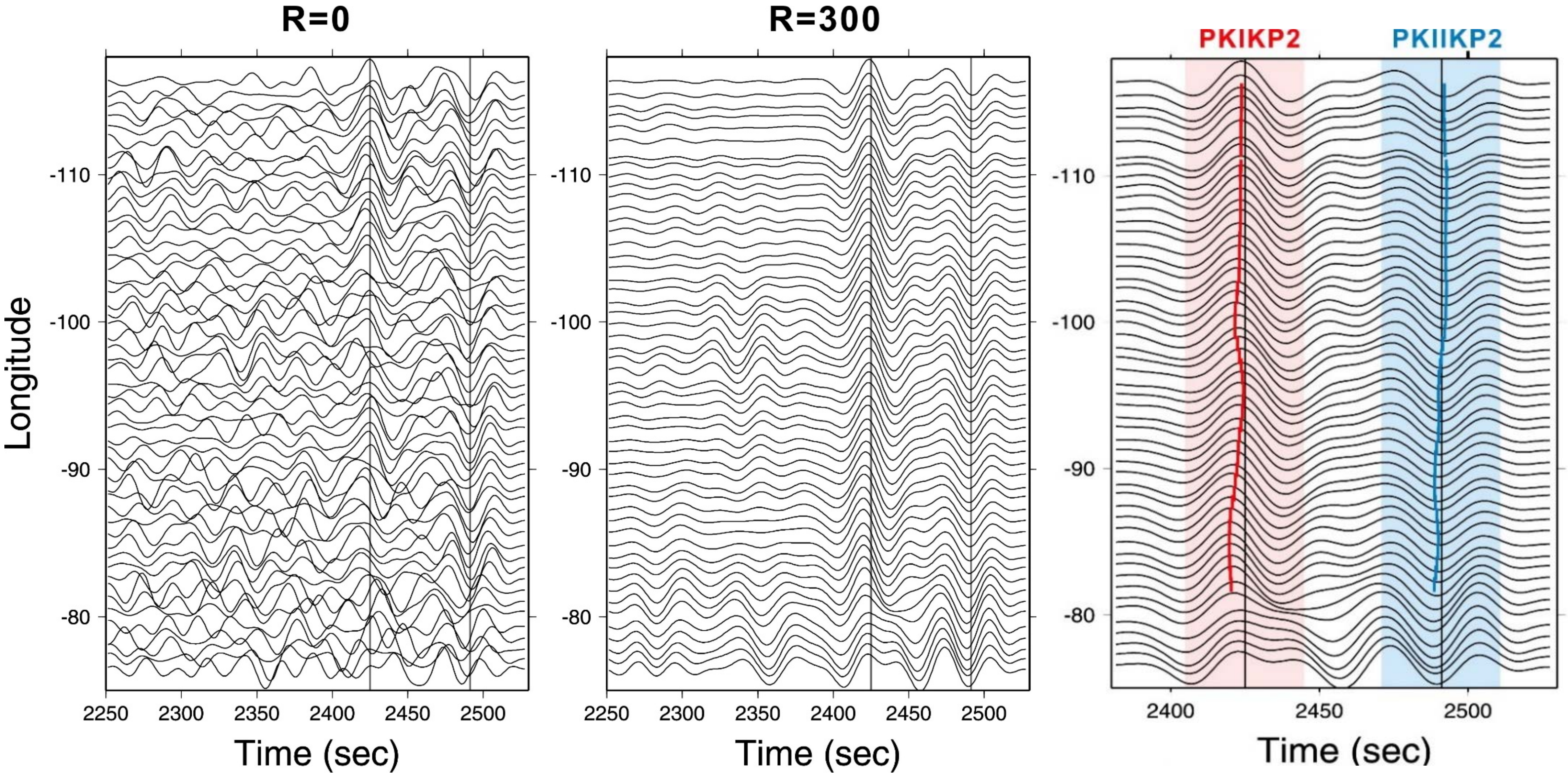

Relative travel time residuals of PKIKP2 and PKIIKP2

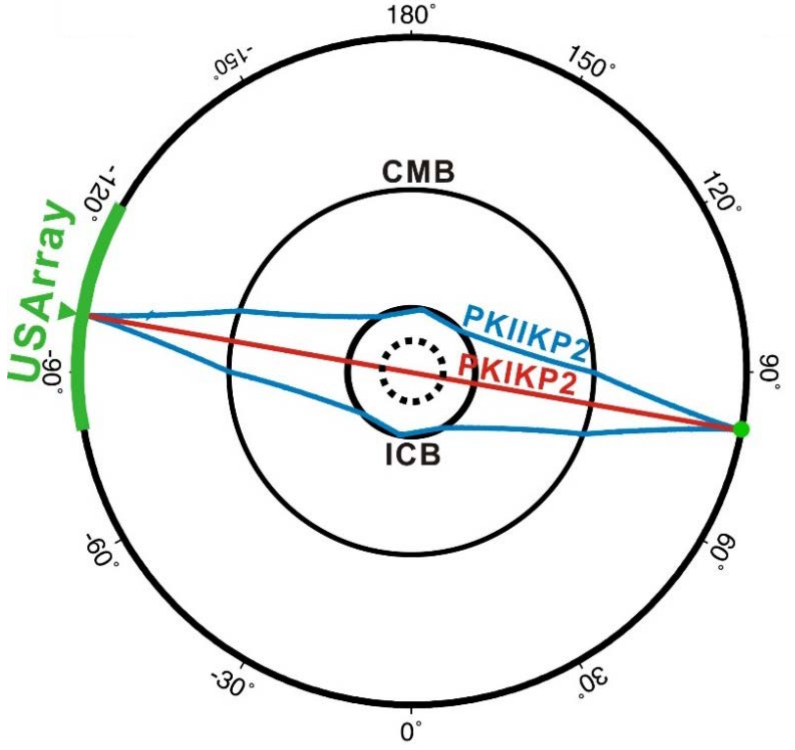

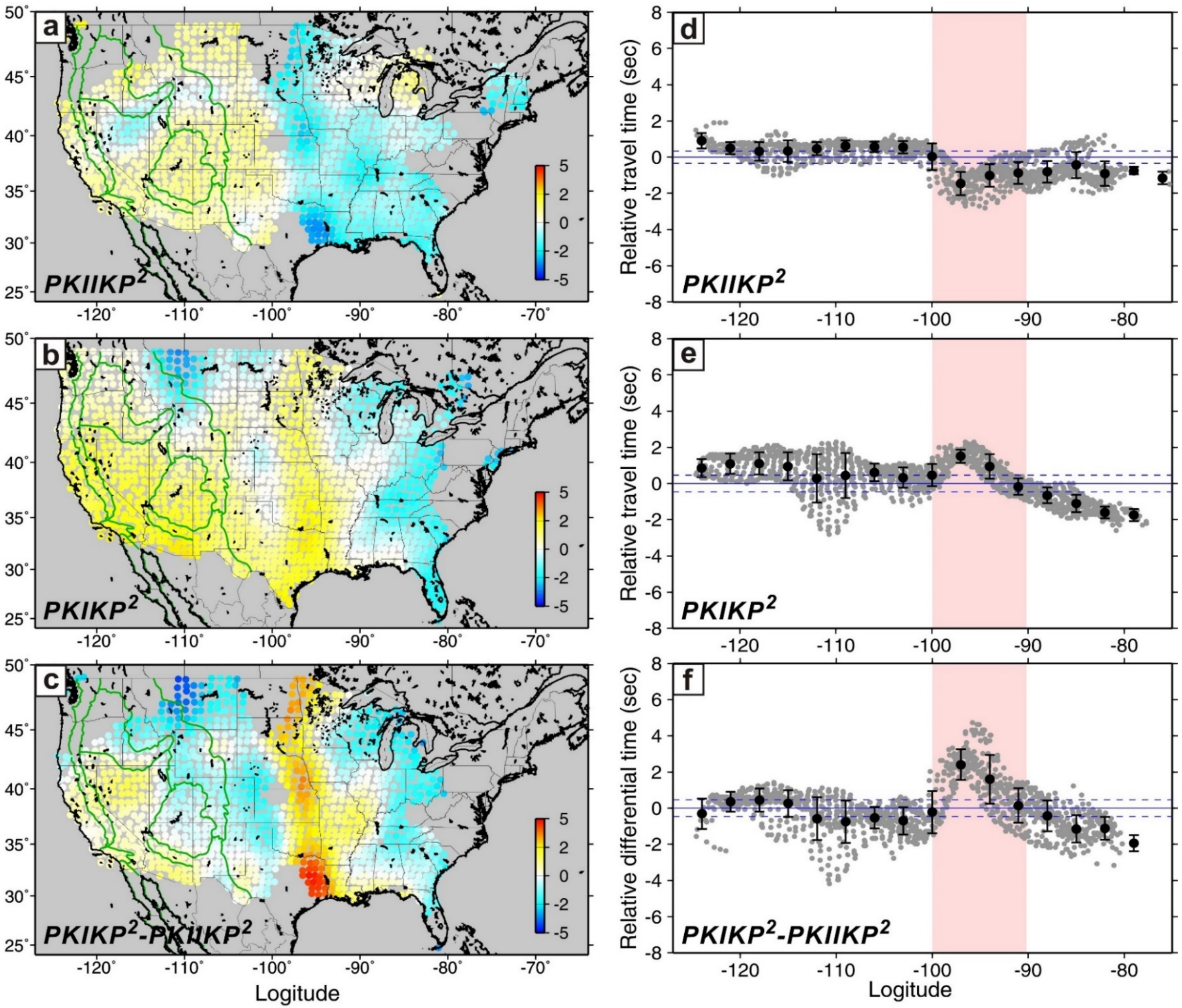

Where the possible anomaly sources are?

– Most likely from inner core, maybe possibly from lowermost mantle

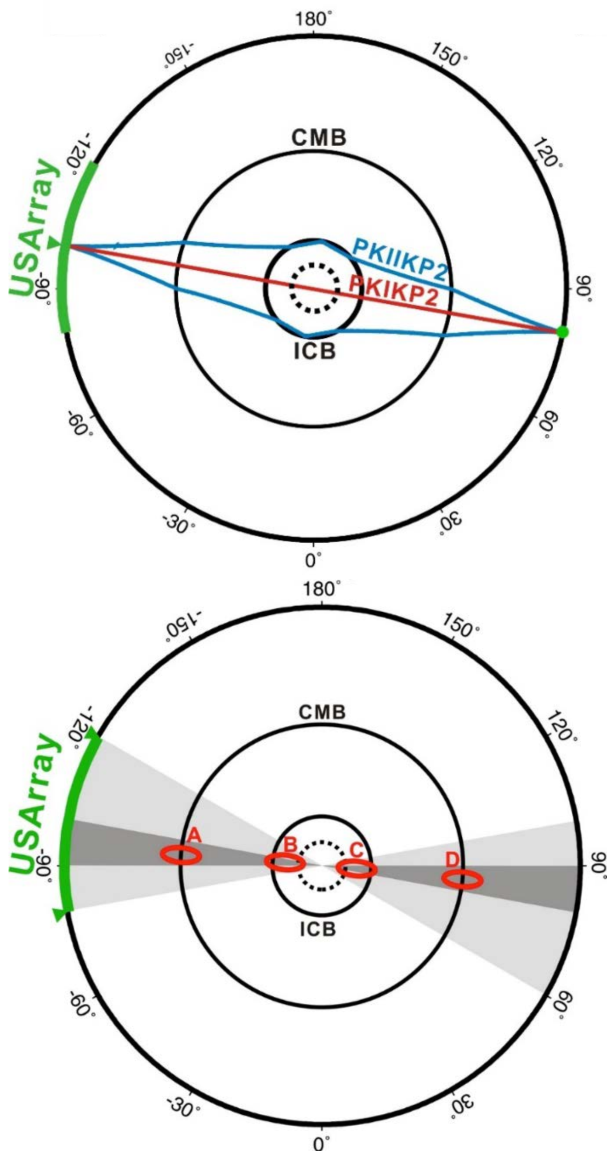

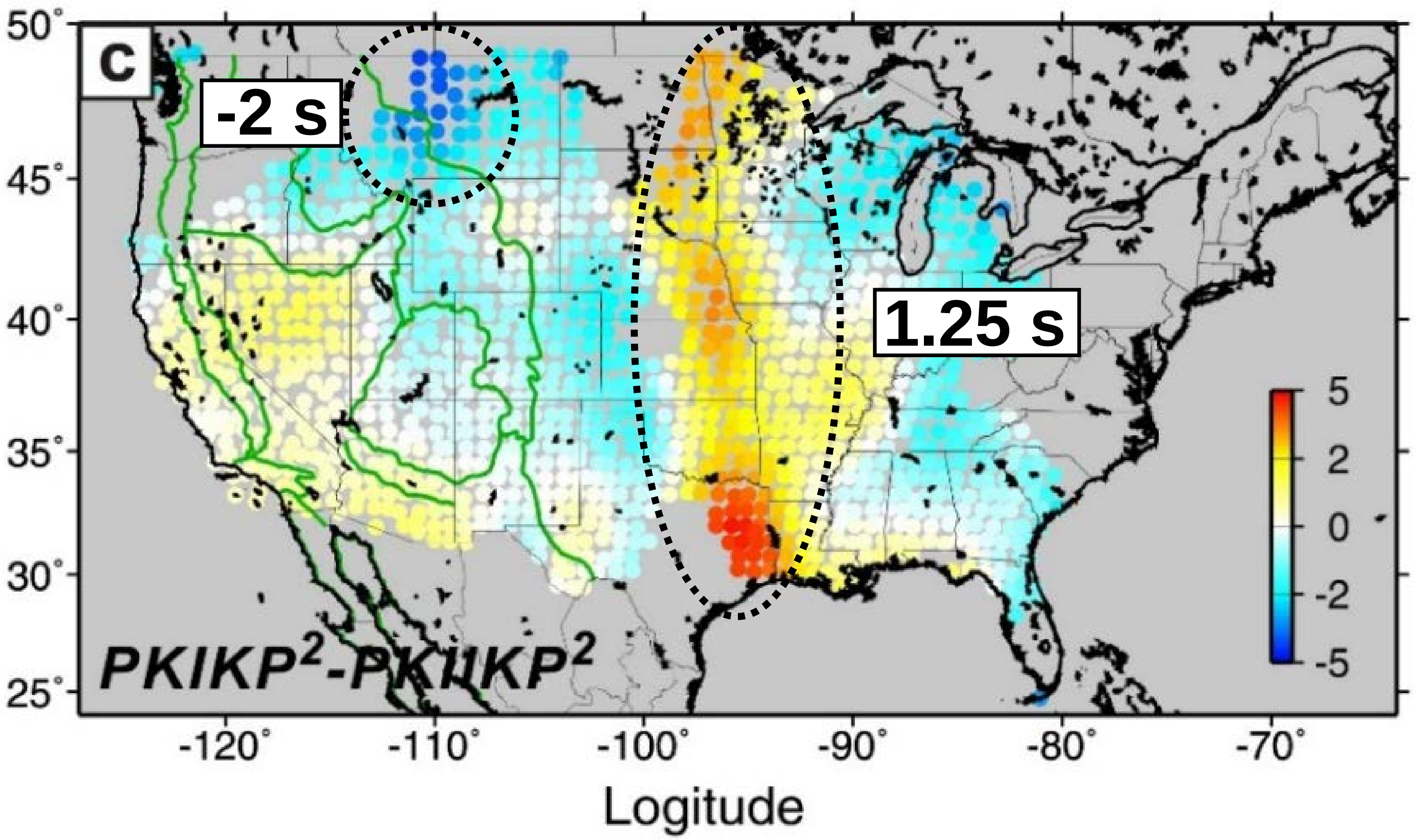

Possible anomaly sources

Anomaly size

$$dt = -\left(\frac{dv}{v}\right)\left(\frac{dl}{v}\right)$$

Velocity perturbation

Background velocity

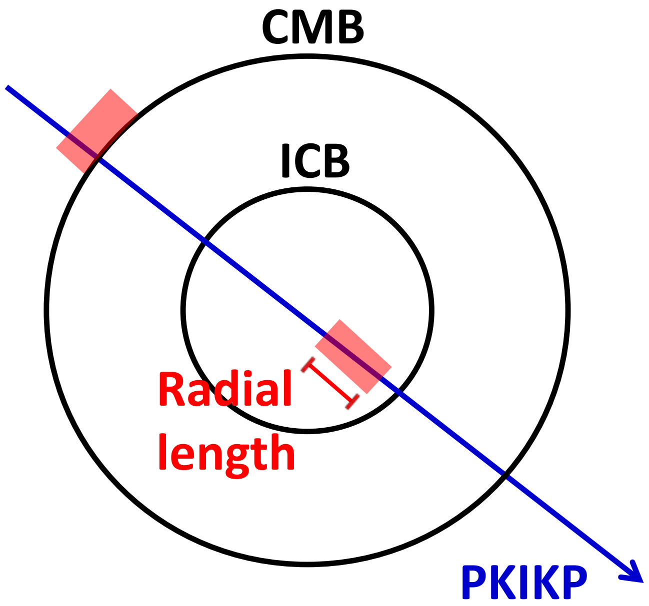

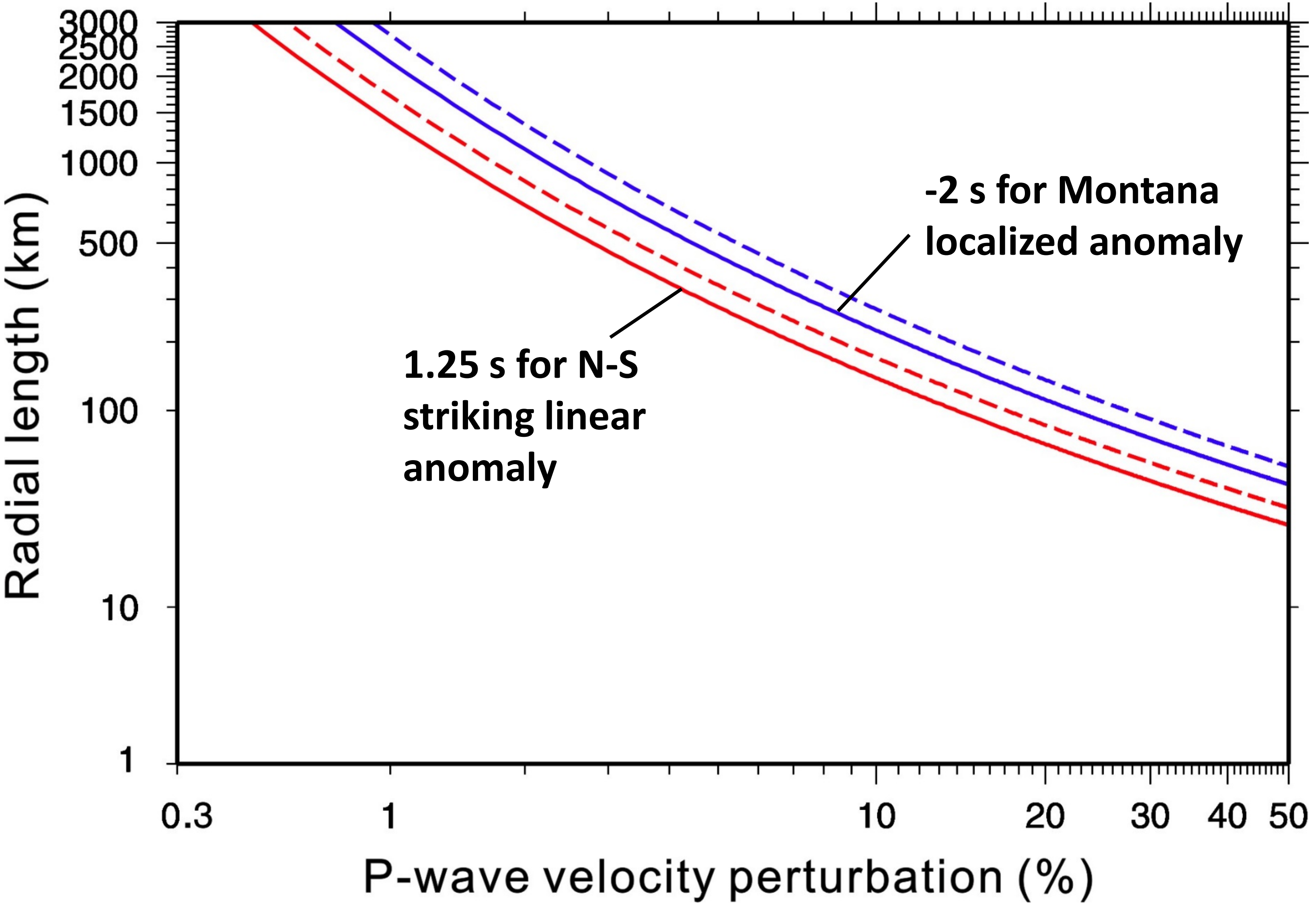

Possible anomaly sources

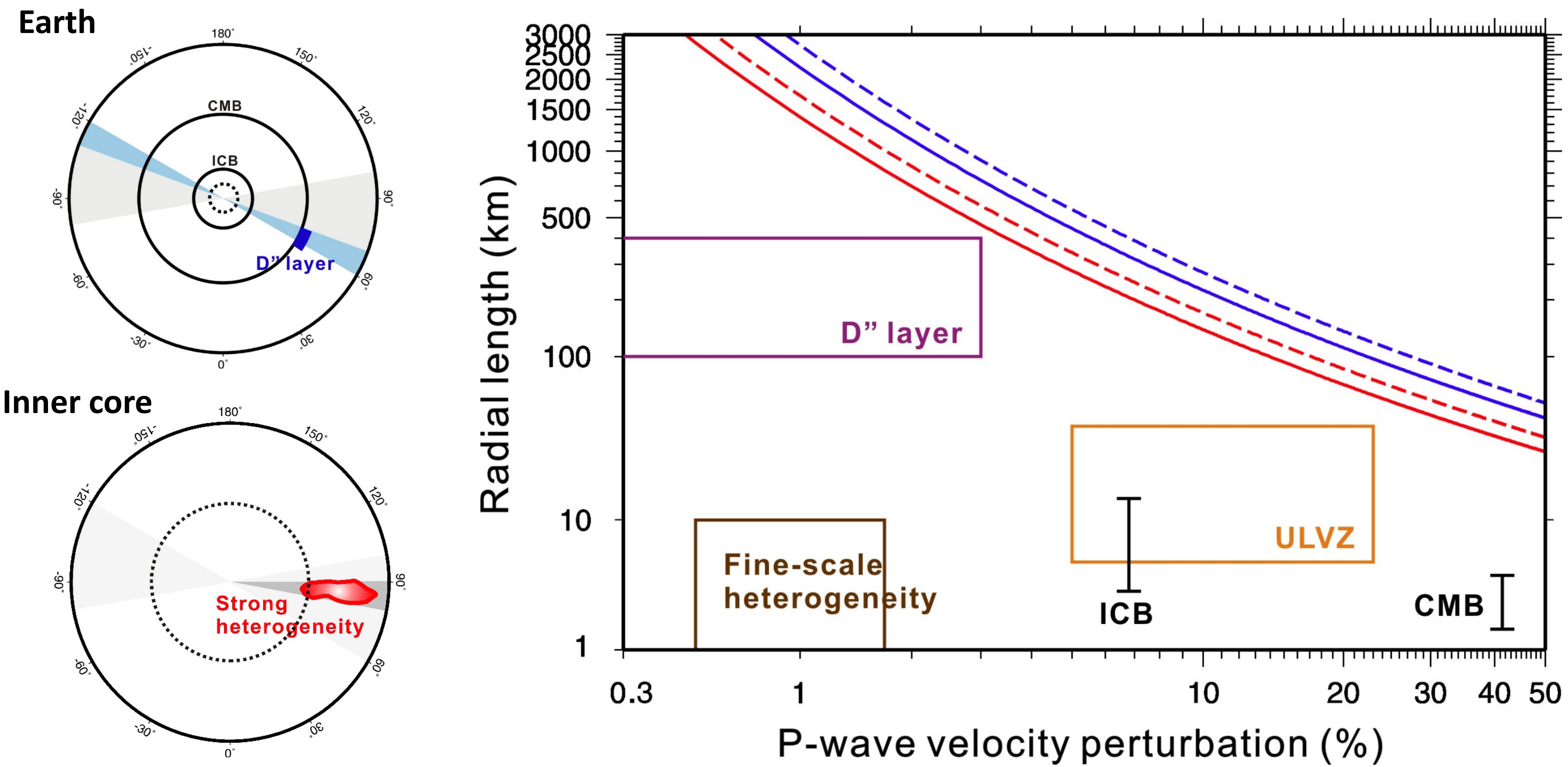

Possible anomaly sources

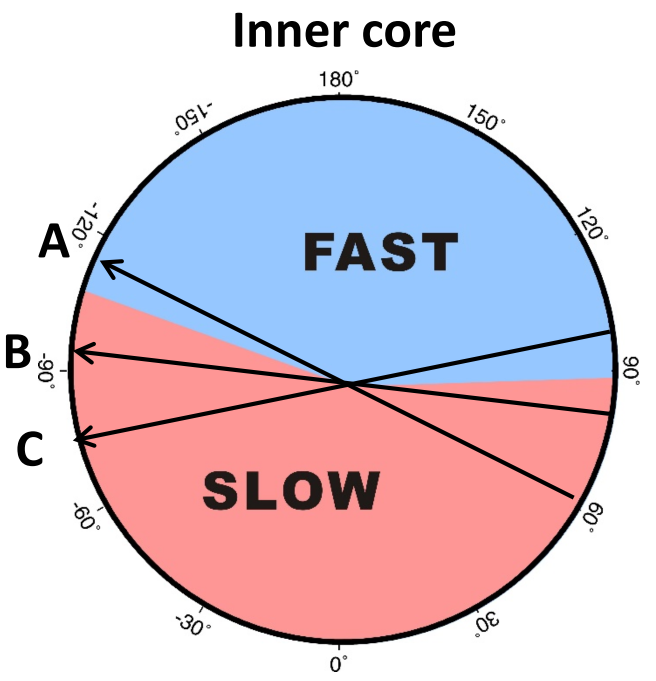

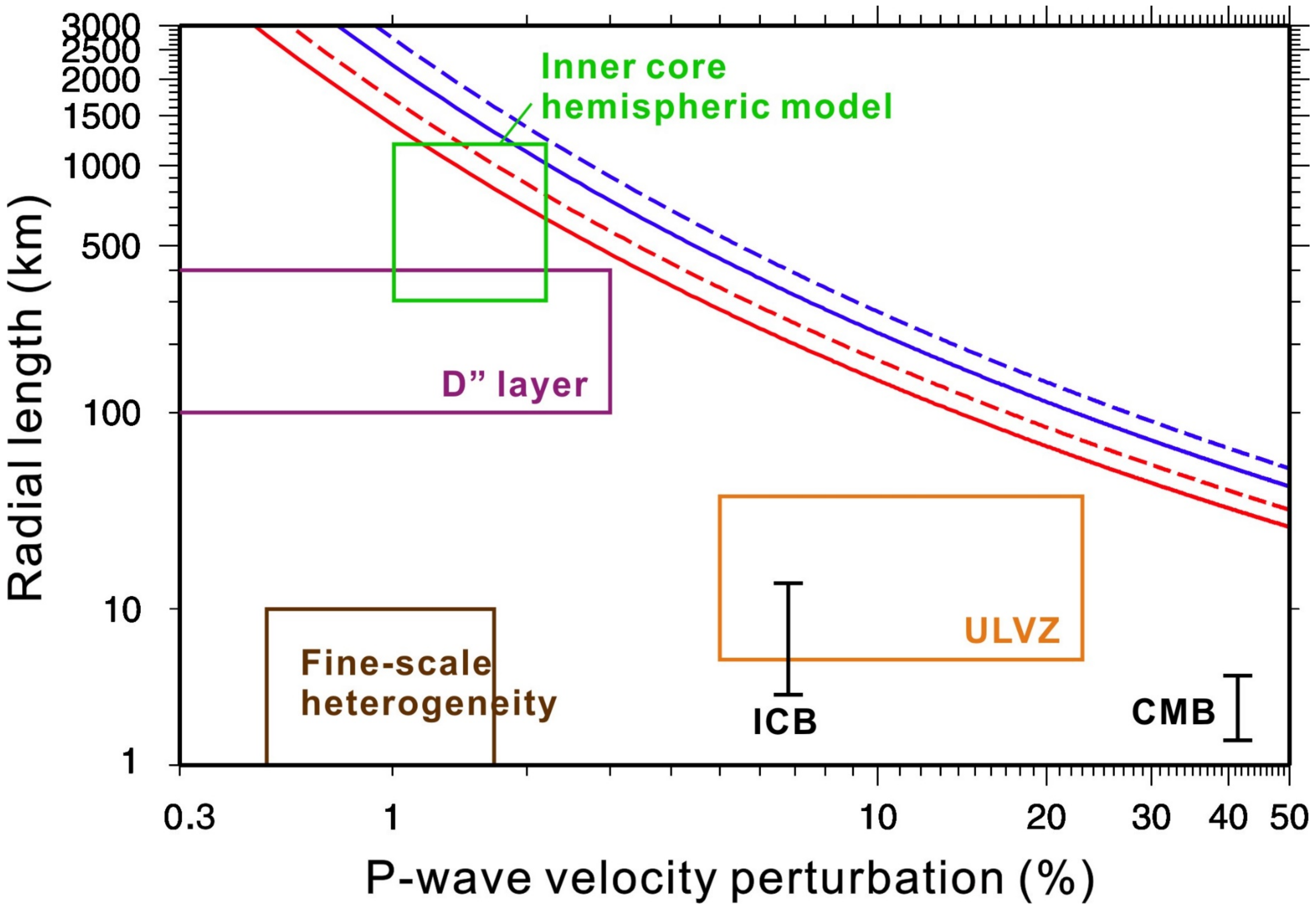

Possible hemispherical model and predictions

− bisected by boundaries at 99°W and 88°E with 1.2% V_P slower in western hemisphere

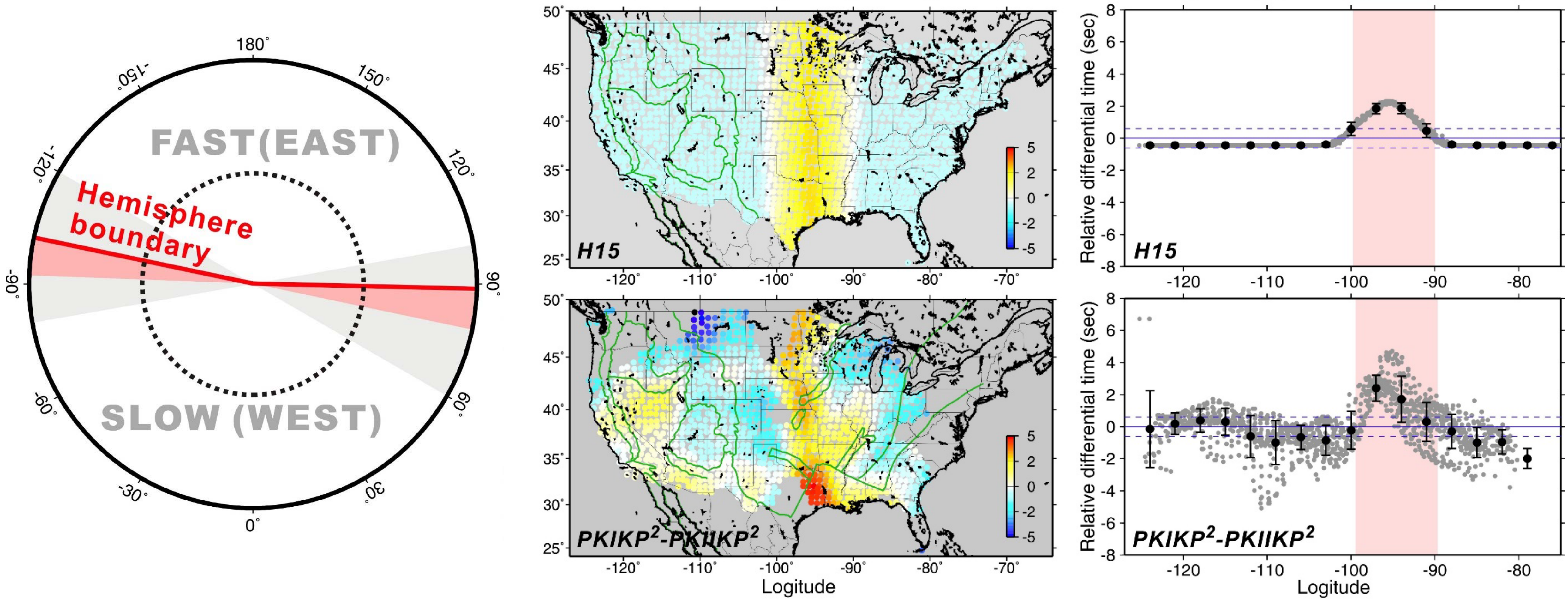

Hemisphere boundary consistency and discrepancy

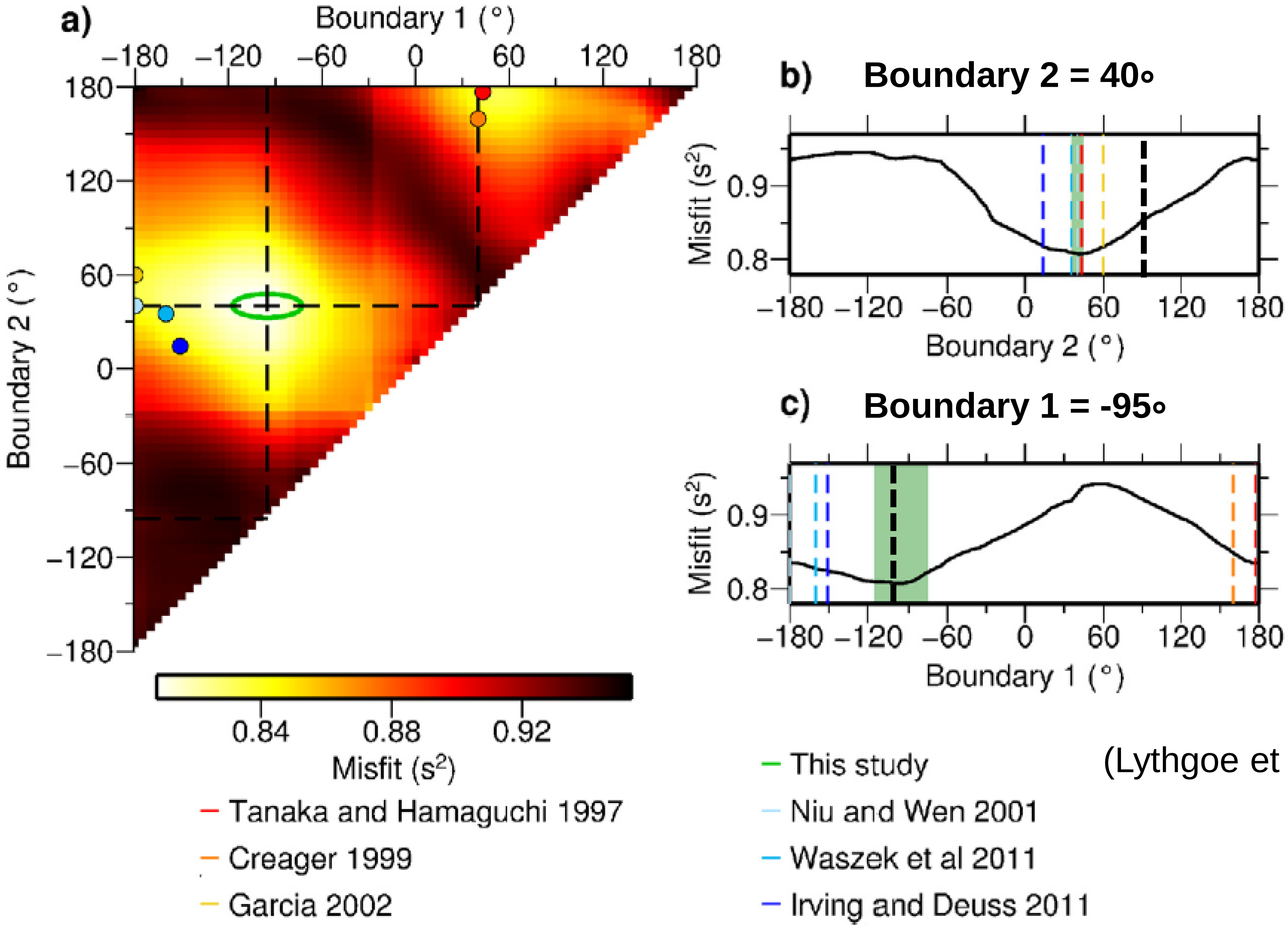

(Lythgoe et al., 2014)

Possible depth dependent boundary (Waszek&Deuss, 2011)

- Different data sets
- Different depth sensitivities

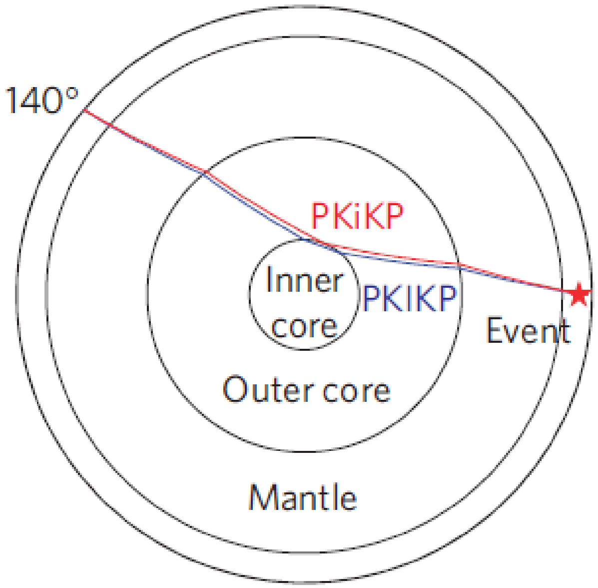

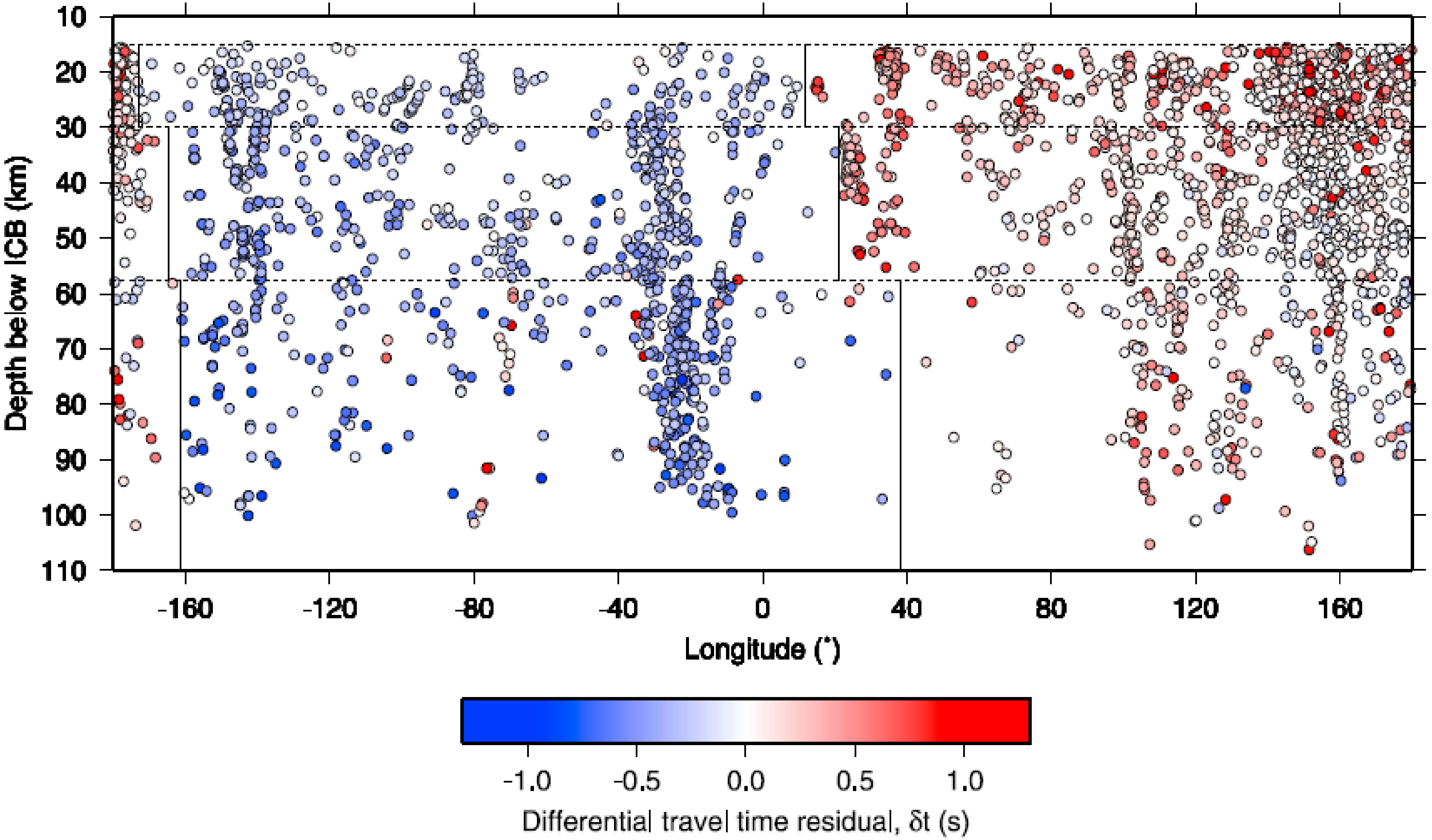

Conclusions

- This study is the first to obtain such dense sampling of inner core structure with seismic interferometry
- The antipodal-distance measurements of $PKIKP^2$ and $PKIIKP^2$ obtained here are rare in earthquake generated body-wave datasets and could be critical to constrain the structure at the very center of the Earth
- The short-wavelength variations in derived travel-time image implies strong, complex structural variability in the deep Earth
- The linear and large (1.25 s) N-S trending anomaly across the center of the U.S. suggests the need for an asymmetric quasi-hemispherical structure in the inner parts of the inner core

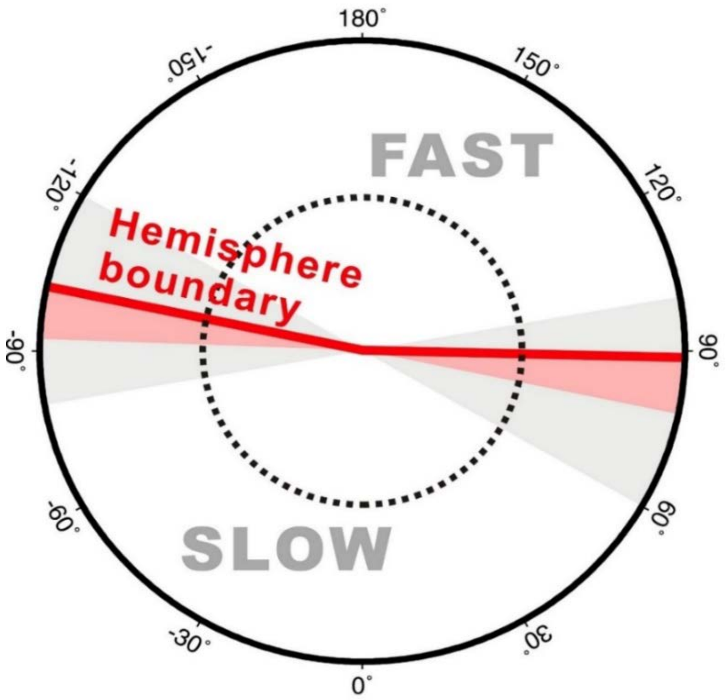

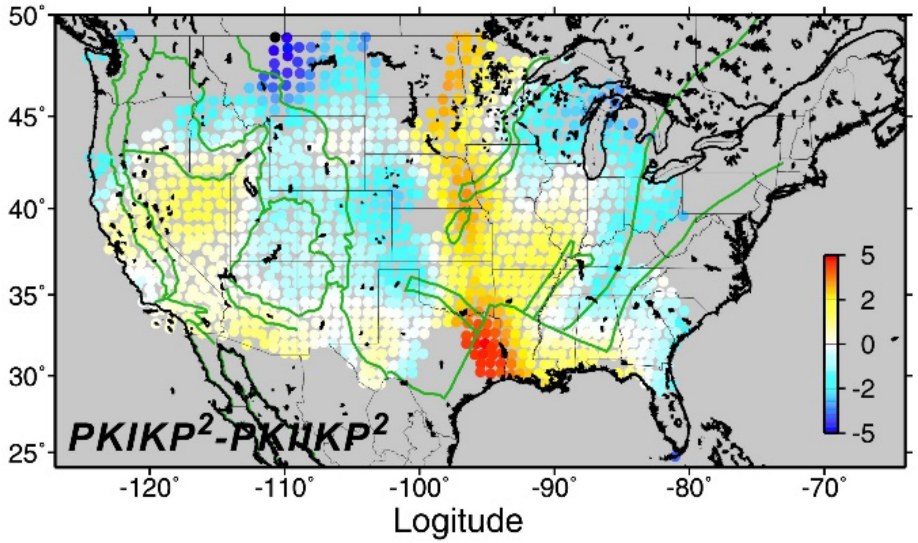

Beyond the inner core

- One of the ultimate goals is to jointly invert all kinds of data we have, including these new interferometry data sets

- Potential bias (mechanism) from body-wave interferometry need to be further investigated

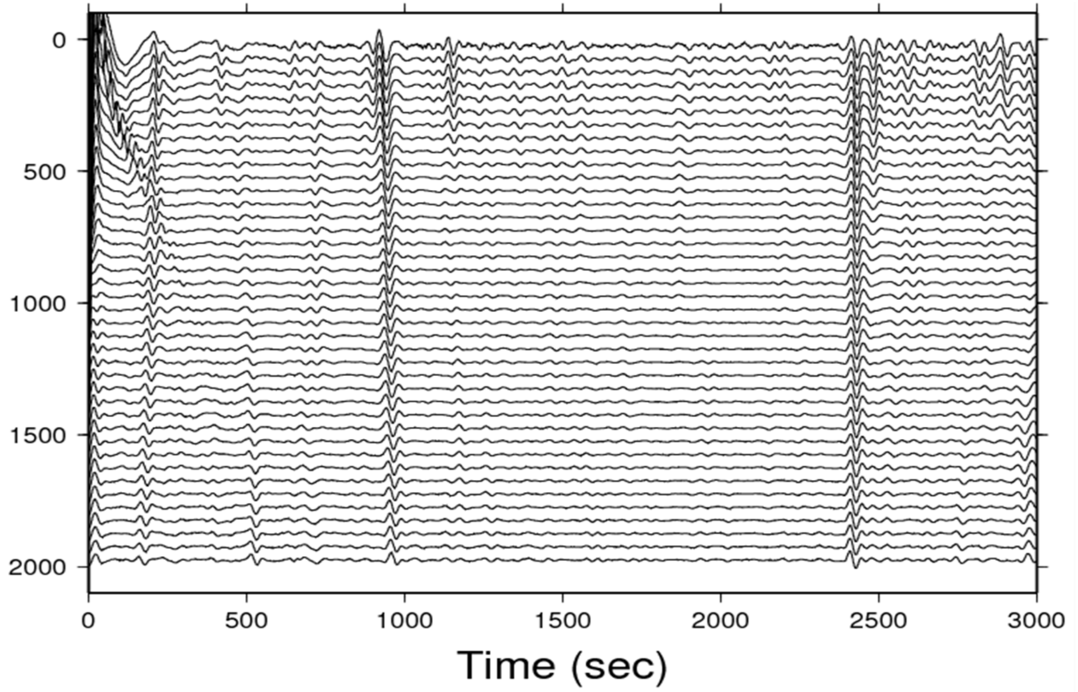

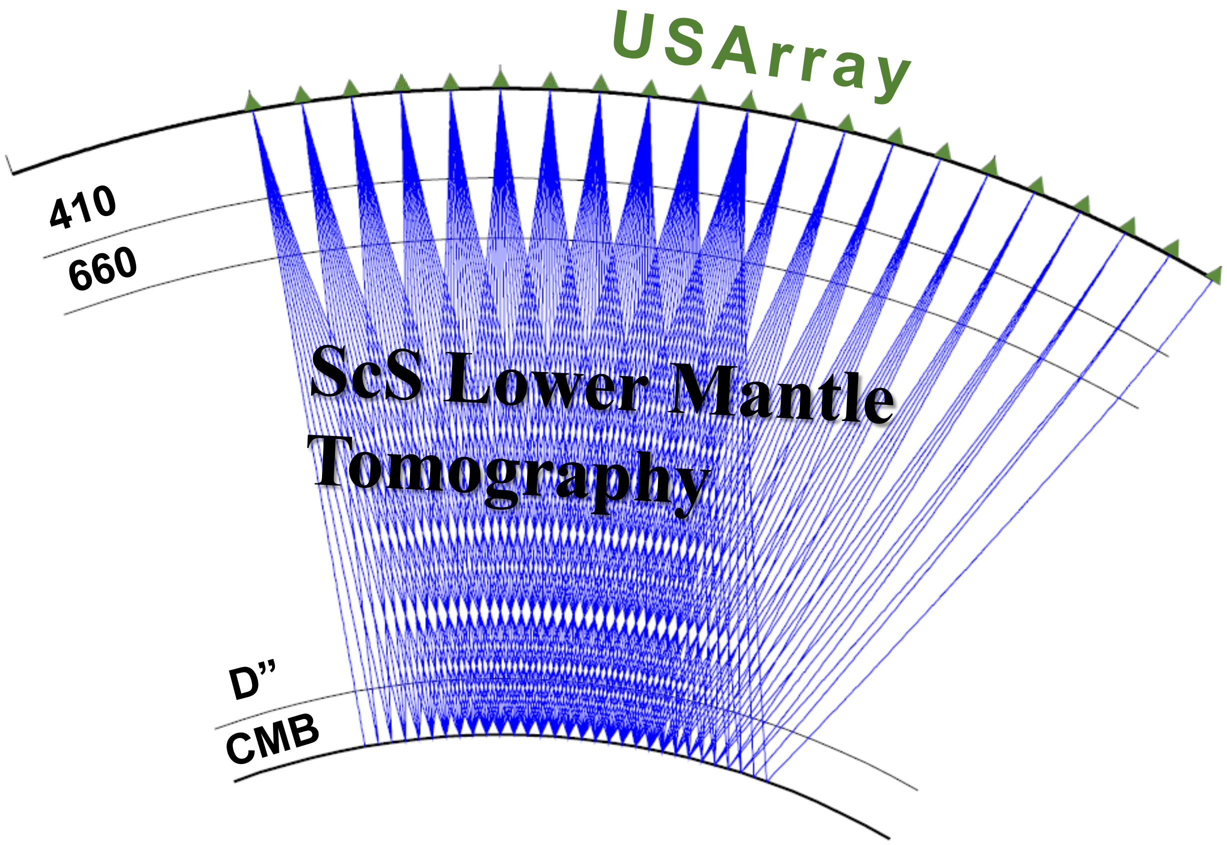

Thanks for your attention!

Presented on April 7, 2017

But what if no earthquakes…

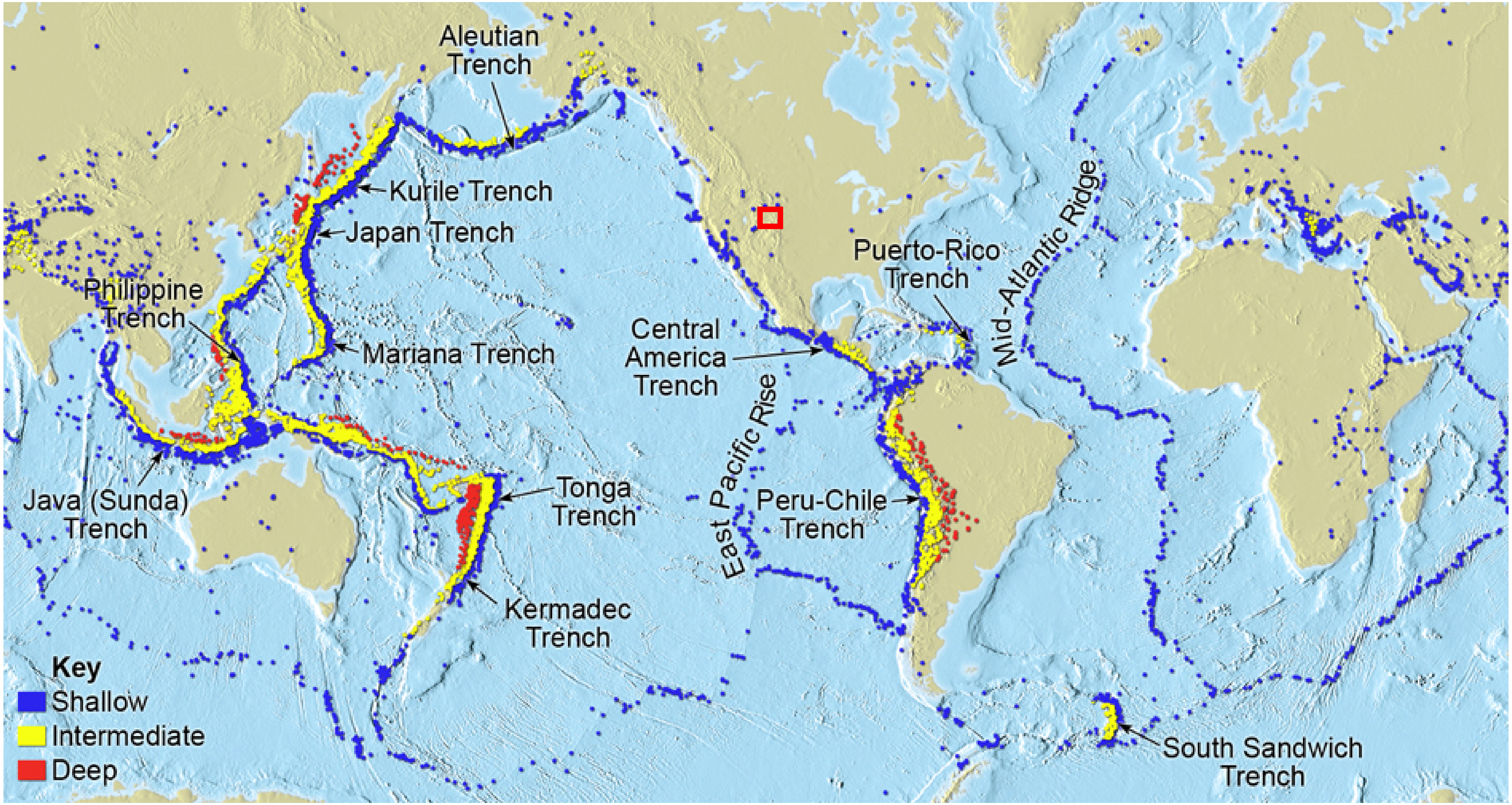

Distribution of shallow-, intermediate-, and deep-focus earthquakes. (Data from NOAA)

Iceland example

– Shallow magma reservoir vs. Deep mantle plume

– The lower crustal structure beneath volcanoes is poorly constrained in general

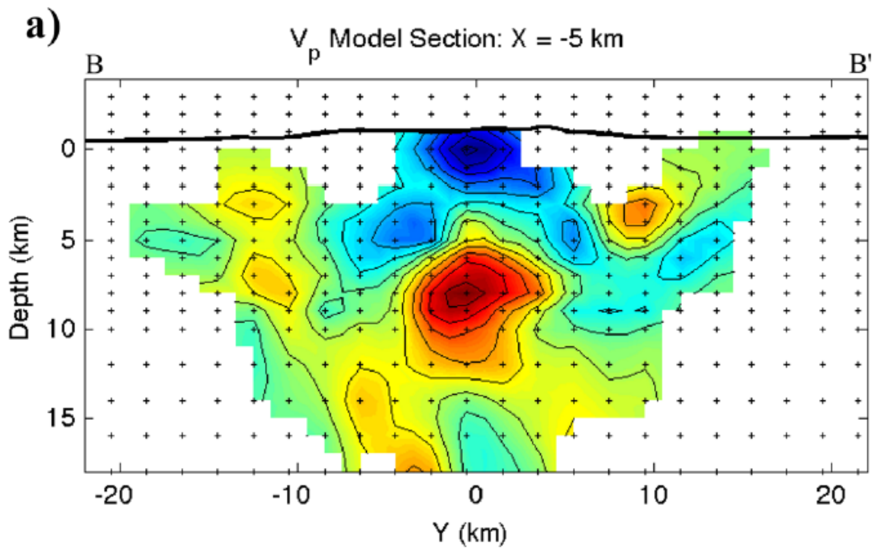

(Mitchell et al., 2013)

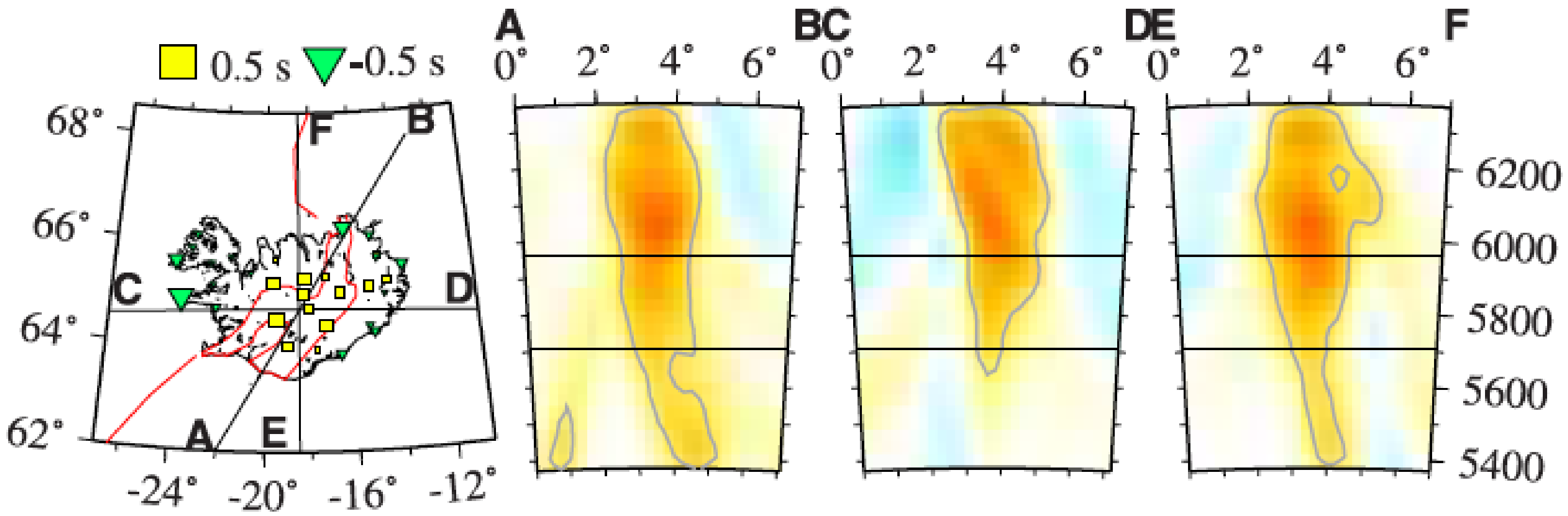

(Hung et al., 2004)

Travel time residuals before/after inversion

- 4 iterations for local earthquake data solely to get a good local model first

- Another 4 iterations for joint inversion integrating both local and teleseismic earthquake data

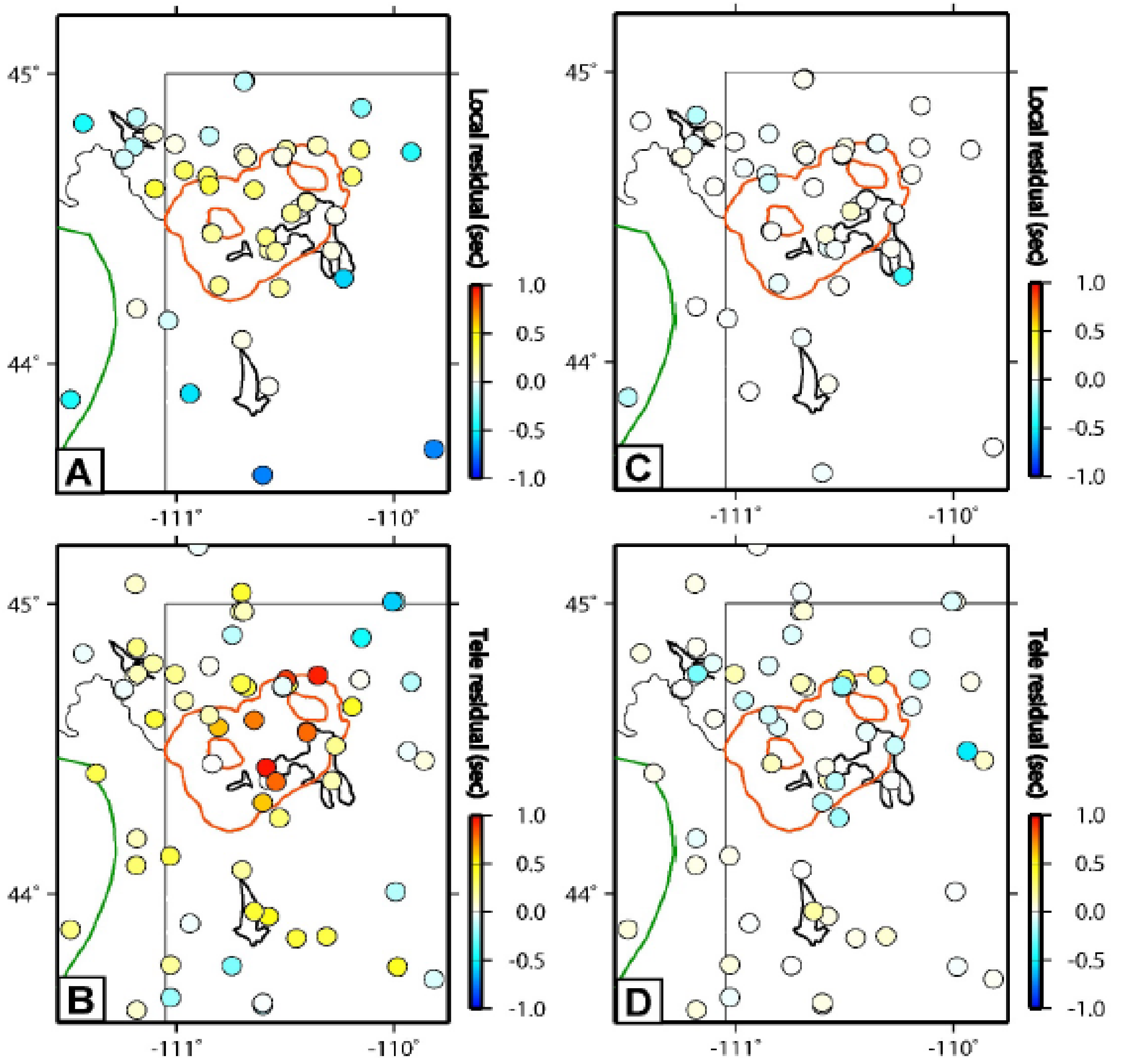

Regularization tests

Damping: 40

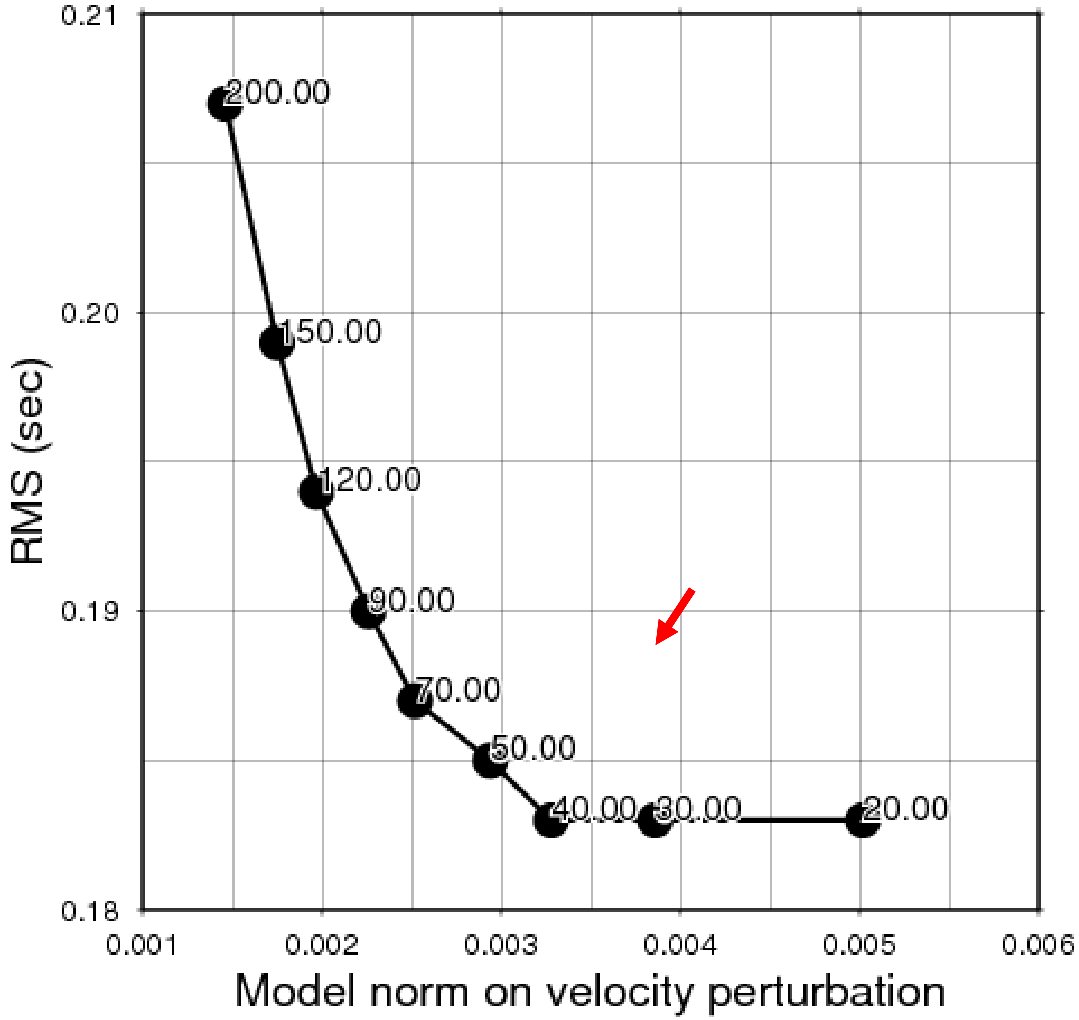

Smoothing: 30

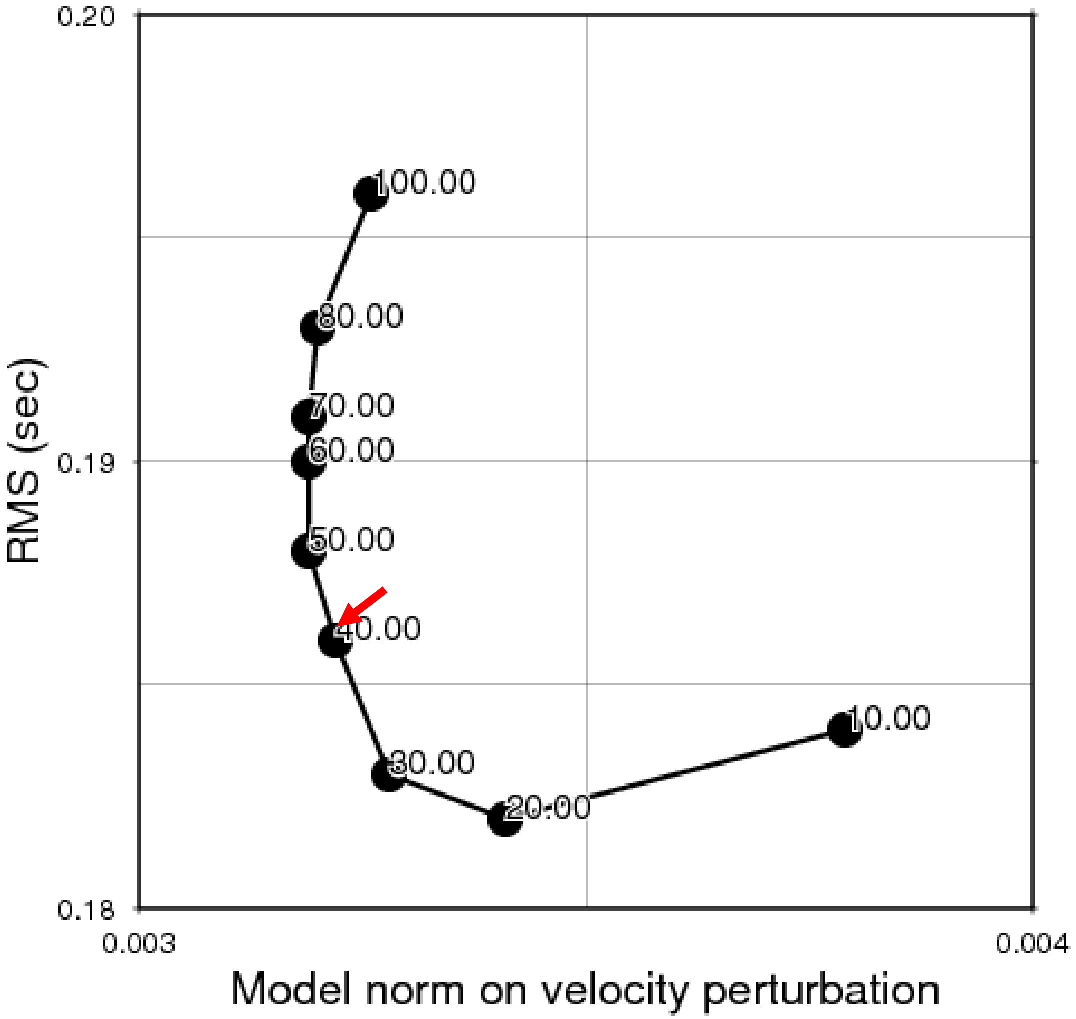

CKB, DWS, *R*

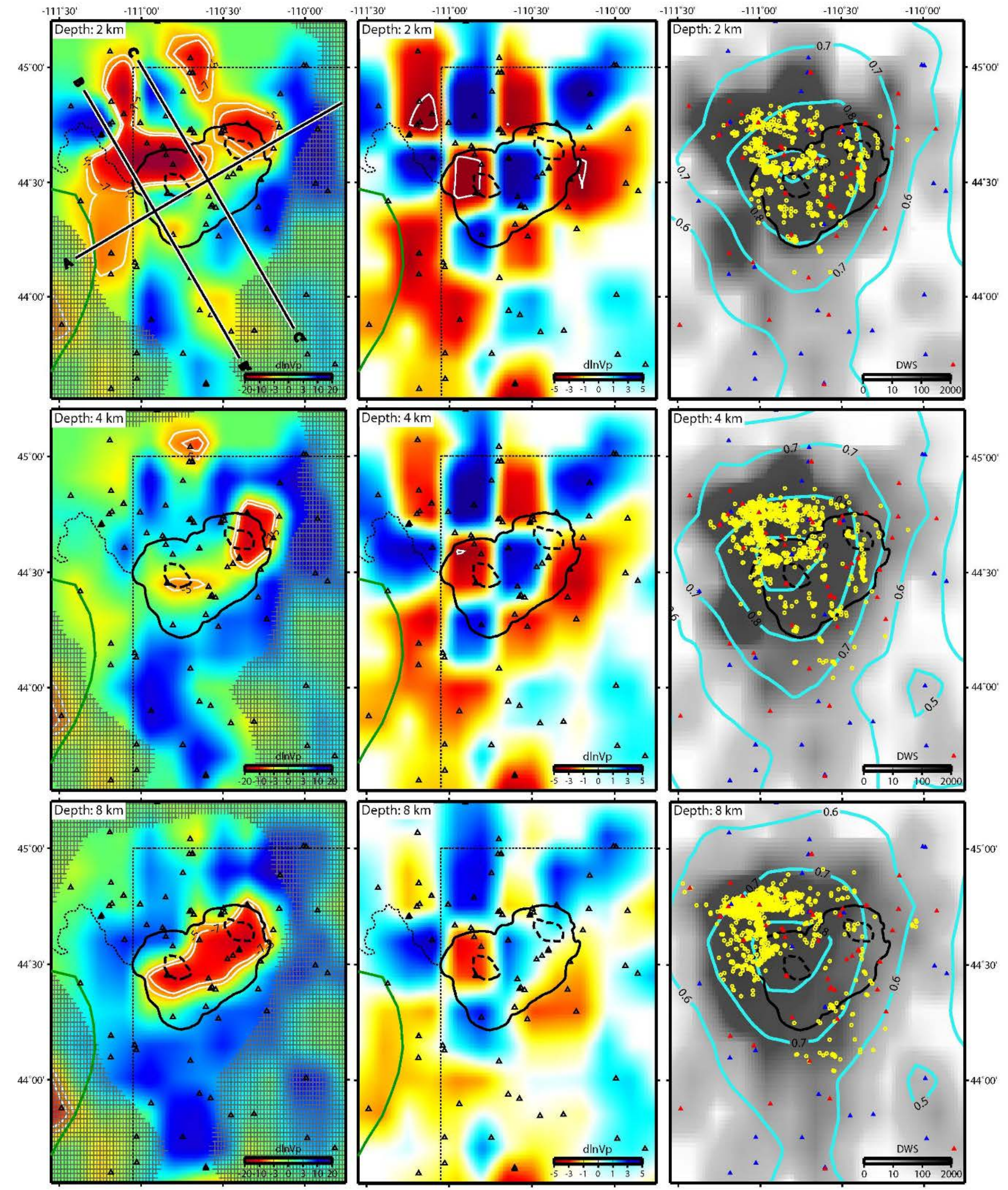
Depth: 2 km
Depth: 4 km
Depth: 8 km
dlnVp
DWS
-111°30'
-111°00'
-110°30'
-110°00'
45°00'
44°30'
44°00'
-20 -10 -3 0 3 10 20
-5 -3 -1 0 1 3 5
0 10 100 2000

CKB, DWS, *R*

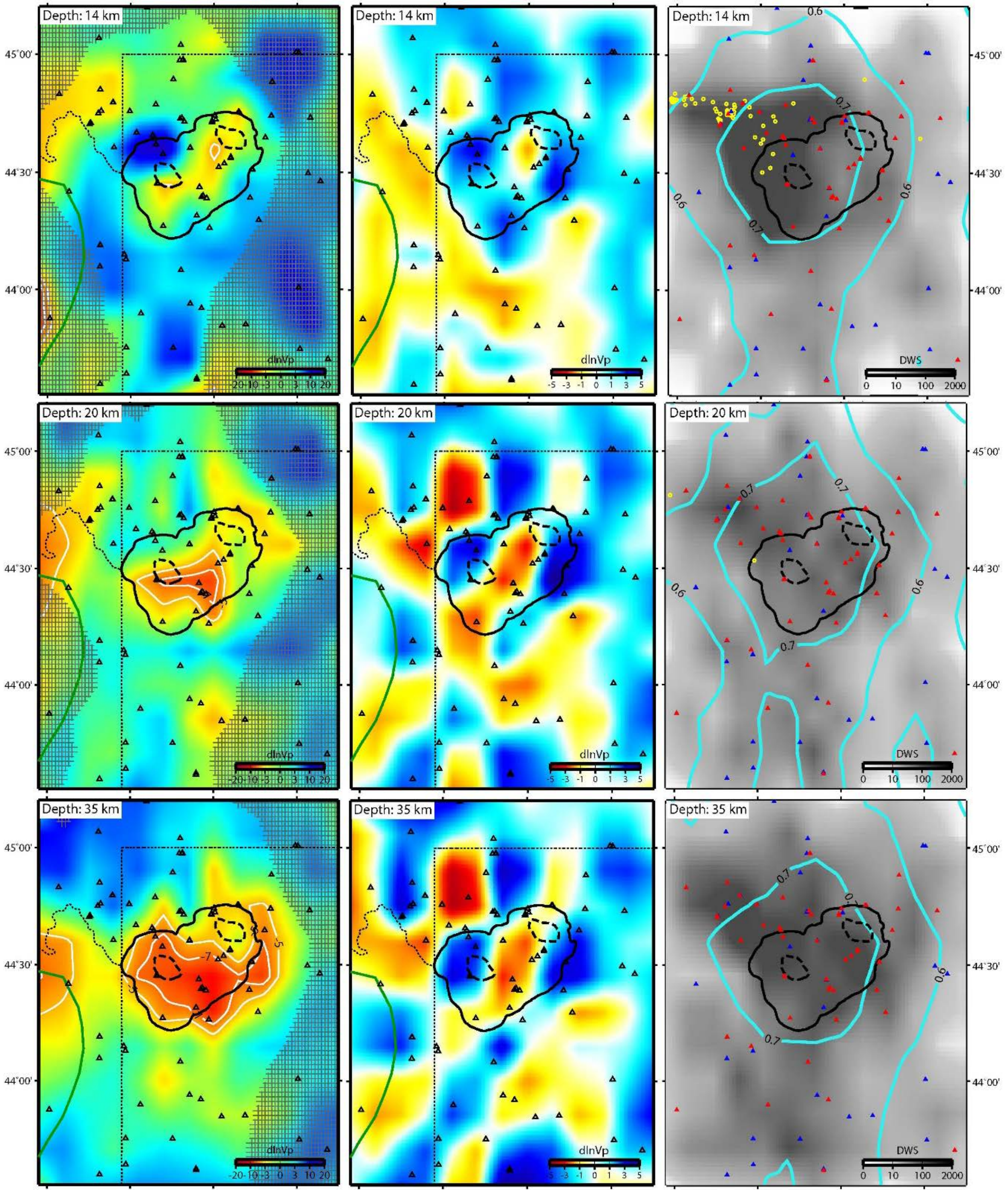

Depth: 14 km
Depth: 20 km
Depth: 35 km
45°00'
44°30'
44°00'
dlnVp
-20 -10 -3 0 3 10 20
-5 -3 -1 0 1 3 5
DWS
0 10 100 2000
0.6
0.7

CKB, DWS, *R*

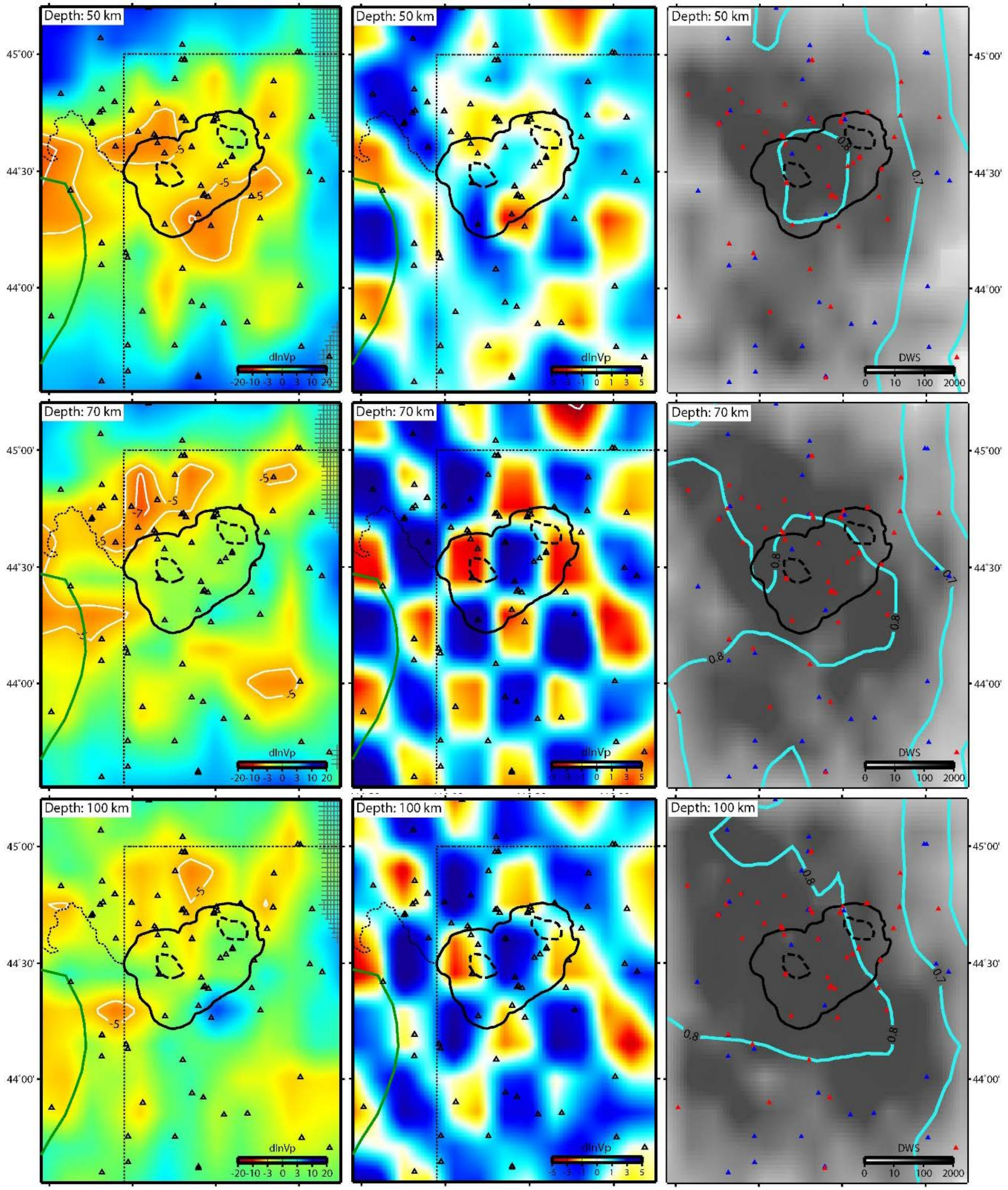

Depth: 50 km
Depth: 70 km
Depth: 100 km
45°00'
44°30'
44°00'
dlnVp
-20 -10 -3 0 3 10 20
-5 -3 -1 0 1 3 5
DWS
0 10 100 2000

Characteristic model tests

- Without lower-crustal low velocity anomaly

- This negative control demonstrates that the lower-crustal magma body is robust

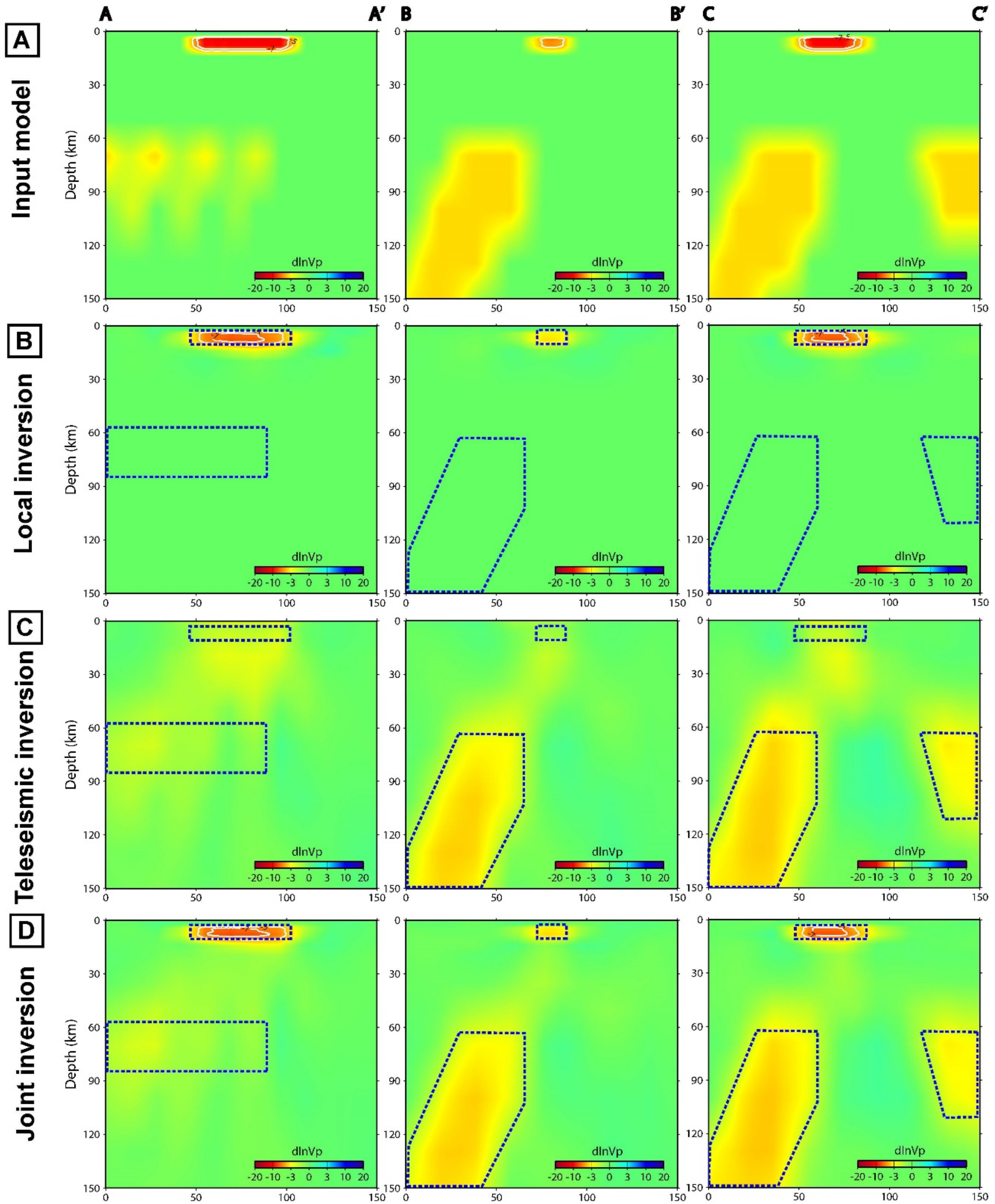

Characteristic model tests

- With noise level of 0.13 s according to the final RMS of travel time residuals of real inversion
- The bottom of the lower crustal anomaly is clearly biased
- Black arrows indicate the smearing artifacts

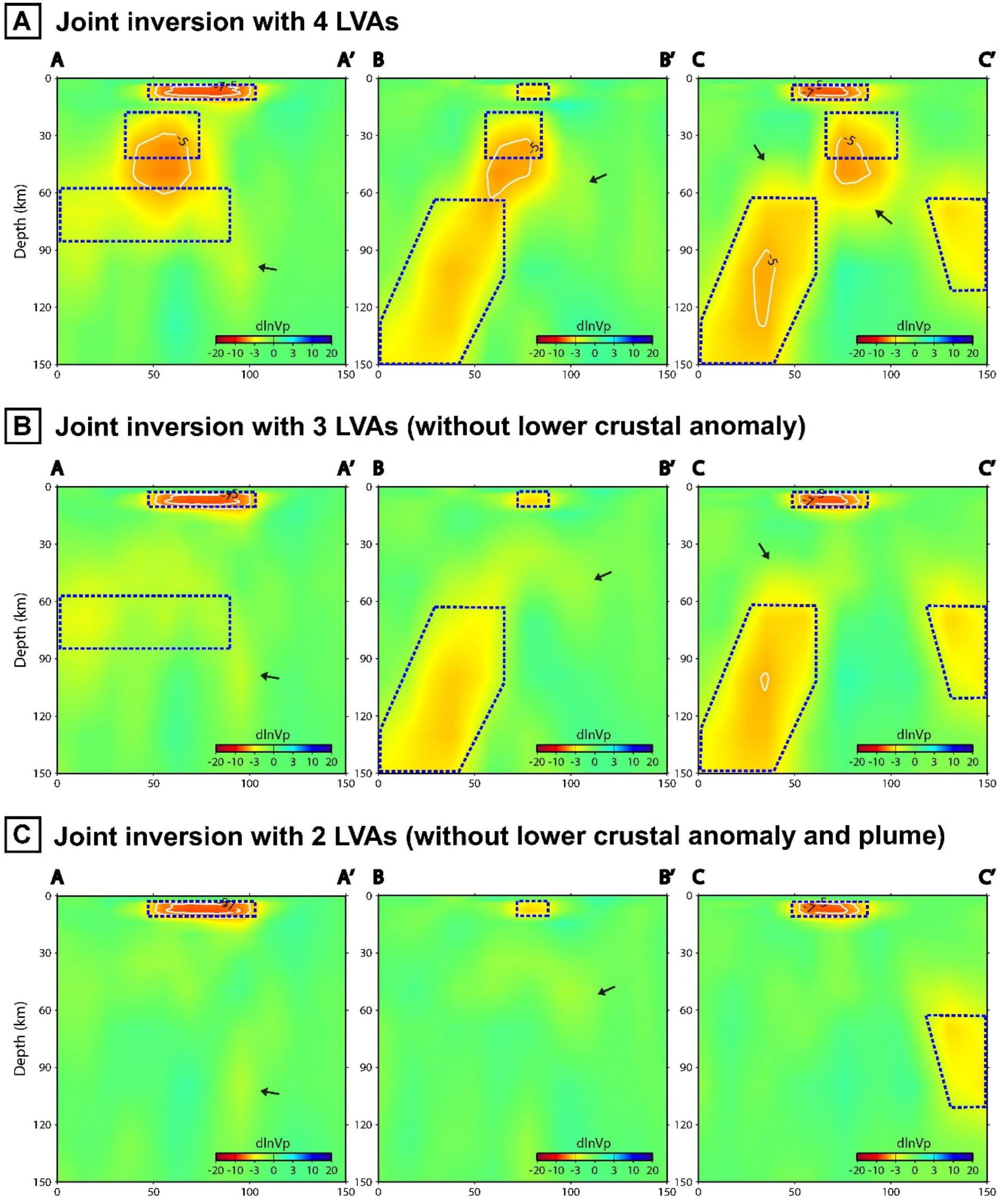

Melt volume calculations

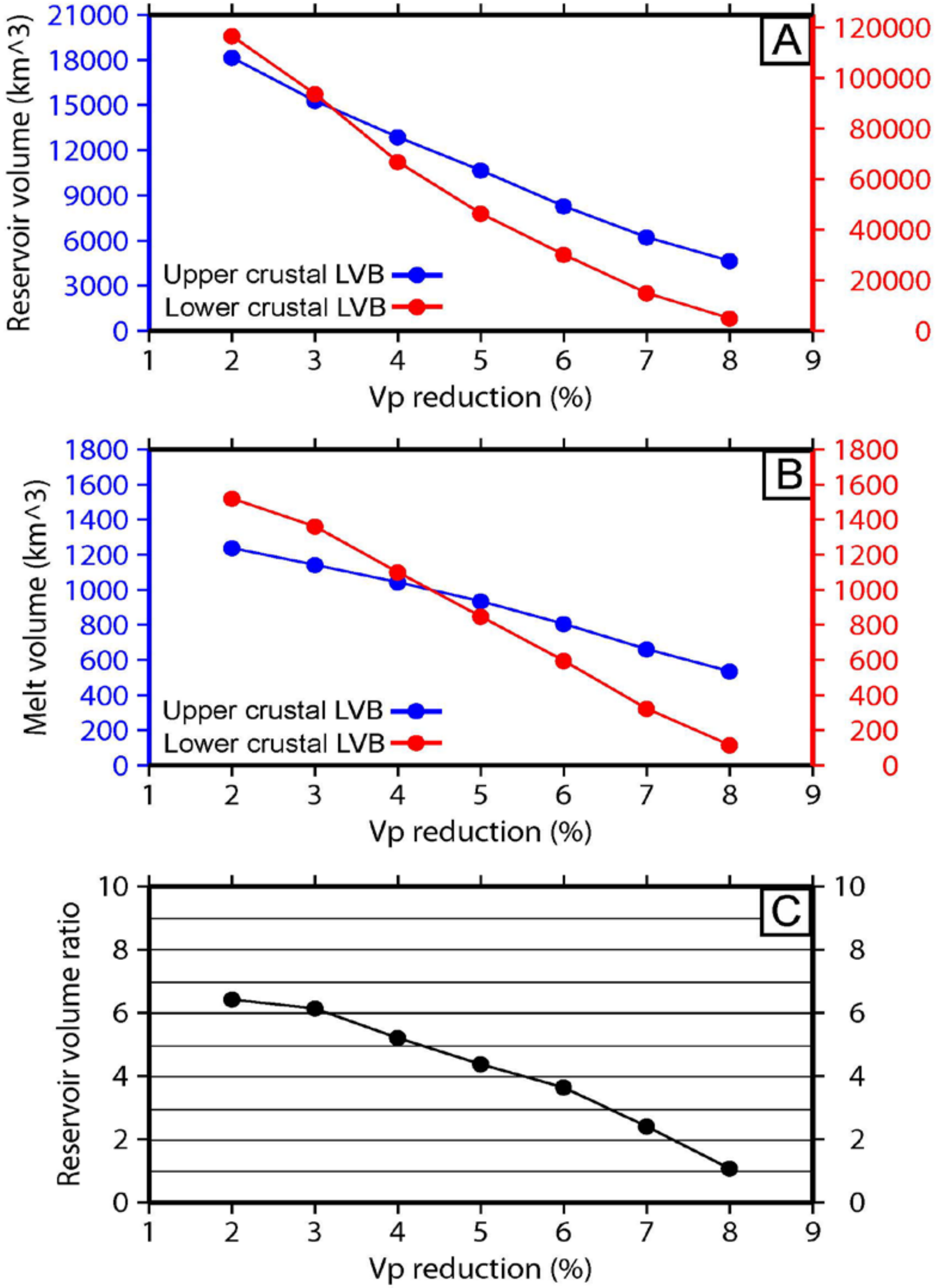

Seismic interferometry

– Open a new area of applications

Tomography (Shapiro et al., 2005)

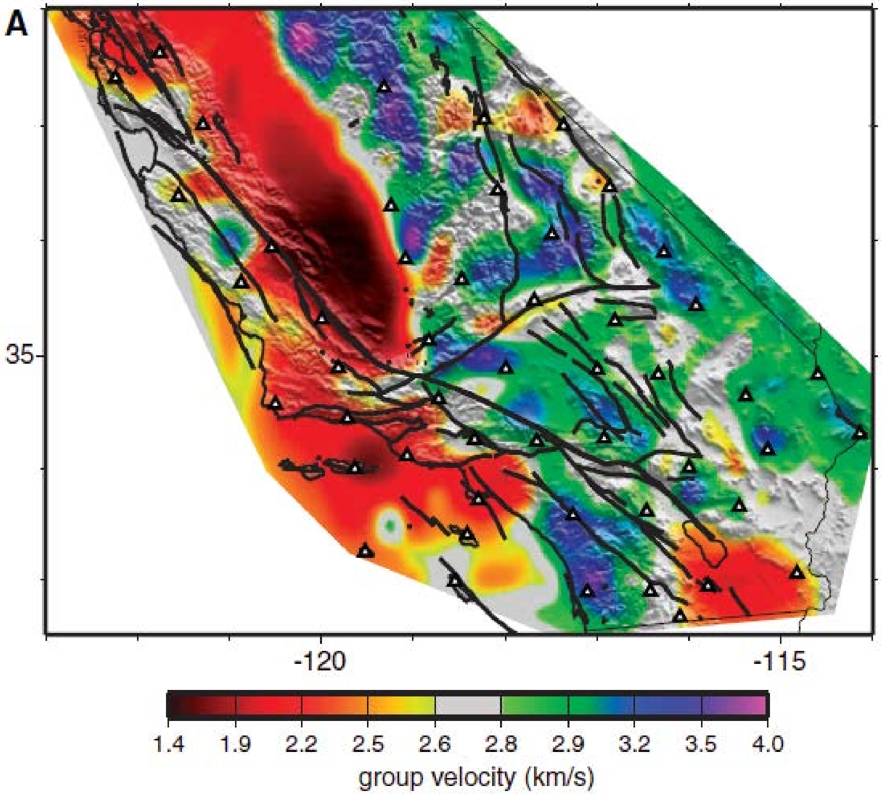

Noise source tracking (Chen et al., 2011)

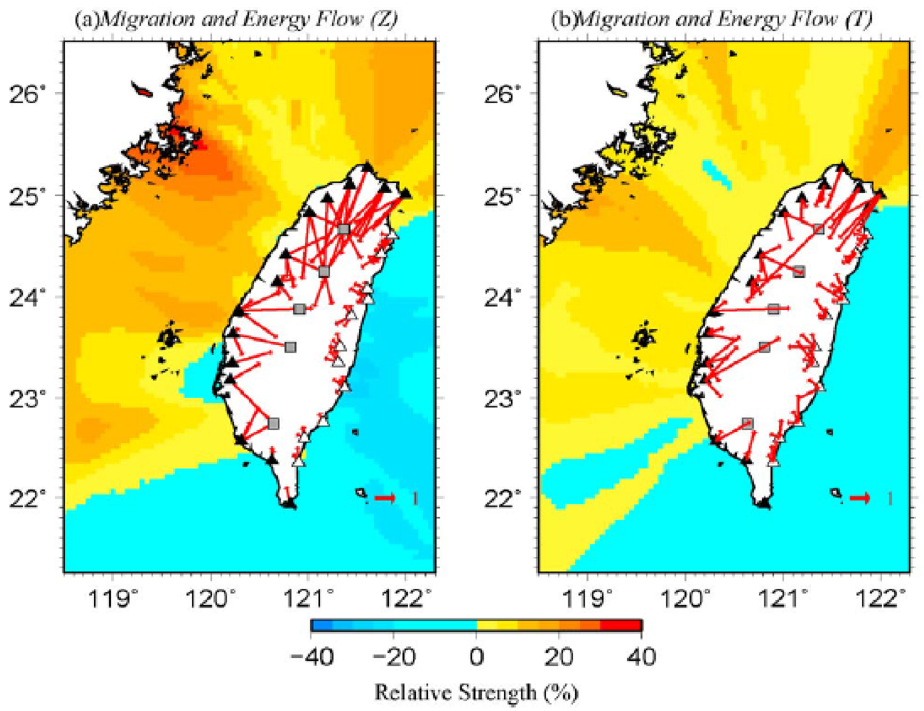

Temporal medium monitoring

(Brenguier et al., 2008)

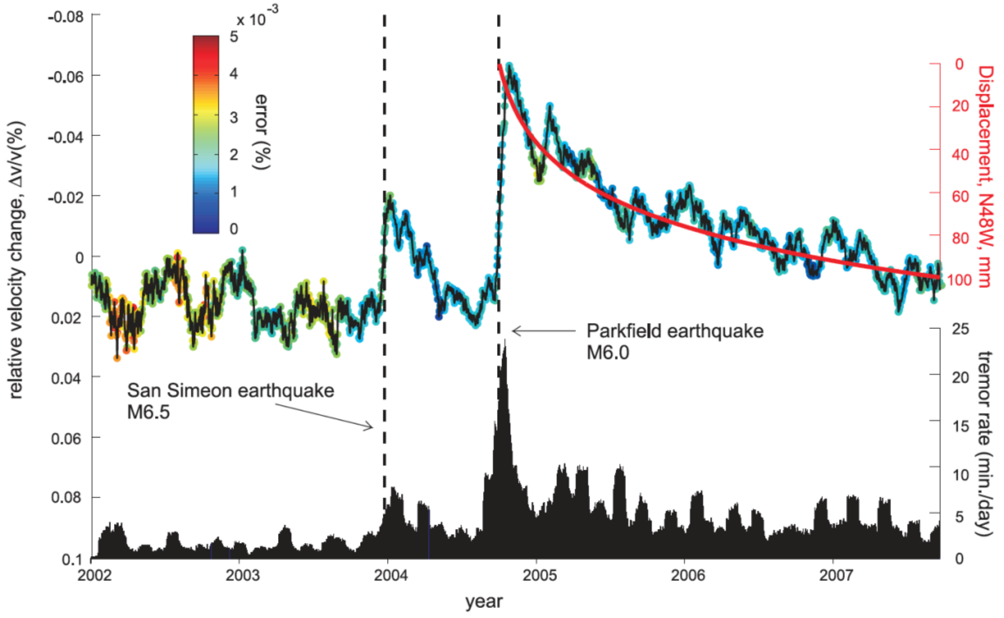

Lin and Tsai, 2013 – Antipodal station pair

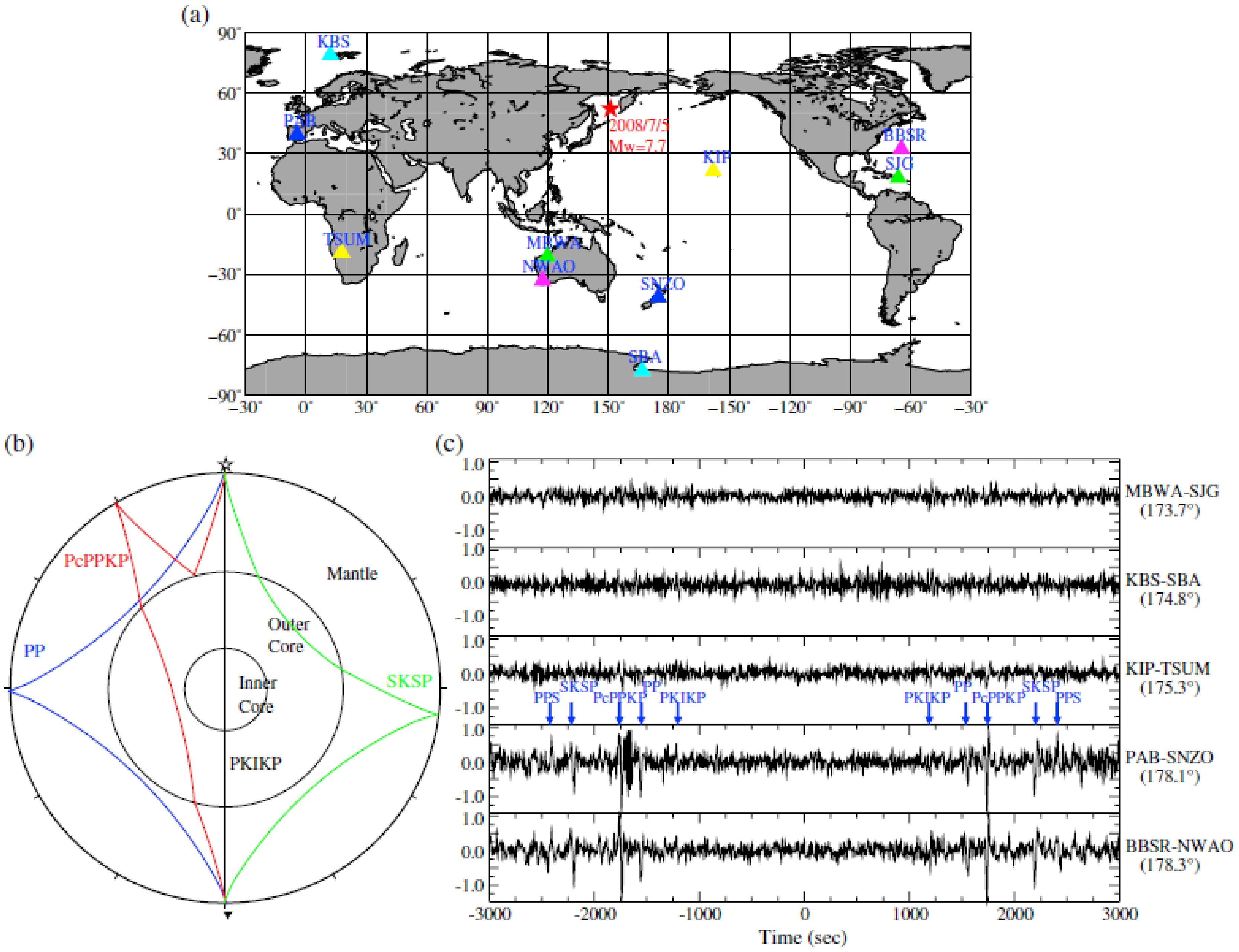

Contamination from mantle heterogeneity

– Reference phase method

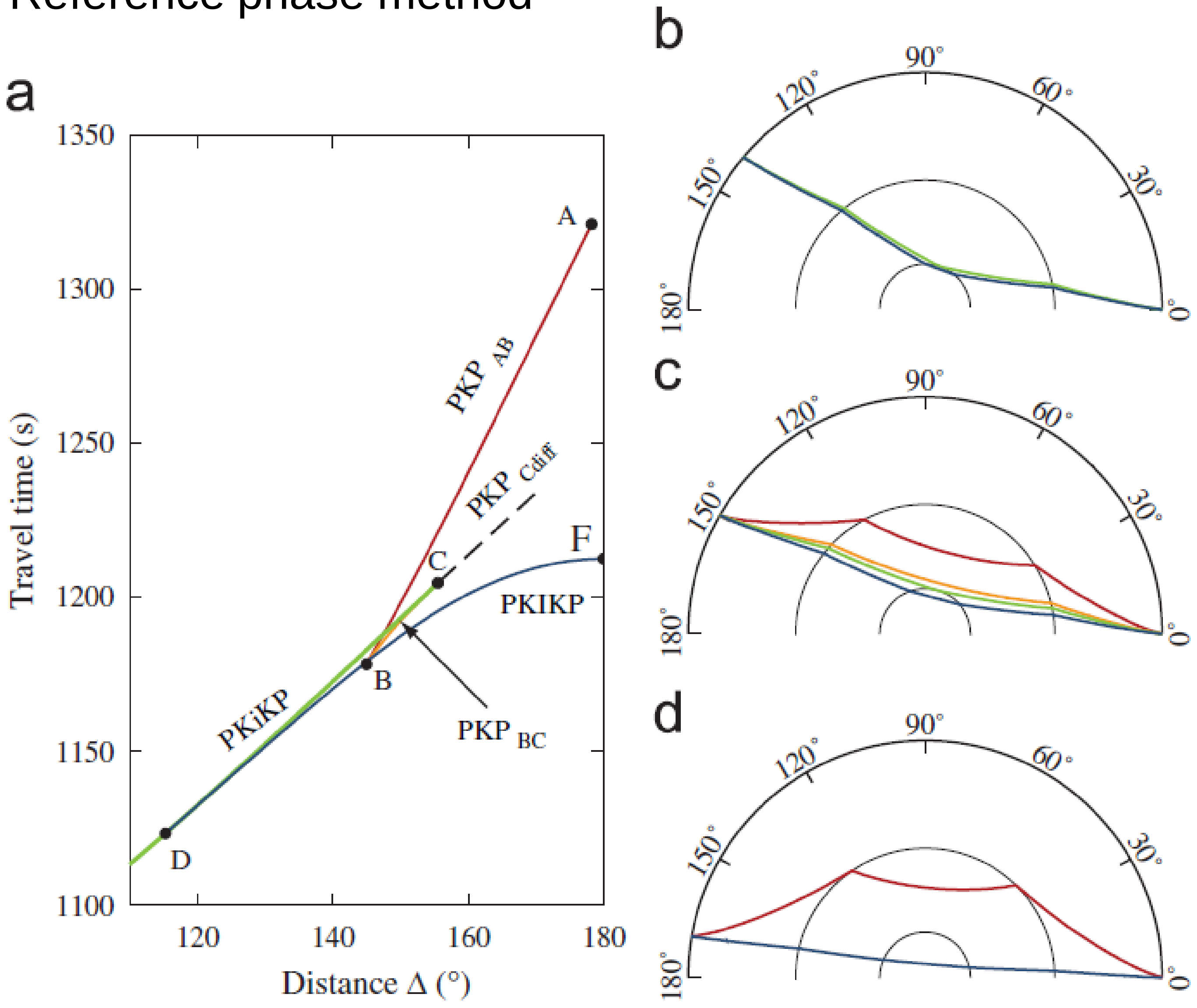

(Deguen, 2012)

– PKIKP & PKIIKP

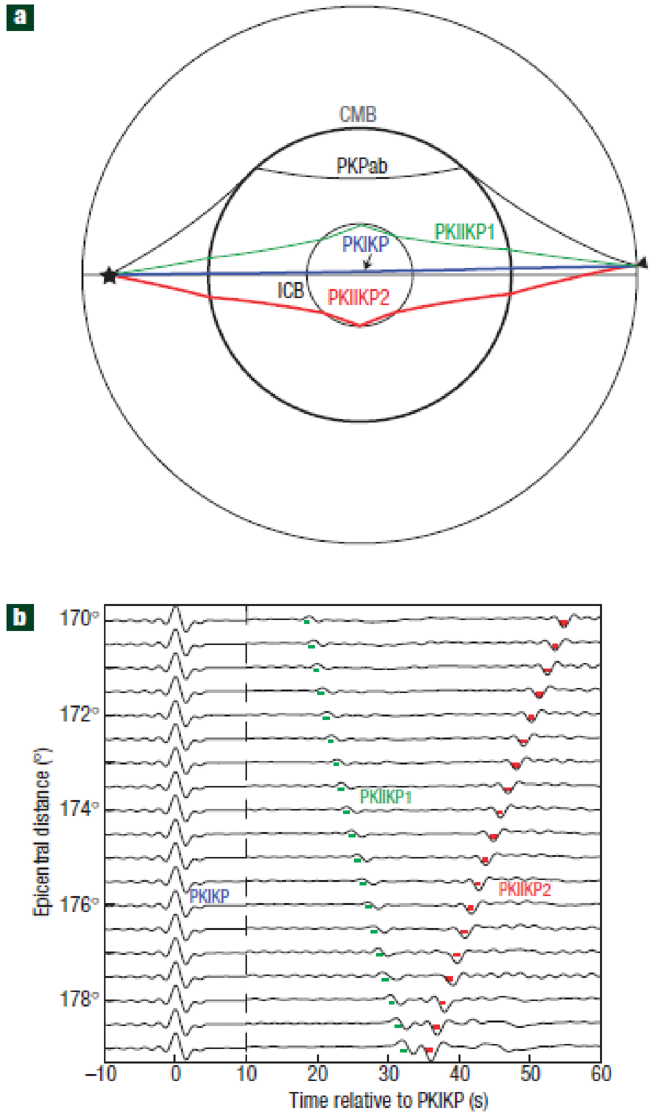

(Niu and Chen, 2008)

Summary of Inner core structure

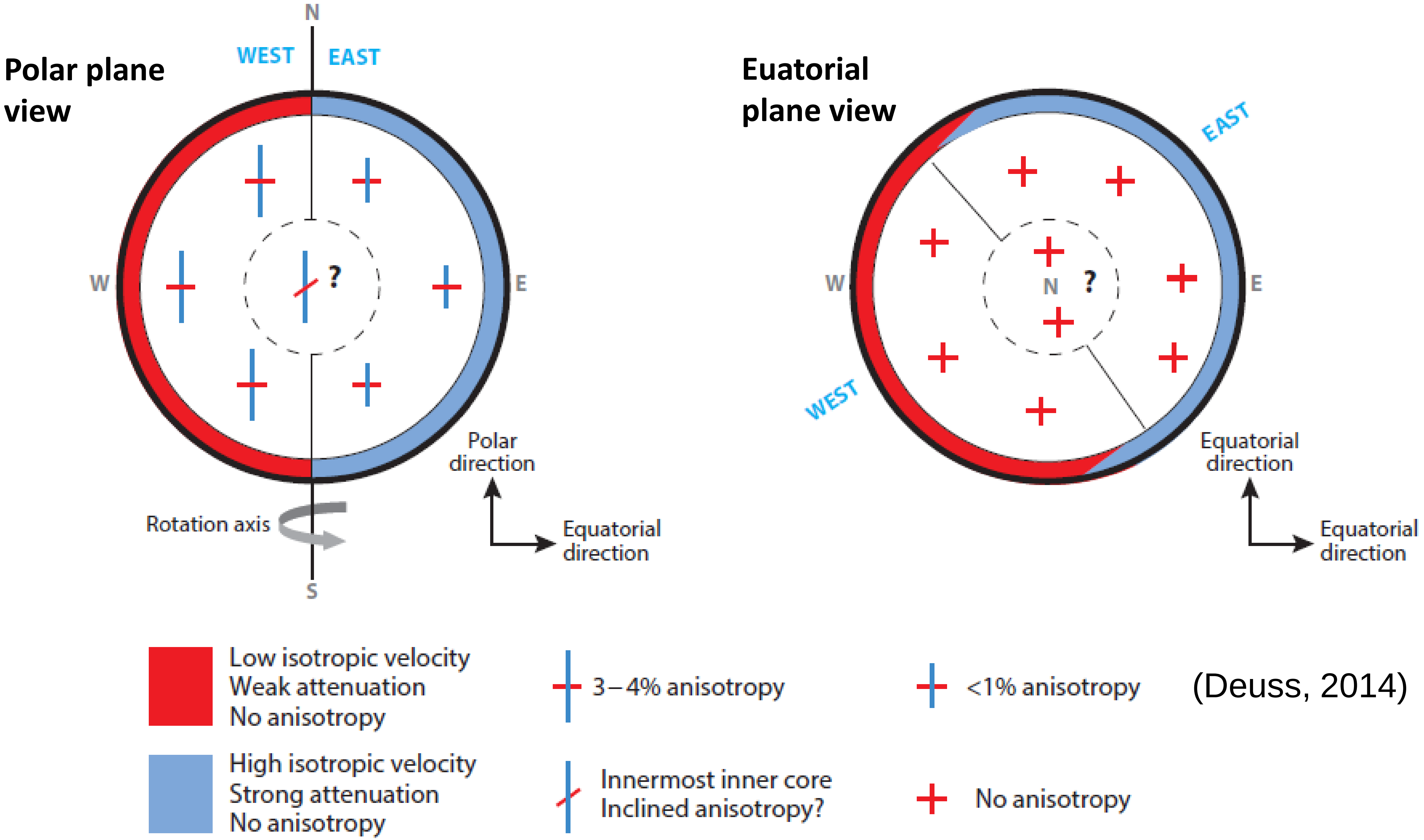

(Deuss, 2014)

Two recent studies..

Lygoes et al., 2014

− East-West Hemisphere boundary

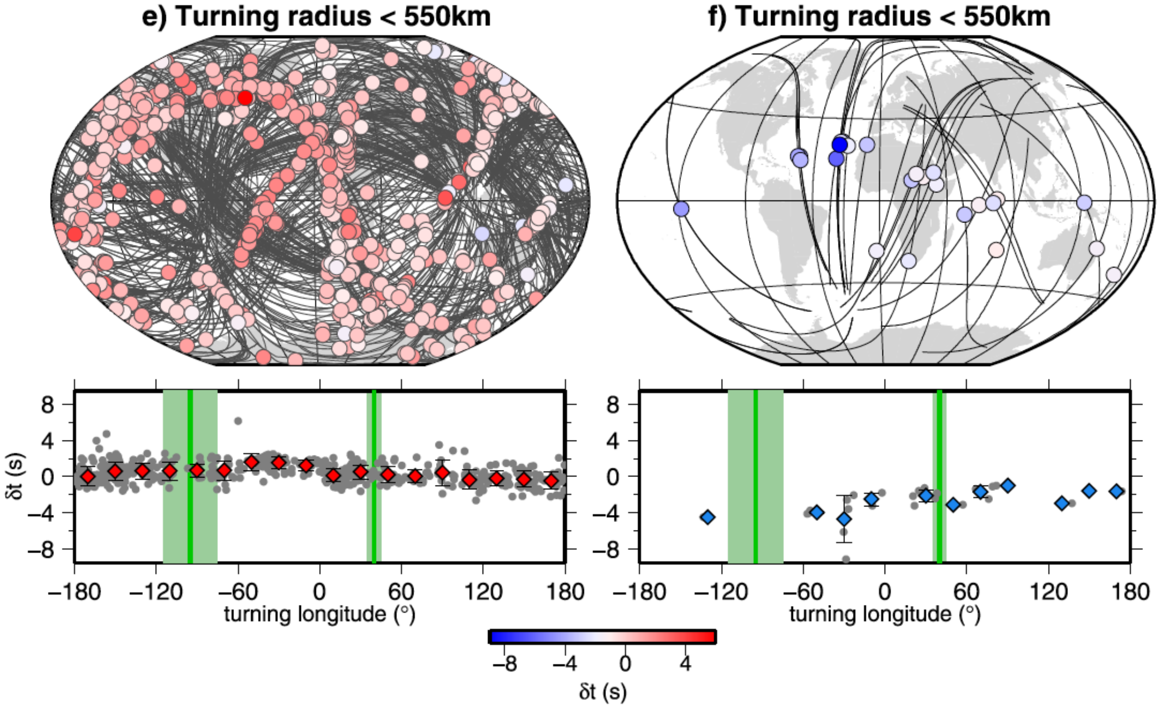

Wang et al., 2015

− Innermost inner core anisotropy

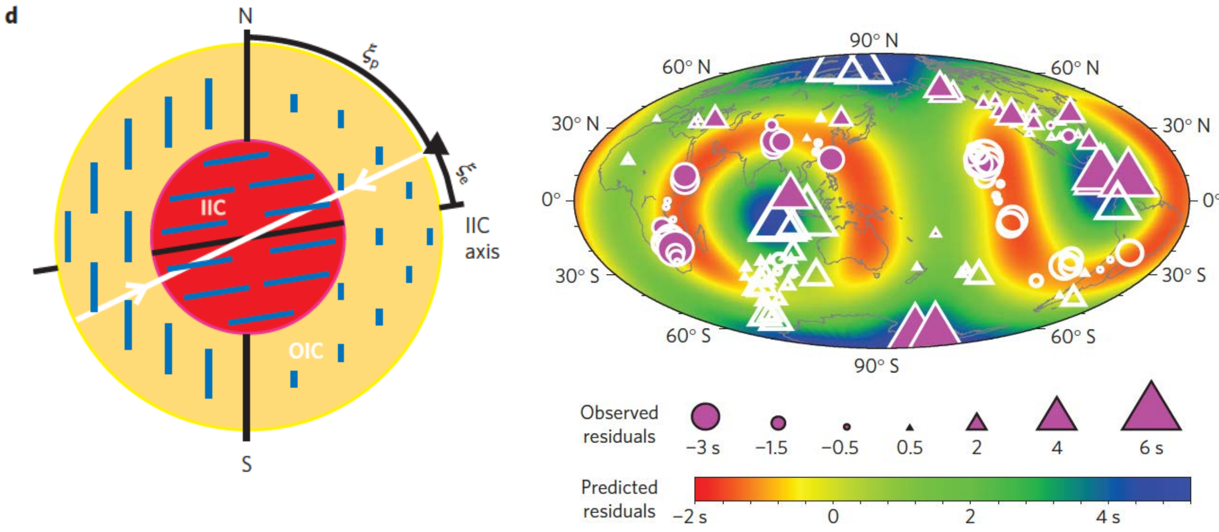

This study

– Instead of continuous noise record, late coda of large earthquakes my be more efficient

143 Global $M_W \geqq 7$ Earthquake

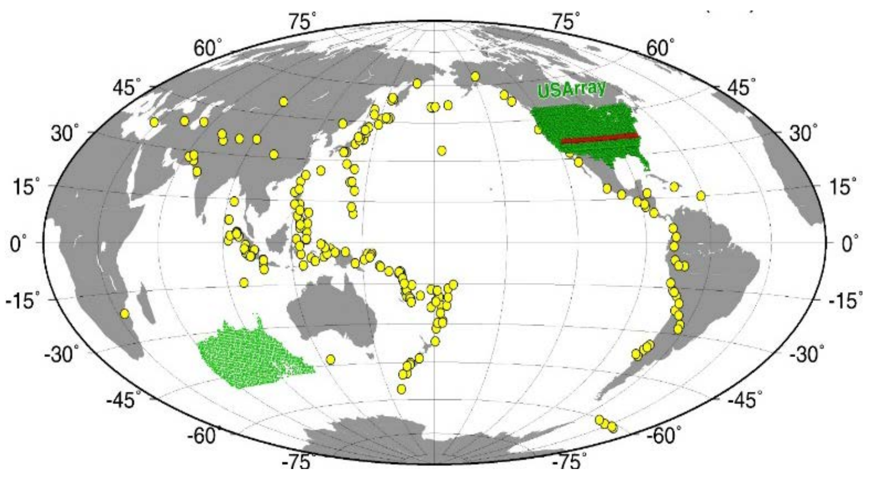

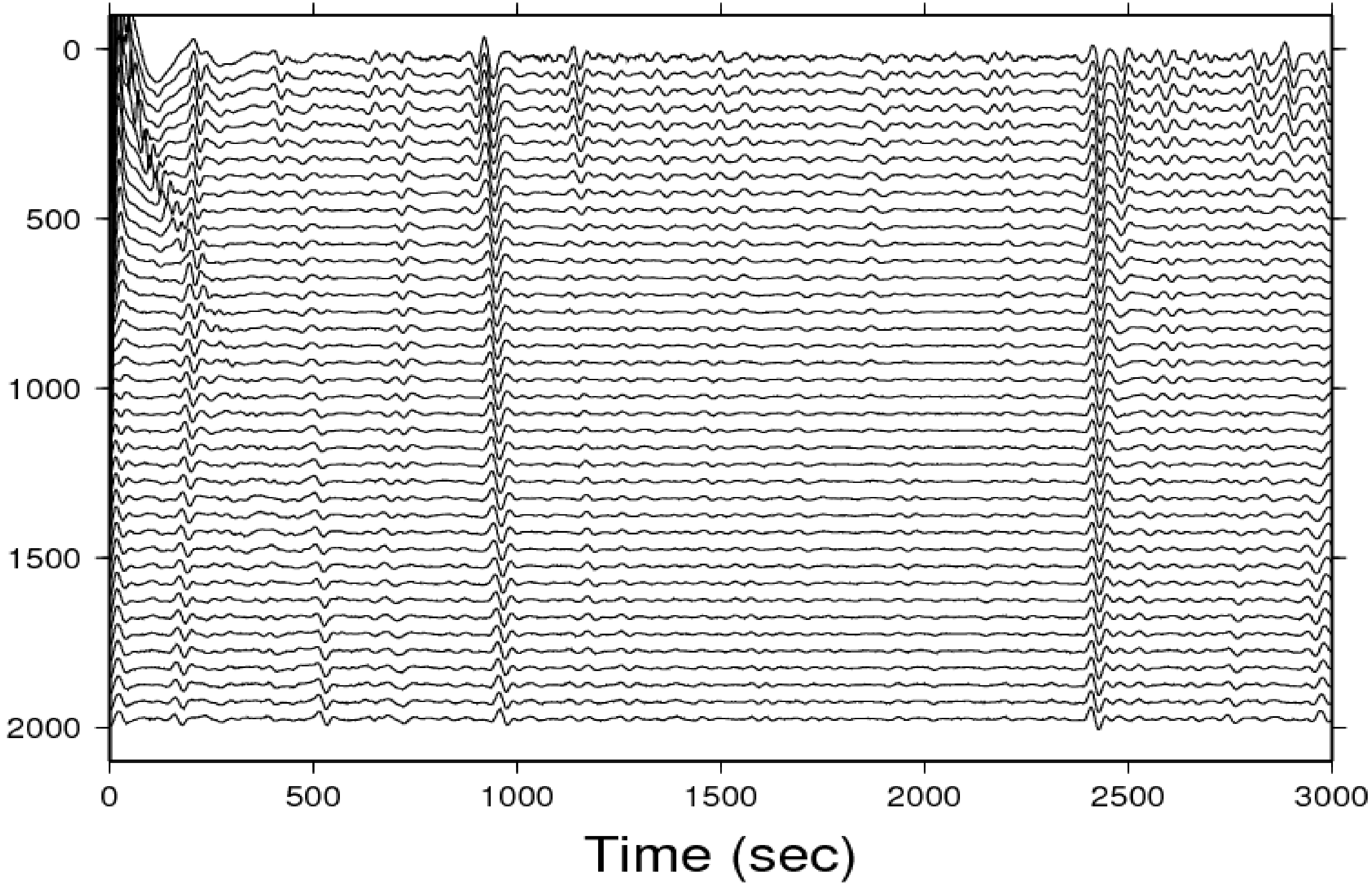

Velocity model corrections

– Schmandt and Lin (2014) for the depth of 0 - 1000 km beneath the US
– Li et al. (2008) for elsewhere globally

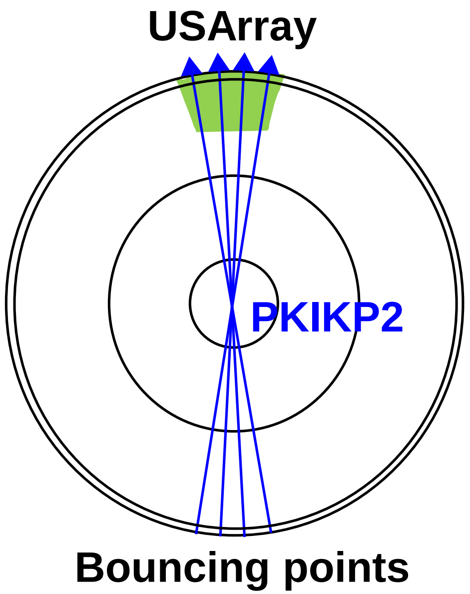

Corrected by PKIIKP2 phase

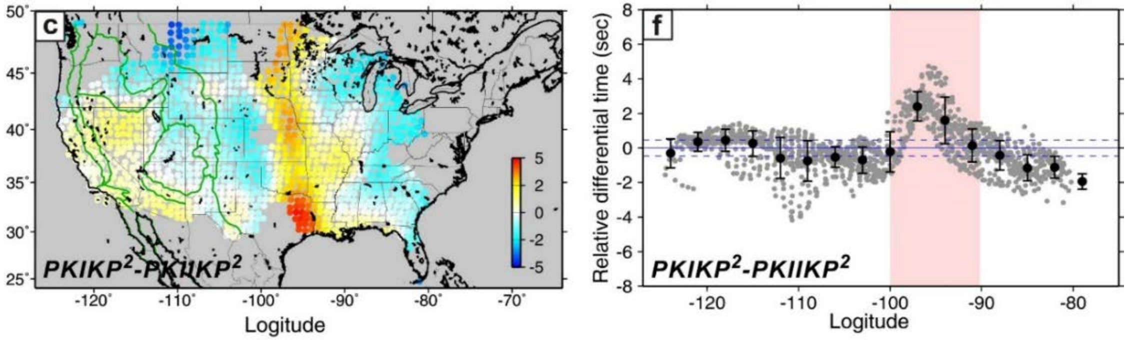

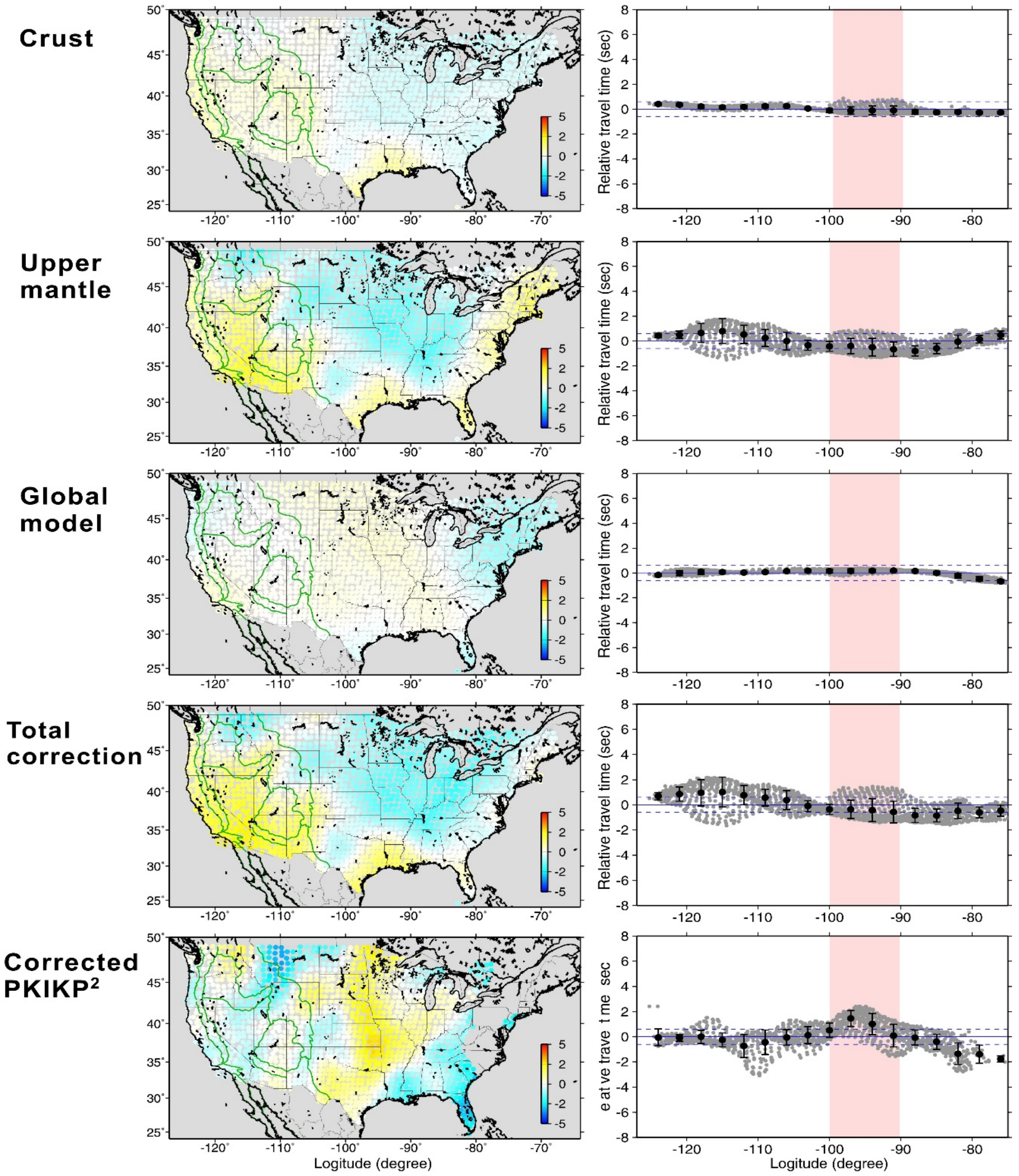

Radius test from 0 to 1000 km

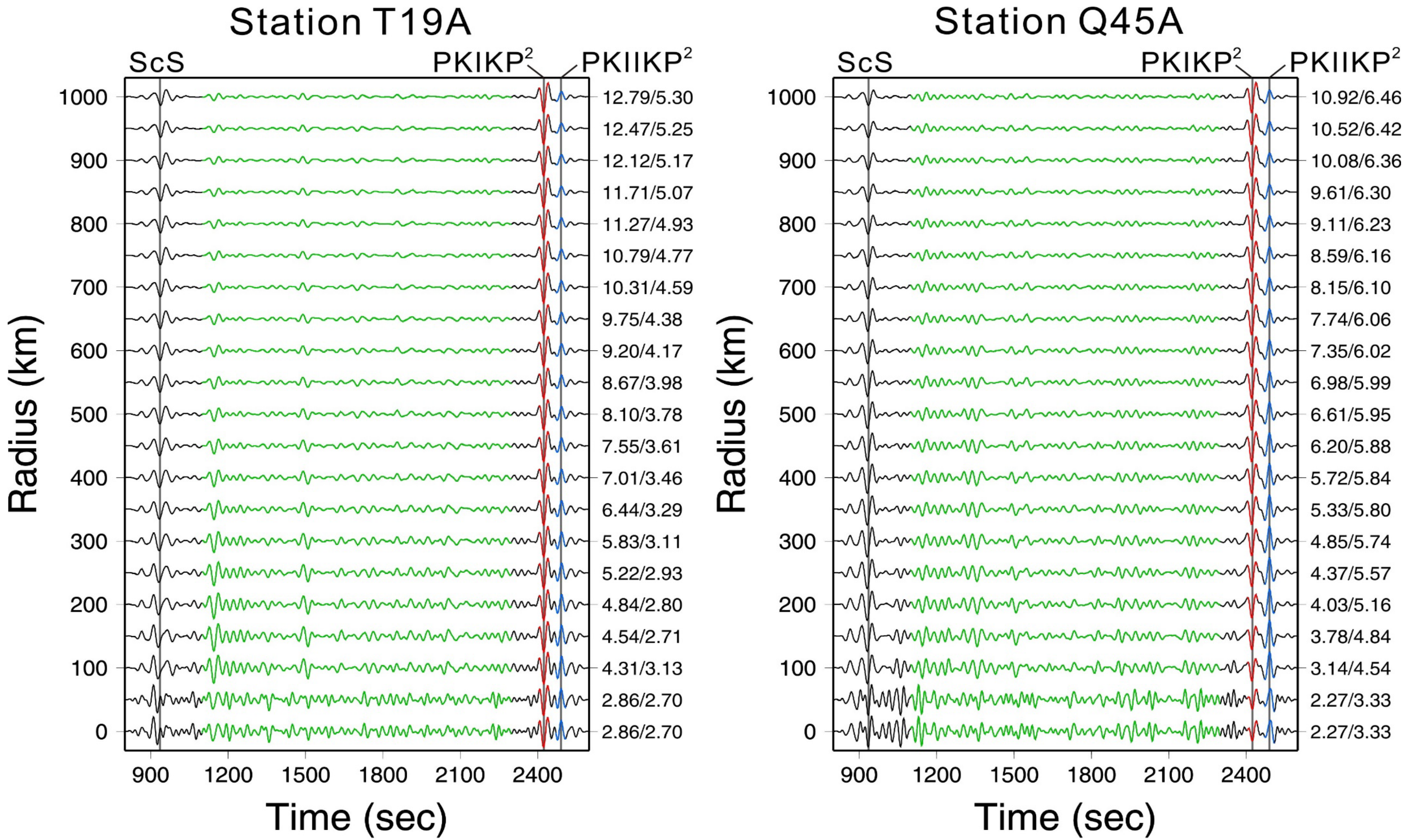

Uncertainty test with odd/even events

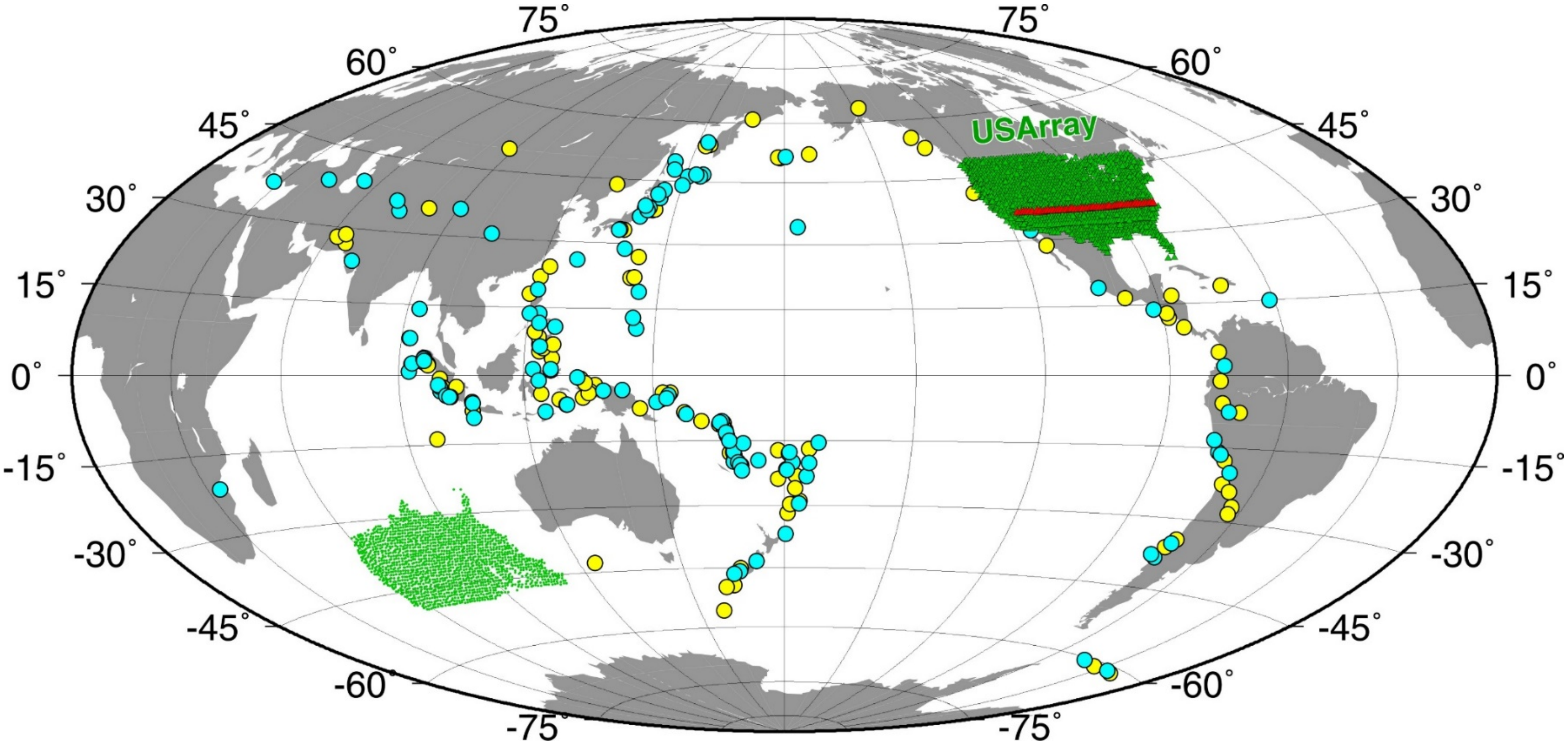

Uncertainty test with odd/even events

PKIKP^2 ~ 0.46 s

PKIIKP^2 ~ 0.33 s

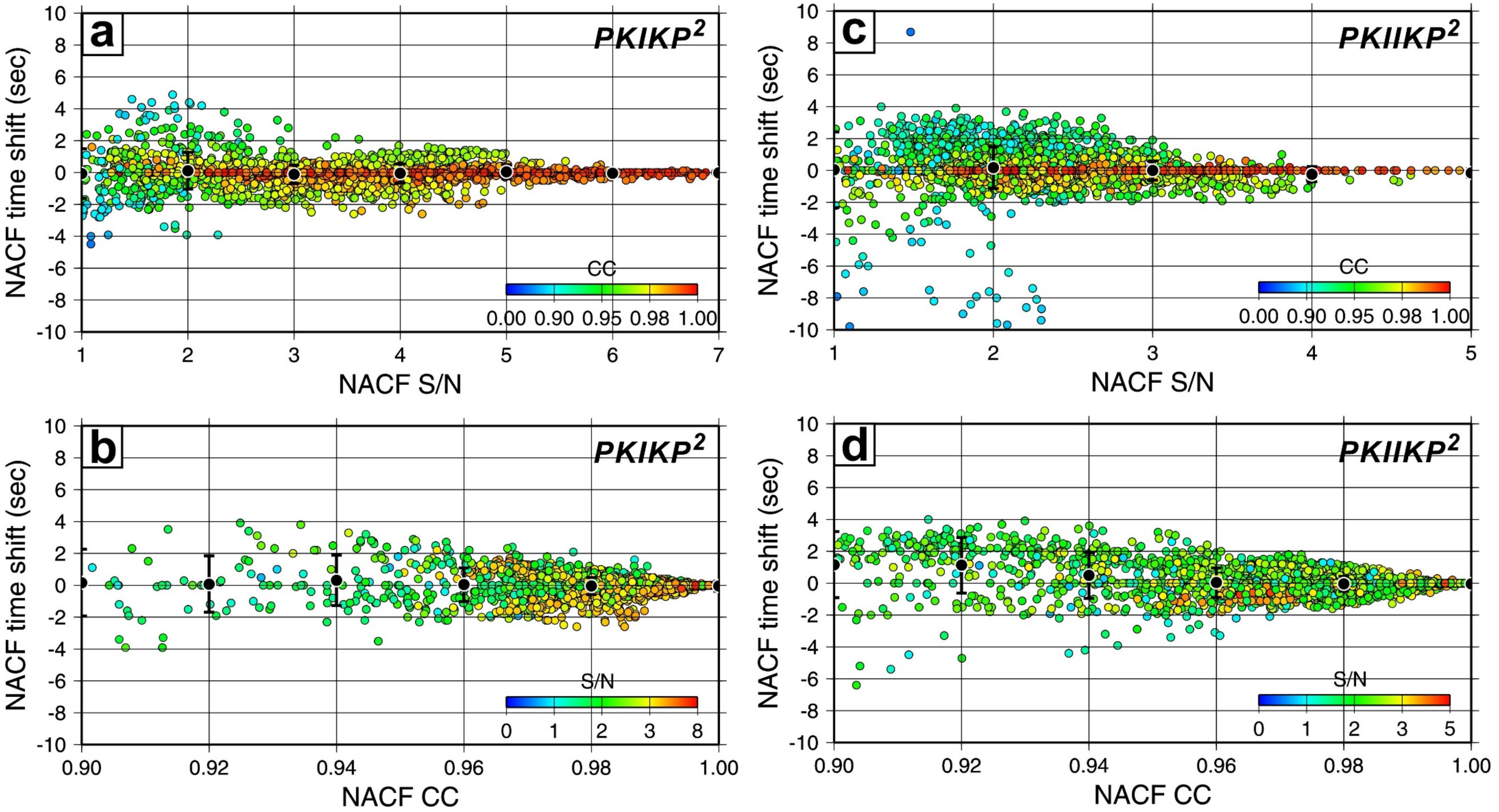

Finite-frequency analysis for PKIKP^2

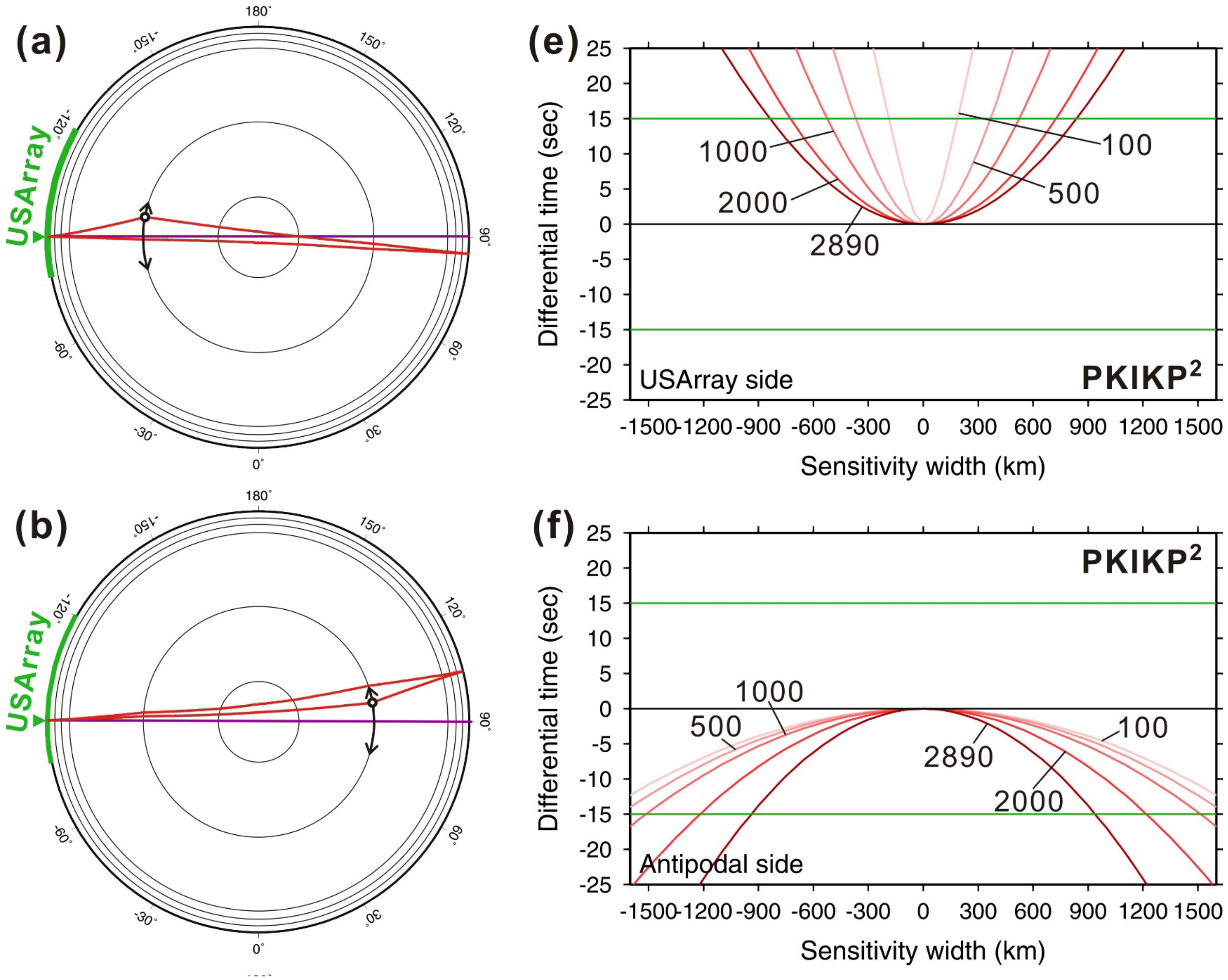

Finite-frequency analysis for PKIIKP^2

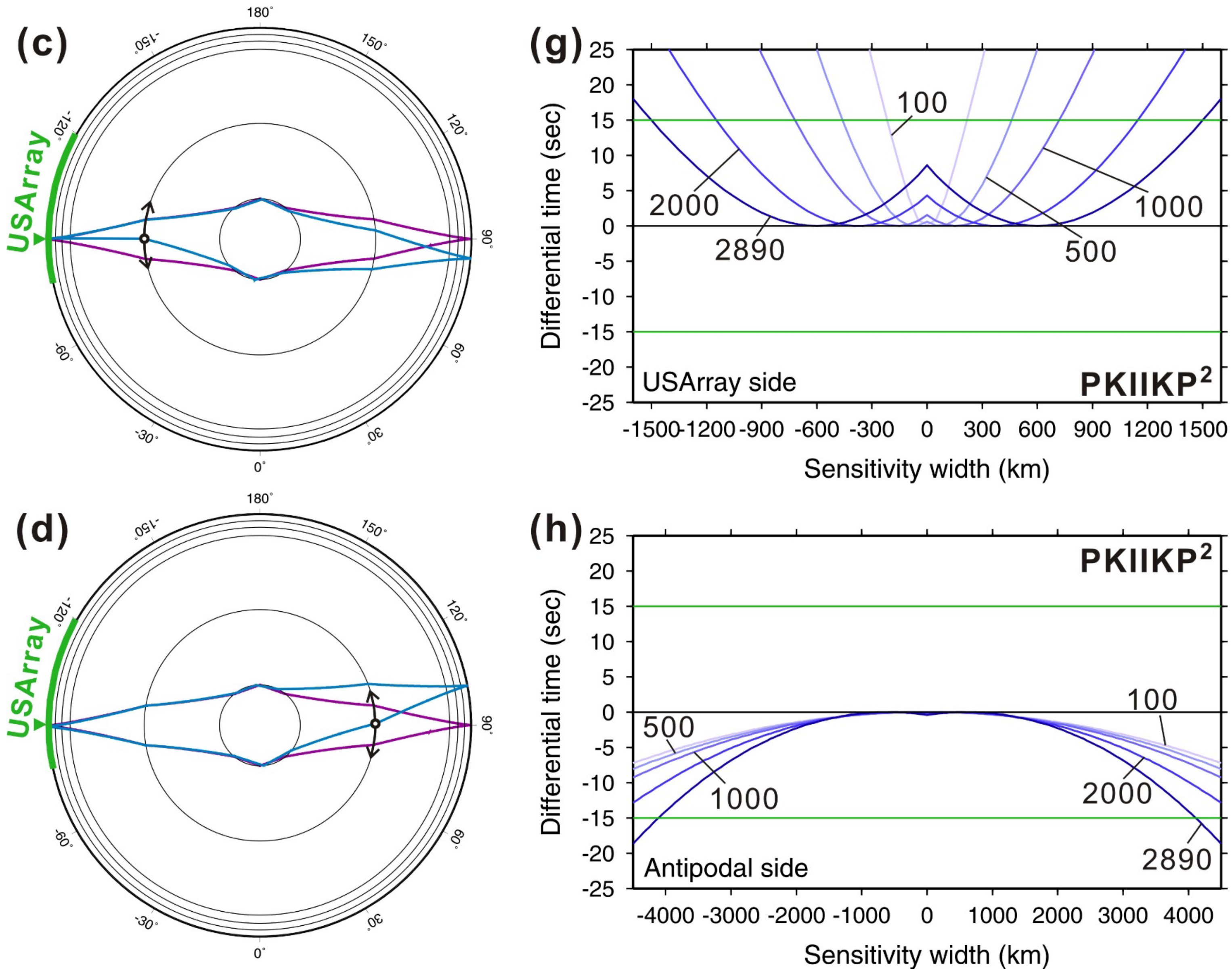

Lowermost mantle sensitivities of PKIKP² and PKIIKP²

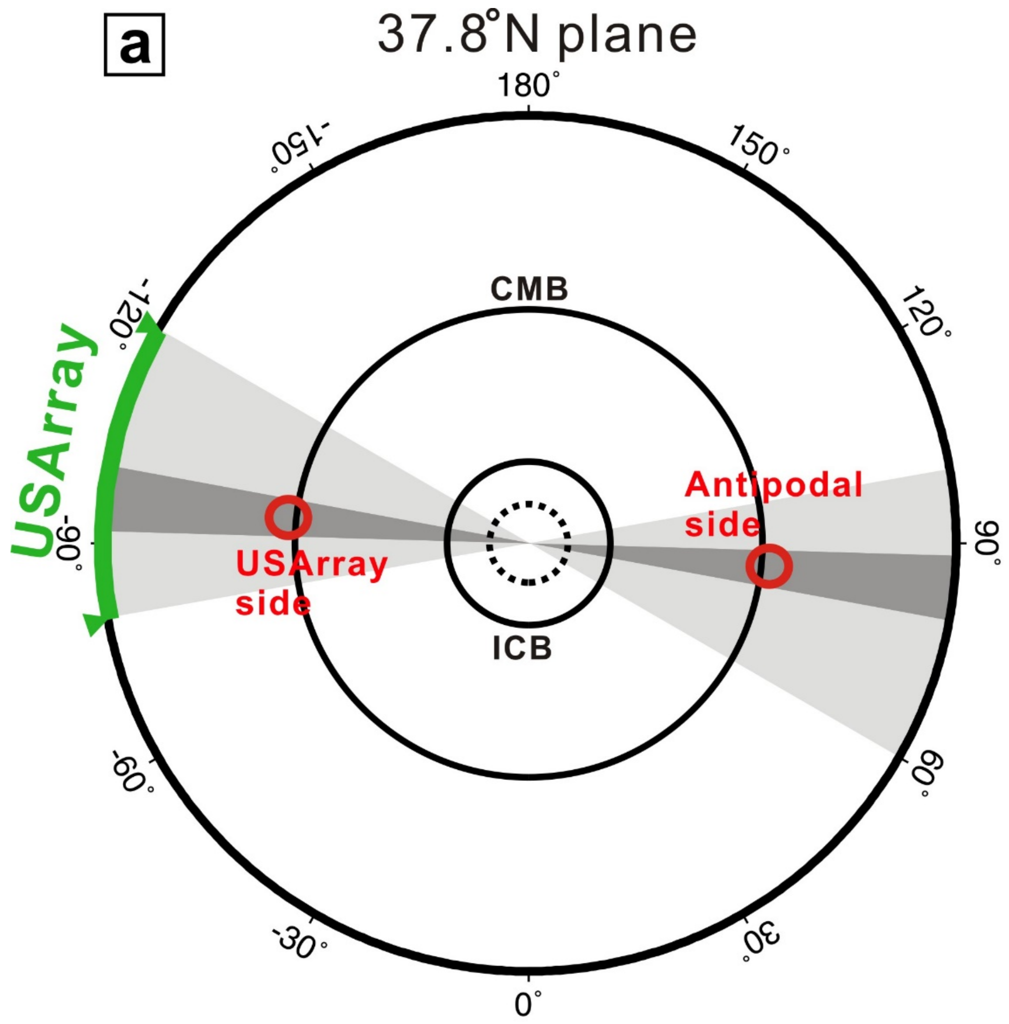

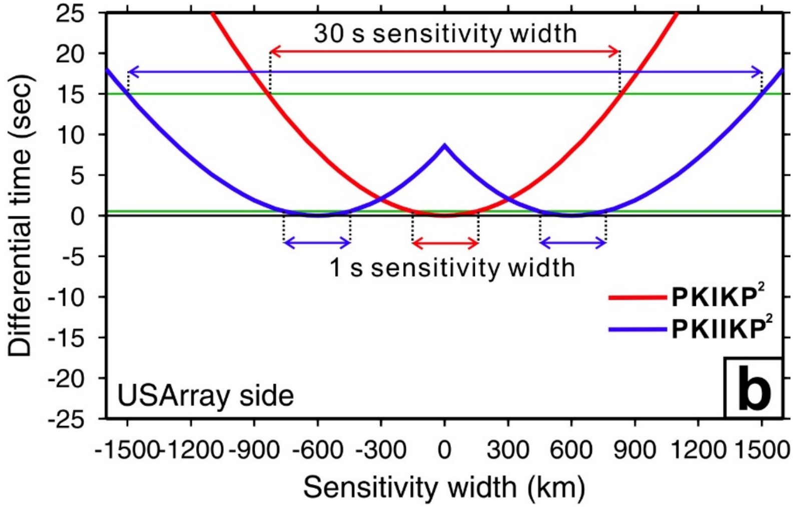

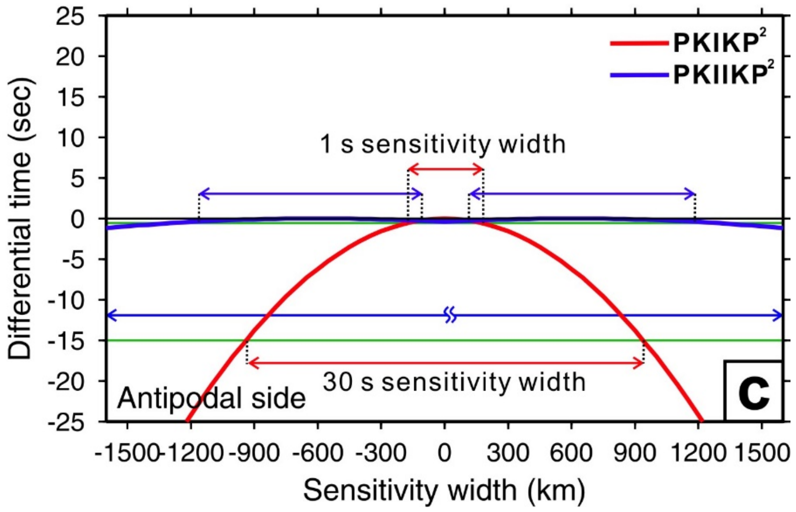

Fresnel zone visualization (Liu and Tromp, 2008)

P’P’

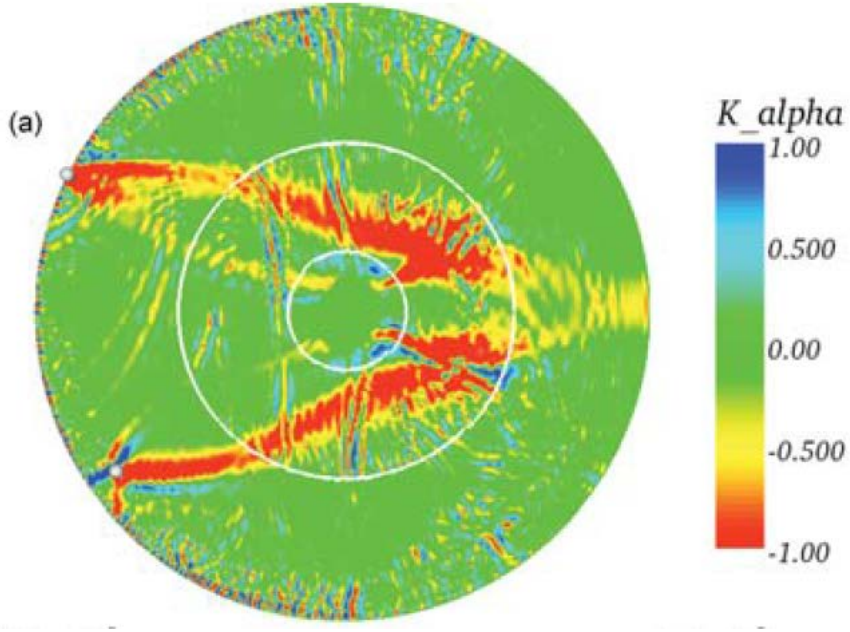

PKIKP

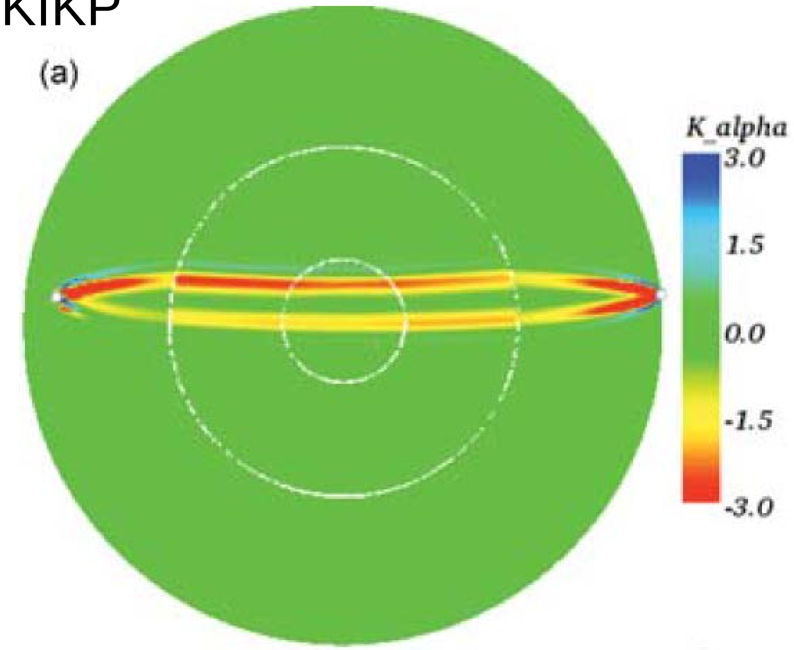

PP

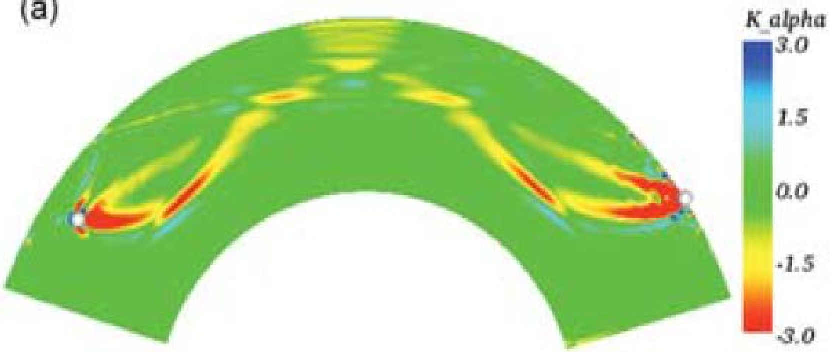

Predictions of different inner core models

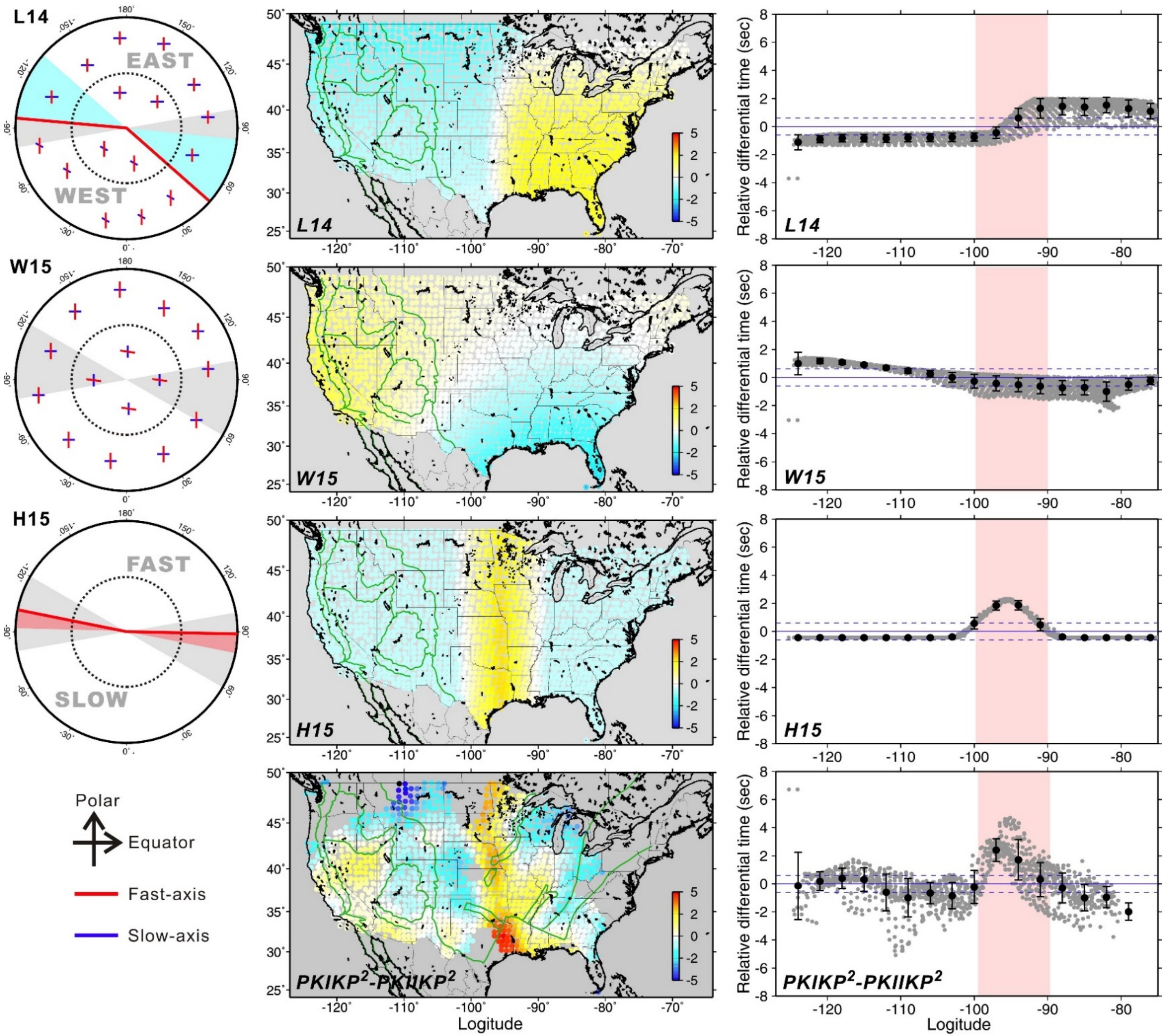

A proof-of-concept test using numerical approach

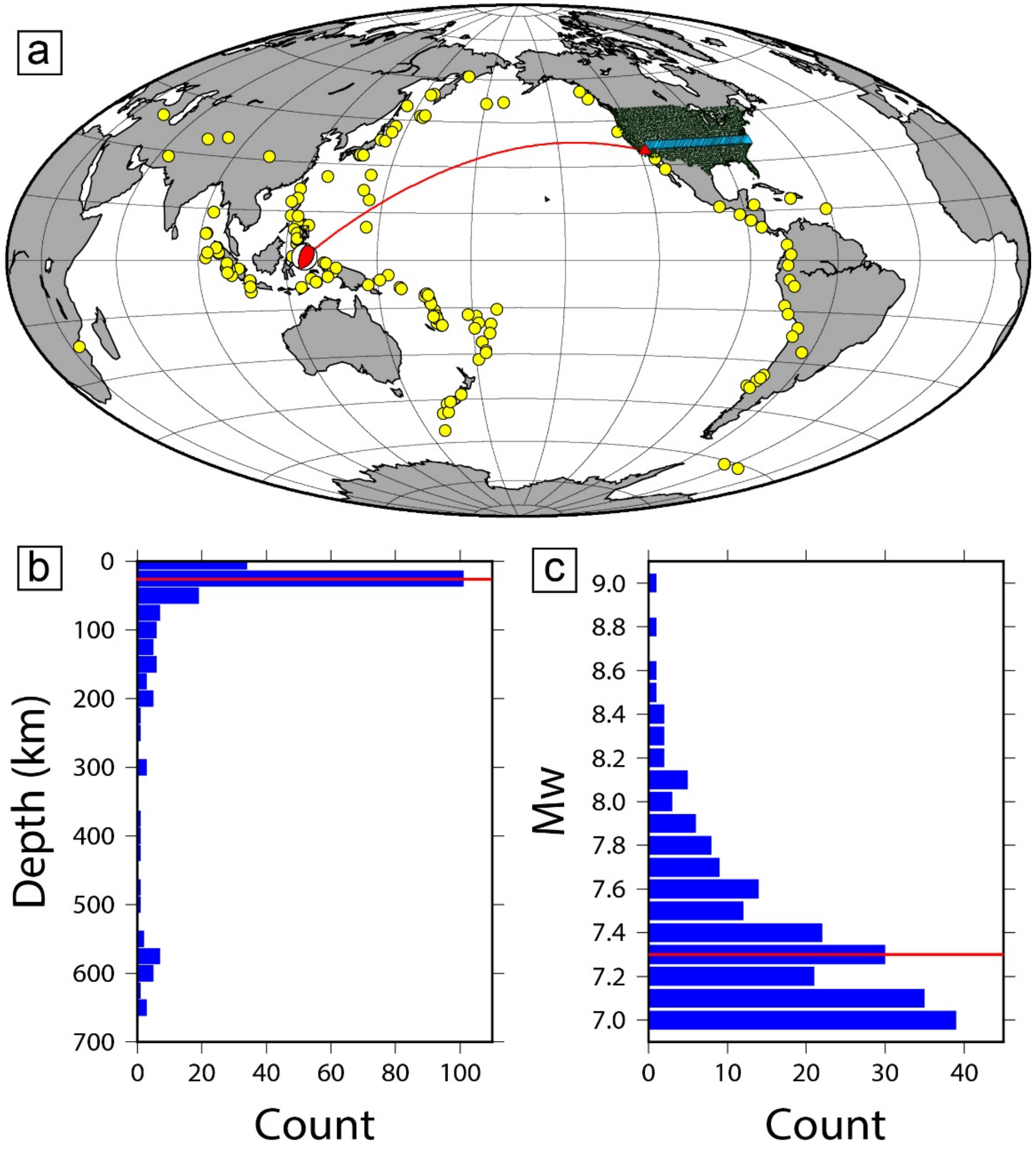

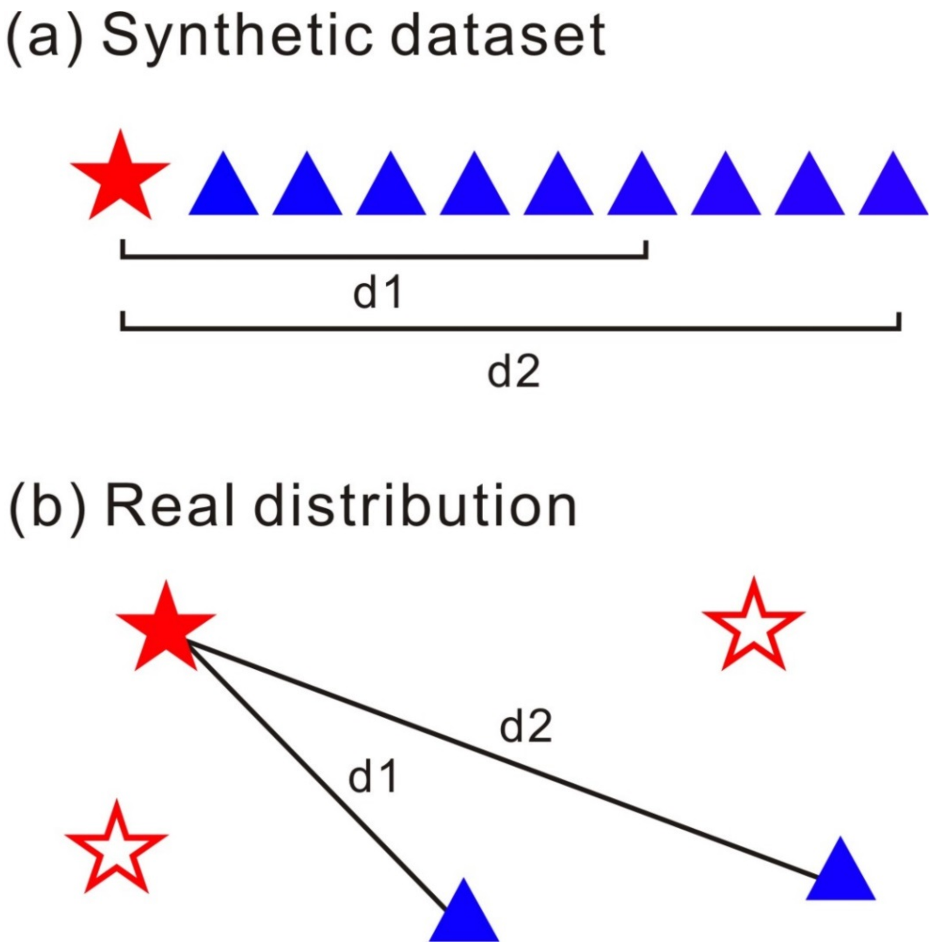

A proof-of-concept test using numerical approach

– comparison between observational CCFs and synthetic CCFs

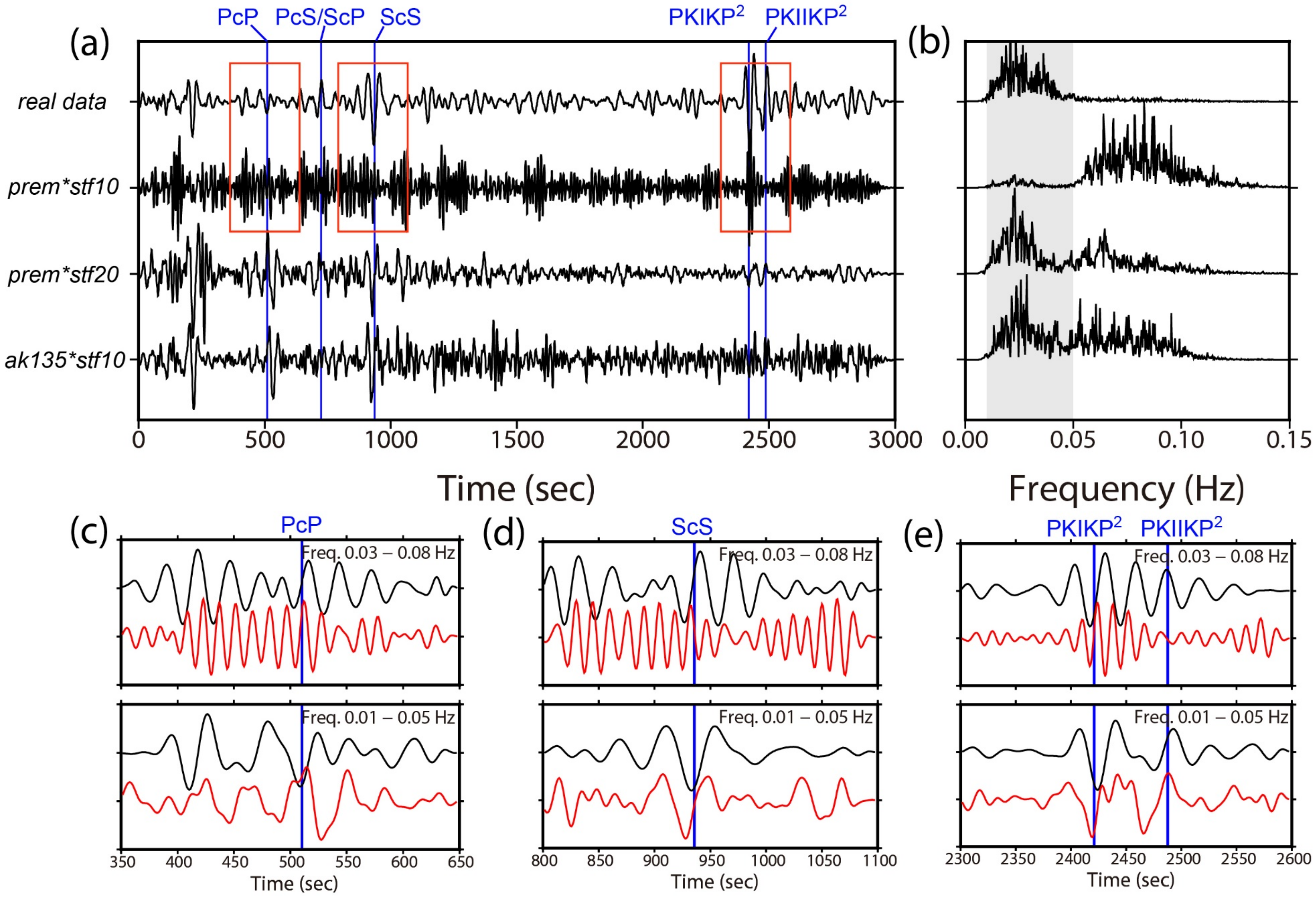

A proof-of-concept test using numerical approach

– comparison between synthetic CCFs using Model *prem* and *prem+IMIC*

– A 500-km-radius and 10% faster Vp will advance the PKIKP2 by 18 s

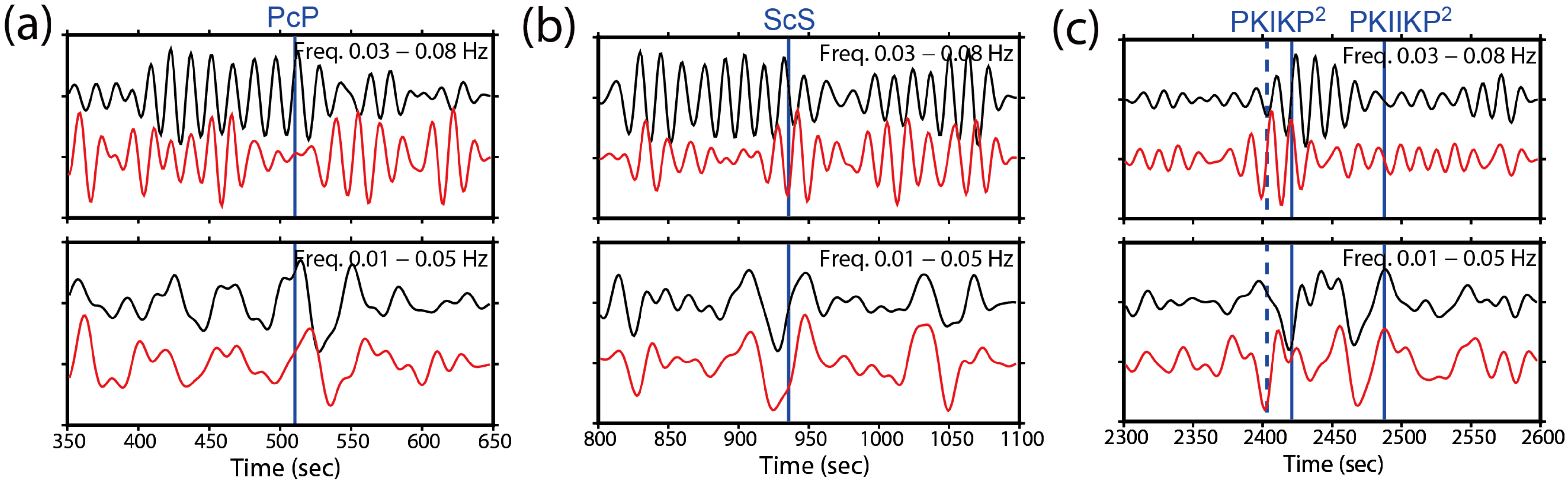

A proof-of-concept test using numerical approach

– effect of source distributions on ACFs and CCFs along a E-W linear array